






Universitat Autònoma de Barcelona

ADVERTIMENT. L'accés als continguts d'aquesta tesi queda condicionat a l'acceptació de les condicions d'ús establertes per la següent llicència Creative Commons:  http://cat.creativecommons.org/?page_id=184

ADVERTENCIA. El acceso a los contenidos de esta tesis queda condicionado a la aceptación de las condiciones de uso establecidas por la siguiente licencia Creative Commons:  <http://es.creativecommons.org/blog/licencias/>

WARNING. The access to the contents of this doctoral thesis it is limited to the acceptance of the use conditions set by the following Creative Commons license:  <https://creativecommons.org/licenses/?lang=en>

UNIVERSITAT AUTONOMA DE BARCELONA

FACULTAT DE BIOCIENCIES

**Molecular basis of shade tolerance: identification of
novel components**

Wenting QIN

2022



UNIVERSITAT AUTONOMA DE BARCELONA

FACULTAT DE BIOCIENCIES

Doctoral program of Plant Biology and Biotechnology

PhD thesis

**Molecular basis of shade tolerance: identification of
novel components**

Dissertation presented by Wenting QIN for the degree of Doctor of Plant Biology and Biotechnology at Autonomous University Barcelona. This work was performed in the Centre for Research in Agricultural Genomics.

Director

Tutor

Author

Dr. Jaume Martínez García Dr. Jaume Martínez García Wenting QIN

Barcelona, September 2022

ACKNOWLEDGEMENTS

Time flies and my PhD studies are coming to an end. Looking back on the past four years, I saw a lot to be grateful and cherished. I would like to express my heartfelt thanks to everyone who has helped me. Because of your help and guidance, I can overcome difficulties and solve doubts.

First, I would like to thank my supervisor Jaume Martínez-García. When we first met four years ago, his gracious smile and humorous words eased my nervousness and anxiety, I was quickly integrated into the new ground. During my PhD study, he carefully guided my experiments, gave me a lot of encouragement and help, and told me to "accumulate a lot". In addition to teaching me scientific knowledge and experimental skills, he also taught me more ways to think and solve problems. "It is better to teach a man to fish than to give him a fish." These principles have benefited me immensely.

Also, I am very grateful for the work of everyone who contributed to these two projects, and many thanks to all the CRAG (Barcelona) and IBMCP (Valencia) service staffs who helped me when needed. To all members of Lab 205 (CRAG) and Lab 005 (IBMCP), both current and no longer in this lab. It is a pleasure to be a part of this lab and to be with you for so many years.

Thanks to the China Scholarship Council for providing me the fellowship. Thanks to all my relatives and friends who care about me. Finally, a special thanks to my mom. Mom has always supported me behind my back, and her selfless love and care for me is what keeps me going.

SUMMARY

To deal with the limitation of light that might cause the shade cast by neighboring vegetation, plants have evolved two different and divergent strategies: avoidance, like *Arabidopsis thaliana* and tolerance, like *Cardamine hirsuta*. When shaded, shade-avoider species display a suite of traits and responses to adapt growth and development as a way to “escape” from shade, called globally the shade avoidance syndrome (SAS). Among these traits are found accelerated elongation of stems (hypocotyls and internodes) and leaf petioles, also elevated leaf angles to the horizontal, reduced branching and early flowering. Conversely, shade-tolerant species do not outgrow the neighboring plants (i.e., their hypocotyls do not elongate in response to plant shade). While the molecular basis of shade avoidance has been heavily studied, such as several transcriptional regulators are central to plant responses to vegetation proximity, including the positive regulator PHYTOCHROME INTERACTING FACTORS (PIFs) and the antagonistic ELONGATED HYPOCOTYL 5 (HY5) and LONG HYPOCOTYL IN FAR-RED 1 (HFR1). However, much less is known about how shade tolerance works, so we are beginning to explore how shade tolerant-plants modulate vegetation proximity by using *C. hirsuta*, a close relative of *A. thaliana*. We demonstrated that *C. hirsuta* HFR1 interacted weaker with COP1 than *A. thaliana* HFR1, which causes it to have higher biological activity and stability. In addition, *C. hirsuta* HY5 inhibits hypocotyl elongation in both shade and white light conditions by constraining the growth-related hormones, such as auxin. Moreover, *C. hirsuta* PIF7 has a role in promoting hypocotyl elongation in shade but only in a phytochrome A (phyA) deficient background. We show that a higher activity of negative regulators, including HFR1 and HY5, whereas a lower activity of positive regulators, like PIF7 when compared to *A. thaliana*, resulting in the shade tolerance habit of *C. hirsuta*. Besides, PROTEOLYSIS6

(PRT6) may be a newly *A.thaliana* shade avoidance regulator, which affects several aspects of plant development, including delayed dark induced senescence (DIS), thermal induced morphogenesis (TIM) and shade-induced hypocotyl elongation. Mutations in different locations of the PRT6 gene may cause differential responses of hypocotyls to shade.

RESUMEN

Para hacer frente a la limitación de luz que podría causar la sombra proyectada por la vegetación vecina, las plantas han desarrollado dos estrategias diferentes y divergentes: evitación, como *Arabidopsis thaliana* y tolerancia, como *Cardamine hirsuta*. Cuando están sombreadas, las especies que evitan la sombra muestran un conjunto de rasgos y respuestas para adaptar el crecimiento y el desarrollo como una forma de "escapar" de la sombra, lo que se denomina globalmente síndrome de evitación de la sombra (SAS). Entre estos rasgos se encuentran elongación acelerada de tallos (hipocotilos y entrenudos) y pecíolos de las hojas, ángulos elevados de las hojas con respecto a la horizontal, ramificación reducida y floración temprana. Por el contrario, las especies tolerantes a la sombra no crecen más que las plantas vecinas (es decir, sus hipocotilos no se alargan en respuesta a la sombra de la planta). Si bien la base molecular de evitar la sombra se ha estudiado mucho, como varios reguladores transcripcionales que son fundamentales para las respuestas de las plantas a la proximidad de la vegetación, incluido el regulador positivo FACTORES DE INTERACCIÓN CON FITOCROMOS (PIF) y el antagonista HIPOCOTILO 5 ELONGADO (HY5) e HIPOCOTILO LARGO EN LEJOS -ROJO 1 (HFR1). Sin embargo, se sabe mucho menos sobre cómo funciona la tolerancia a la sombra, por lo que estamos comenzando a explorar cómo las plantas tolerantes a la sombra modulan la proximidad de la vegetación mediante el uso de *C. hirsuta*, un pariente cercano de *A. thaliana*. Demostramos que *C. hirsuta* HFR1 interactuó más débilmente con COP1 que *A. thaliana* HFR1, lo que provocó que tuviera mayor actividad biológica y estabilidad que. Además, *C. hirsuta* HY5 inhibe el alargamiento del hipocótilo tanto en condiciones de sombra como de luz blanca al restringir las hormonas relacionadas con el crecimiento, como la auxina. Además, *C. hirsuta* PIF7 tiene un papel en la promoción de la elongación del

hipocótilo en la sombra, pero solo en un fondo deficiente de fitocromo A (phyA). Mostramos que una mayor actividad de los reguladores negativos, incluidos HFR1 y HY5, mientras que una menor actividad de los reguladores positivos, como PIF7 en comparación con *A. thaliana*, da como resultado el hábito de tolerancia a la sombra de *C. hirsuta*. Además, PROTEOLYSIS6 (PRT6) puede ser un nuevo regulador de evitación de la sombra de *A. thaliana*, que afecta varios aspectos del desarrollo de la planta, incluida la senescencia inducida por la oscuridad retrasada (DIS), la morfogénesis inducida térmicamente (TIM) y el alargamiento del hipocótilo inducido por la sombra. Las mutaciones en diferentes lugares del gen PRT6 pueden causar respuestas diferenciales de los hipocotilos a la sombra.

ABBREVIATIONS

ABBREVIATIONS

R	Red light
FR	Far-red light
B	Blue light
SAS	Shade avoidance syndrome
PhyA	Phytochrome A
PhyB	Phytochrome B
Cry	Cryptochrome
Pr	Inactive red-absorbing phytochrome form
Pfr	Active far-red-absorbing phytochrome form
At	<i>Arabidopsis thaliana</i> (<i>A. thaliana</i>)
At^{WT}	<i>A. thaliana</i> wild type (Col-0)
Col-0	Columbia-0 ecotype of <i>A. thaliana</i>
Ch	<i>Cardamine hirsuta</i> (<i>C. hirsuta</i>)
Ch^{WT}	<i>C. hirsuta</i> wild type (OX)
OX	<i>C. hirsuta</i> Oxford ecotype
bHLH	Basic helix-loop-helix
HFR1	LONG HYPOCOTYL IN FAR-RED 1
ChHFR1	<i>C. hirsuta</i> HFR1
<i>chfr1</i>	<i>C. hirsuta</i> mutant in ChHFR1
<i>hfr1</i>	<i>A. thaliana</i> mutant in AtHFR1
COP1	CONSTITUTIVE PHOTOMORPHOGENIC 1
HY5	ELONGATED HYPOCOTYL 5
<i>chy5</i>	<i>C. hirsuta</i> mutant in ChHY5
<i>hy5</i>	<i>A. thaliana</i> mutant in AtHY5
PIF7	PHYTOCHROME INTERACTING FACTOR 7
chpif7	<i>C. hirsuta</i> mutant in ChPIF7
<i>pif7</i>	<i>A. thaliana</i> mutant in AtPIF7
<i>pifq</i>	<i>A. thaliana</i> PIFQ quadruple mutant
<i>sis1</i>	<i>C. hirsuta</i> mutant slender in shade 1
W+FR	White light supplemented with far-red
W	Continuous white light

VP	Val-Pro motifs
MST	Microscale thermophoresis
GFP	Green fluorescence protein
HA	Influenza hemagglutinin
GUS	β -glucuronidase
SDS-PAGE	Sodium dodecyl sulfate - polyacrylamide gel electrophoresis
k_D	Dissociation constant
AtCRY1	<i>A. thaliana</i> cryptochrome 1
pU6	U6 promoter
pU3	U3 promoter
PAM	Protospacer adjacent motif
NLS/bHLH	Nucleus in basic helix-loop-helix
Q-rich	Glutamine-rich
APB	Active phyB binding
DEGs	Differentially expressed genes
SE	Standard error
PVDF	Polyvinylidene fluoride
GA	Gibberellin
IAA	Indol-3 acetic acid
ABA	Abscisic acid
BR	Brassinosteroid
PSI and PSII	Photosystems I and II
NPQ	Non-photochemical quenching
CF	Chlorophyll fluorescence
Fv/Fm	The maximum quantum yield of PSII
ϕPSII	The effective quantum yield of PSII
PPDF	Photosynthetically active photon flux density
DIS	Dark-Induced Senescence
TIM	Thermal-induced morphogenesis
HY5ox	The over expression HY5 line
HFR1ox	The over expression HFR1 line
EF1α	<i>ELONGATION FACTOR 1α</i>

qPCR	Real time quantitative PCR
Cbu-P	<i>Capsella bursa-pastoris PHA</i>
Cbu-S	<i>Capsella bursa-pastoris SCH</i>
Cru	<i>Capsella rubella</i>
Sir	<i>Sisymbrium irio</i>
Aal	<i>Arabis alpina</i>
EMS	Ethyl-methanesulfate
eva	Seedlings are ever green and attenuated in shade and TIM
adm	Seedlings have attenuated DIS and enhance hypocotyl elongation in shade and TIM
eden	Seedlings have attenuated DIS and enhanced hypocotyl elongation in shade but attenuated elongation in TIM
B₁F₂	F ₂ segregating population have been backcrossed once
B₂F₂	F ₂ segregating population have been backcrossed twice
df	Degrees of freedom
AF	Allele frequency
SNPs	The single nucleotide polymorphisms
UTRs	Untranslated regions
CDS	Coding sequence
GED1	GREENING AFTER EXTENDED DARKNESS
PRT6	PROTEOLYSIS 6

TABLE OF CONTENTS

Table of Contents

GENERAL INTRODUCTION	1
1. Light serves as a crucial signal for the development of plants.....	1
2. Plant adaptations to vegetation proximity	2
3. Shade and light perception and signaling in shade avoiders.....	5
3.1 Phytochromes perceive the R:FR signal.....	5
3.1.1 Phytochromes transfer the R:FR signal to PIFs.....	6
3.1.2 Activated PIFs induce the expression of growth-related genes .	7
3.2 Cryptochrome: blue light receptors	9
3.3 Perception of UV-B	10
4. Variety of plant strategies to vegetation proximity	10
4.1 Different response at seedling stage	10
4.2 Different response in adult plants	12
5. Additional conditions related with shade signaling	13
5.1 Dark-Induced Senescence (DIS) on leaves	13
5.2 Thermal-Induced Morphogenesis (TIM).....	15
OBJECTIVES.....	17
CHAPTER I.....	19
1. Introduction.....	21
2. Result	22
2.1 The increased HFR1 abundance in <i>C. hirsuta</i> is due to differences in interaction with COP1	22
2.1.1 ChHFR1 VP peptide had a weaker interaction with COP1 than AtHFR1	22
2.1.2 VP regions determine the different stability of HFR1 orthologue proteins.....	26

2.1.3 Other regions participate in conferring differences in HFR1 stability.....	27
2.2 HY5 and PIF7 both are required for shade tolerance habit of <i>C. hirsuta</i>	29
2.2.1 Plasmid construction and mutant identification	29
2.2.2 ChHY5 protein is more stable than AtHY5.....	40
2.2.3 HY5 and PIF7 have less effect on shade-regulated gene expression in <i>C. hirsuta</i>	41
3. Discussion.....	53
3.1 COP1-interacting domain controls At/ChHFR1 stability	53
3.2 ChPIF7 and ChHY5 have roles in shade tolerance in <i>C. hirsuta</i>	55
3.3 ChHY5 and ChPIF7 are less affected by shade	56
4. Materials and method.....	58
4.1 Plant material and growth conditions	58
4.2 Generation of constructs for transient expression.....	59
4.3 Construction of transgenic lines.....	59
4.4 Measurement of hypocotyl length	61
4.5 Gene expression analyses.....	61
4.6 Floral dip	61
4.7 Agroinfiltration of <i>N. benthamiana</i> leaves	61
4.8 RNA-sequencing.....	62
4.9 Protein extraction and immunoblotting analyses.....	62
4.10 Protein purification for the MST experiments	63
Supplementary information	64
Reference	70
CHAPTER II.....	87
1. Introduction.....	89
2. Result.....	91

2.1 Characteristics of shade-tolerant plants.....	92
2.1.1 Hypocotyls of shade-tolerant species are unresponsive to warm temperature	92
2.1.2 Shade-tolerant plants show overall a delayed DIS	94
2.1.3 Different early changes in chlorophyll fluorescence levels	96
2.2 Screening from EMS-mutagenized pools.....	100
2.2.1 Selection of mutants displaying a delayed DIS phenotype	100
2.2.2 Additional sequential screenings of the selected mutants with a delayed DIS	103
2.2.3 Chlorophyll levels dropped slowly in mutants	105
2.3 Mapping by sequencing to identify the mutated genes	108
2.3.1 Backcrossing to purify mutants	108
2.3.2 Mapping by sequence revealed candidate mutations	109
3. Discussion	123
3.1 PIF-mediated processes of shade, DIS and TIM are related	123
3.2 A delayed DIS in <i>C. hirsuta</i> is modulated by an attenuated PIF activity.....	125
3.3 Novel molecular components involved in SAS.....	127
4. Materials and methods	130
4.1 Plant material and growth conditions	130
4.2 Pigment Extraction and chlorophyll content quantification	131
4.3 Chlorophyll fluorescence measurements	132
4.4 Genomic DNA extraction for massive sequencing.....	133
Supplement Information	134
Reference	146
GENERAL DISCUSSION	164
CONCLUSIONS.....	171
GENERAL REFERENCE.....	173

GENERAL INTRODUCTION

GENERAL INTRODUCTION

1. Light serves as a crucial signal for the development of plants.

The variety of light conditions seen in natural surroundings has an important influence on plant life. As photoautotrophic and sessile organisms, plants rely on exposure to sunlight for activating the photosynthesis, which transforms the light energy into chemical energy used for driving growth and development. Plants go through a number of developmental stages throughout the life cycle, including germination, seedling establishment, flower induction and seed production, all of which are regulated by light (Smith 2000). Photosynthetically active radiation (PAR, 400–700 nm) refers to this part of the light spectrum that is utilized for photosynthesis, which ranges from 400 nm (around blue light, B) to 700 nm (around red light, R), which also coincides with the visible spectrum for humans (Dannehl, Schwend et al. 2021).

The absorption of radiation in the PAR region of plants is easily affected by external factors, such as the presence of vegetation that throws shade on its surrounding plants, which may diminish the PAR intensity and degrade the quality of the light for driving photosynthesis (Smith 1982) (**Fig 1A**). In addition, plants perceive the proximity of other plants as changes in the relative amounts of red (R) and far-red light (FR), this is so because photosynthetic tissues, such as leaves, preferentially absorb R and B as a source of energy for the photosynthesis. By contrast, plants reflect FR, which mixes with sunlight and results in a mild reduction in the R:FR around them (low R:FR), a signal that informs about the near presence of potentially competing vegetation before actual shading takes place (Casal 2013). When a plant grows under plant canopy shade, the upper chlorophyll and carotenoid photosynthetic pigments present in the leaves strongly absorb the so-called PAR. In comparison, a higher proportion of FR is transmitted through the photosynthetic tissues, which decimates the amount of PAR and strongly lowers the R:FR (very low R:FR)

(Kurepin, Walton et al. 2007). Depending on the presence and density of the vegetation proximity, the growth condition what is affected of plants around them falls into three categories (**Fig 1B**) (Roig-Villanova and Martínez-García 2016):

(i) Unshaded. It can be seen in low density and sparse vegetation communities. As a result of these conditions, the sunlight that reaches the ground is largely unmodified and present high UV-B, B and R. It also retains a relatively high ratio between R and FR (R:FR) of around 1.5.

(ii) Proximity shade. It affects the quality of light without virtually altering the quantity in the PAR range, and vegetation is considered to preferentially reflect FR compared to other wave lengths, so this condition will also have high UV-B, B and R but generate an intermediate or moderate reduction in the R:FR.

(iii) Direct plant canopy shade. It affects not only the quality but also the quantity of light, because photosynthetic pigments from green tissues specifically absorb light from the PAR region, as explained, it causes a strong reduction in UV-B, B and R as well as a very low R:FR. Consequently, under direct plant canopy shade both the amount of PAR and R:FR is strongly reduced.

Either way, the reduction of the R:FR represents a highly reliable signal indicative of the absence of vegetation, or the proximity of non-shading vegetation or canopy shade, a signal that is perceived by the photochromic family of photoreceptors (Fraser, Hayes et al. 2016) (see below).

2. Plant adaptations to vegetation proximity

In many ecosystems in nature, such as in forests, prairies or agricultural communities, plants grow at high or very high densities where the close proximity of neighboring vegetation can result in competition for limited resources, like light (Pierik and de Wit 2014). In some case, the close proximity

of other plants can filter out the light to such low levels that the amount of light is suboptimal and plants eventually die (Bai 2017). As plants cannot move to the best places to absorb light, in contrast to animals, they have evolved multiple systems to monitor and sense the environment, such as a wide range of photoreceptors, and adjust their growth, development and metabolism to optimize the use of sunlight. Photoreceptors are able to convert environmental signals into biological information that can be integrated with the endogenous mechanisms and processes that regulate growth and developmental. As a consequence, plant form can be greatly modulated depending on the environment in which the plant is growing, which gives plants a very plastic development.

When exposed to vegetation proximity or shade, plants have evolved two main strategies to respond: avoidance and tolerance (**Fig 1B**). For shade-avoider plant species, such as *Arabidopsis thaliana*, perception of the low R:FR signal triggers a suite of traits and responses to compete with other plants in the search for more sunlight and escape from shade, which collectively are known as Shade Avoidance Syndrome (SAS) that typically results in an accelerated elongation of hypocotyls, stems and petioles, and a delay in cotyledon and leaf expansion and chloroplast development. Shade-tolerant species, like *Cardamine hirsuta* (Morelli, Paulisic et al. 2020), show particular adaptations under shade environment, including lack of elongation in response to low R:FR (Molina-Contreras, Paulišić et al. 2019).

Generally, activation of SAS responses are detrimental to agricultural production, as it diverts more resources to promote elongation in detriment to harvestable organs, such as leaves, fruits, flowers and seeds (Morgan, Finlayson et al. 2002). On the other hand, this activation could be positive in natural environments, as it helps plants to compete for more resources by pronouncing shoot elongation and upwarding leaf movement (hyponasty) to

consolidate light capture (Franklin 2008). Therefore, understanding how shade-tolerant species work in suppressing the SAS responses could potentially be beneficial to crop production in high planting densities.

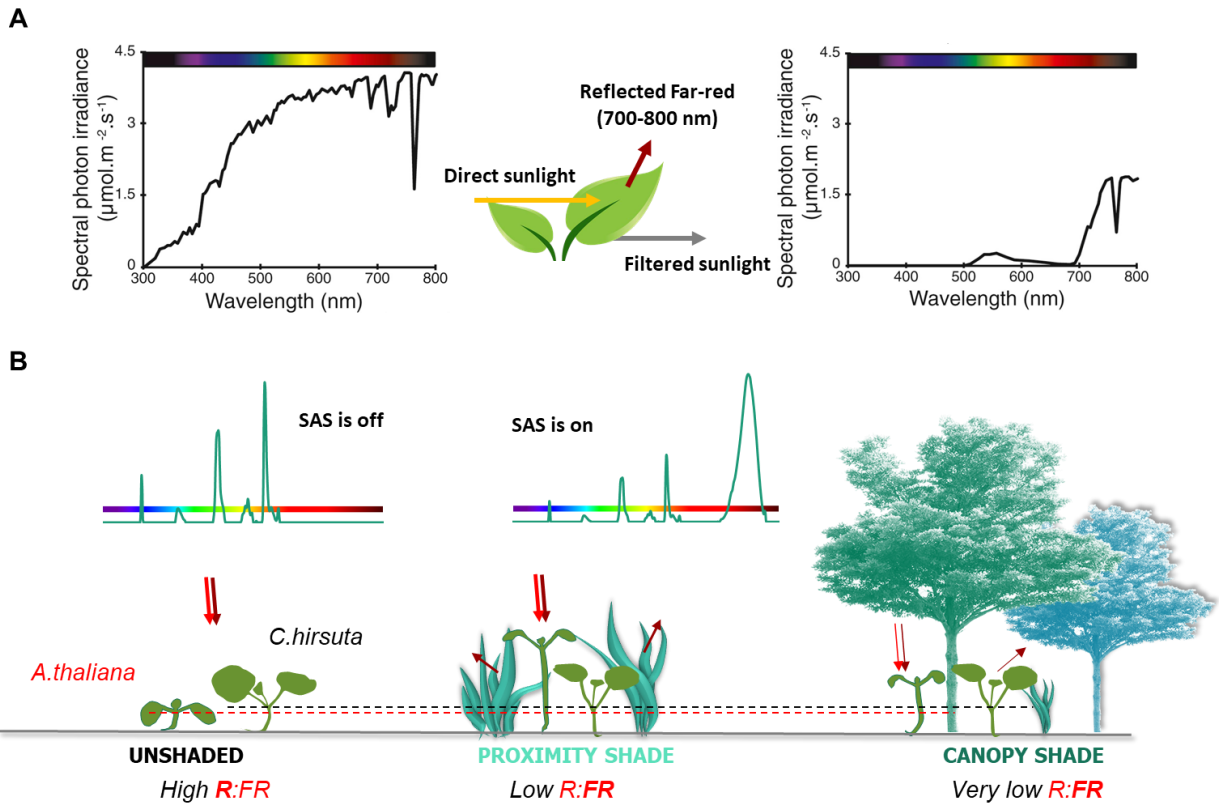


Figure 1. Vegetation filters and reflects part of the light spectrum producing different shade conditions. **(A)** The spectrum of direct sunlight contains blue (450-500 nm), green (500-570 nm), red (R, 620-700 nm), and far-red (FR, 700-750 nm). B and R are preferentially and intensely absorbed by the photosynthetic pigments present in green tissues, while FR is reflected and even transmitted by the leaves. **(B)** Unshaded and shaded conditions in nature have different light characteristics. When vegetation density is low enough to allow direct sunlight to reach an isolated plant, it contains relatively high levels of R and low levels of FR, resulting in a high R:FR ratio. When growing in dense vegetation–areas, FR reflected from nearby plants decreases the R:FR of sunlight, announcing the proximity of vegetation that potentially can result in light competition (proximity shade). Light conditions under a vegetation canopy,

which are characterized by low PAR light intensity caused by light being filtered by the leaves, also results in a very low R:FR ratio (canopy shade). When shade-avoider plants like *A. thaliana* detect a reduction in the R:FR caused by the presence of neighboring vegetation (either proximity or canopy shade) responds by inducing a series of adaptive reactions, such as promoting the elongation of hypocotyls and reducing the size of cotyledons, in order to escape shade and outcompete their neighbors. By contrast, shade tolerant plants, such as *C. hirsuta*, are suited for survival in low light conditions, and do not react by elongating when they detect the low R:FR signals (Kami, Lorrain et al. 2010, Fiorucci and Fankhauser 2017).

3. Shade and light perception and signaling in shade avoiders

3.1 Phytochromes perceive the R:FR signal

Phytochromes are R and FR-absorbing photoreceptors that sense the light changes caused by the presence of neighboring vegetation that potentially can compete for light (Keuskamp and Pierik 2010) (**Fig 2**). Phytochromes act as molecular switches between two photoconvertible forms in response to R and FR exposure: an inactive R-absorbing Pr form and an active FR-absorbing Pfr form. As in natural environments light is polychromatic and R:FR changes in response to the proximity of other plants, the balance between the active and inactive forms of the phytochromes changes in a R:FR-dependent manner. When plants grow with a high R:FR, the photo-equilibrium is displaced towards the active Pfr form and SAS is suppressed. By contrast, with a low R:FR, this equilibrium is displaced to the inactive Pr form and SAS is induced (Hersch, Lorrain et al. 2014).

Phytochromes are encoded by a small gene family that in *A. thaliana* is formed by 5 genes (*PHYA-PHYE*). Under proximity vegetation, phyB is the primary regulator in repressing plant responses to shade; phyD and phyE act

with phyB in suppressing SAS responses at the adult stage, like internode and petiole elongation (Roig-Villanova and Martínez-García 2016). Genetic analyses also show that phyA and phyB have antagonistic actions in shade. Indeed, when plants grow under canopy shade (very low R:FR), phyA accumulates and it is strongly activated to prevent the excessive elongation of the seedling caused by the deactivation of phyB (Martínez-García, Gallemí et al. 2014). Therefore, the regulation imposed by the low R:FR perception are the rapid changes in the balance of active photoreceptors. Other aspects of the light environment that are also affected by the proximity of vegetation, such as the amount of B, are perceived by a different group of photoreceptors, the B-light absorbing cryptochromes (Tissot and Ulm 2020).

3.1.1 Phytochromes transfer the R:FR signal to PIFs

Shade-induced changes in the abundance of active Pfr form are translated into changes in gene expression via the interaction of phytochromes with the PHYTOCHROME INTERACTING FACTORS (PIFs), a group of basic helix-loop-helix (bHLH) transcription factors (Qi, Liu et al. 2020). Under high R:FR, the interaction of active phyB with PIFs reduces their stability and/or activity, inhibiting the SAS. However, under low R:FR, the active phyB inactivates, which results in PIFs accumulation and/or activation. This causes rapid changes in the expression of dozens of *PHYTOCHROME RAPIDLY REGULATED (PAR)* genes (Roig-Villanova and Martínez-García 2016), activating a transcriptomic cascade (**Fig 2**). All these components form a regulatory network important for the implementation of the shade-regulated responses.

Genetic analyses indicate that most PIFs play a role as positive regulators of the hypocotyl elongation, like PIF4, PIF5, and PIF7 act early in the phytochrome signaling pathways to promote the SAS by inhibiting auxin repressor (Leivar, Tepperman et al. 2012) (Lorrain, Allen et al. 2008, Jia, Kong

et al. 2020). In addition, under shade with high intensities of PAR, PIF-mediated auxin production is primarily responsible for SAS, whereas under shade with low PAR, PIF4 and PIF5 increase the sensitivity of plants to auxin (Hersch, Lorrain et al. 2014). Arabidopsis plants PIF quartet (PIFQ: PIF1, PIF3, PIF4 and PIF5) and PIF7 promote SAS by upregulating the transcription of *YUCCA* (*YUC*) genes, encoding enzymes which control a rate-limiting step of auxin biosynthesis (Müller-Moulé, Nozue et al. 2016, Zhou, Zhang et al. 2018), and participate in regulating other two growth hormones: gibberellins (GAs) and brassinosteroids (BRs) (Jaillais and Vert 2012). Therefore the defective mutants *pifq* (loss of function in PIF1, PIF3, PIF4 and PIF5) and *pif7* (loss of function in PIF7) plants produce short petioles and display a reduced response to shade (Hornitschek, Kohnen et al. 2012, Xie, Liu et al. 2017).

3.1.2 Activated PIFs induce the expression of growth-related genes

Related the PAR factors, genetics indicates that several of them act as negative (like LONG HYPOCOTYL IN FAR RED1 (HFR1), PAR1/HELIX LOOP HELIX 1 (PAR1), PAR2 and PIF3-LIKE1 (PIL1)) or positive (like PIF sub-family) SAS regulators. As negative regulators, they dimerize with the HLH domain of PIF proteins, and the resulting heterodimers are not functional in DNA-binding, hence preventing PIFs from interacting with the promoters of their target genes to inhibit the growth (Roig-Villanova, Bou-Torrent et al. 2007). These negative regulators of SAS responses, whose expression is promoted by plant shade or proximity, generate a negative feedback that has been proposed to reduce the strength of the elongation responses, acting as a gas-and-brake mechanism for control of the SAS responses (Ruberti, Sessa et al. 2012). By contrast, regulators, PIFs, whose stability but not expression is increased by simulated shade, act as positive players that promote cell growth and regulate expression of some PAR genes, such as HFR1 and PIL1 (Lorrain, Allen et al. 2008, Hornitschek, Kohnen et al. 2012, Leivar, Tepperman et al. 2012, Zhang, Mayba

et al. 2013). On the other hand, ELONGATED HYPOCOTYL5 (HY5), a member of the bZIP transcription factor family, which is a SAS negative regulator. In some cases, HY5 was shown to inhibit the function of PIFs by directly competing for binding to G-boxes in target gene promoters (Favero 2020). Besides, the growth repressing DELLA proteins were found to interact directly with transcriptional regulators PIF3 and PIF4 to control the expression of growth-promoting genes and activate SAS responses (Hauvermale, Ariizumi et al. 2012). Also auxin, which is the dominant SAS physiological regulator, is activated by PIF proteins through the TAA1/SAV3 pathway and accumulates in low R:FR light (Sairanen, Novák et al. 2012).

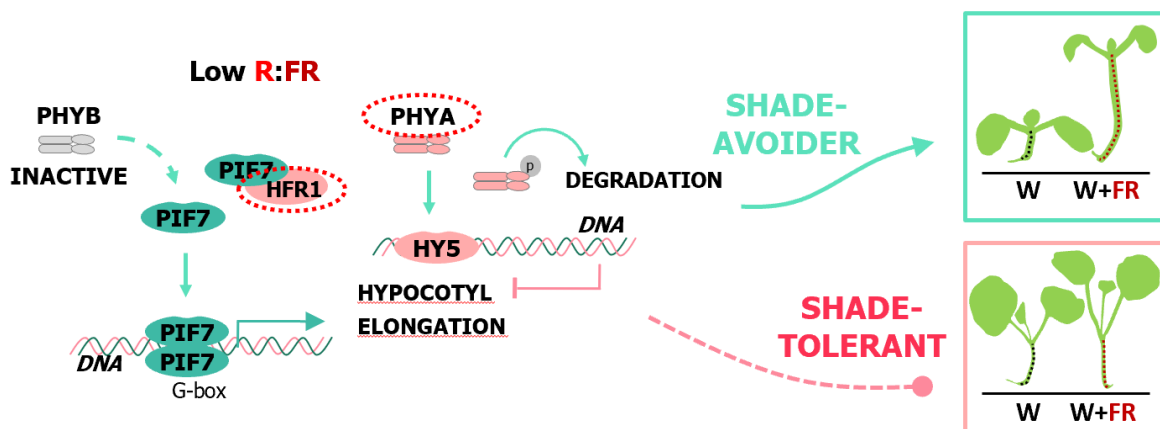


Figure 2. Phytochromes and PIFs are important actors in the shade signaling cascade. Phytochromes sense the presence of nearby vegetation by detecting reductions in the R:FR. Under low R:FR, hypocotyl elongation is modulated by PIF-induced signaling cascades. HFR1 and HY5 operate as negative modulators. Shade avoider plants *A. thaliana* and shade tolerant plants *C. hirsuta* have different strategies for responding (Pierik and Testerink 2014, Sheerin and Hiltbrunner 2017).

3.2 Cryptochrome: blue light receptors

When actual shading happens, the light absorption due to chlorophylls present in above photosynthetic tissues specifically depletes sunlight in R and B wavelengths. Therefore, plants growing below a vegetation canopy are exposed to low B. This light conditions can cause a shade avoidance-like response, which is mainly dependent on cryptochrome (CRY) photoreceptors, with PIF4 and PIF5 play supporting roles (Casal 2013, Pedmale, Huang et al. 2016). In *A. thaliana* and other plants there are two genes encoding CRYs, *CRY1* and *CRY2*. *CRY1* is light-stable, whereas *CRY2* is light labile and only acts in low B. Different from the phytochromes, low B-induced phenotypes involve the interaction of *CRY1* with SUPPRESSOR OF PHYTOCHROME A 1 (*SPA1*) (Holtkotte, Ponnu et al. 2017), *SPA1* proteins bind CONSTITUTIVELY PHOTOMORPHOGENIC 1 (*COP1*). In addition, *CRY1*-*SPA1* interaction complex affects some *COP1*-targeted transcription factors by function with E3 ubiquitin ligase involved in protein degradation (Pierik and de Wit 2014). Thereby *CRY1*-*SPA1* inhibits *SPA1*-*COP1*, *COP1* targets can be accumulated in low B, such as the growth-promoting bZIP transcription factor *HY5* (Liu, Zuo et al. 2011, Lu, Zhou et al. 2015). And some published results have indicated that *A. thaliana* seedlings show enhanced hypocotyl elongation in low B environment even stronger than under low R:FR (Djakovic-Petrovic, Wit et al. 2007), this has been confirmed also in other species as well, like tobacco (Pierik and de Wit 2014) and *Stellaria longipes* (Sasidharan, Chinnappa et al. 2008). Because the reduction of B wavelengths does usually occur in nature combined with low R:FR, the phytochrome- and cryptochrome-mediated light signaling interact in the control of shade avoidance to enhance the elongation responses. This enhancement likely occurs through suppression by B-mediated depletion of negative SAS regulators, such as *HFR1* and *HY5*, which are also induced by low R:FR conditions (de Wit, Keuskamp et al. 2016).

3.3 Perception of UV-B

UV-B (290–315 nm) is another light waveband which also gets depleted in shade condition. UV-B RESISTANCE 8 (UVR8) is the photoreceptor that senses UV-B. It regulates downstream growth-regulating components in *A. thaliana*, such as HY5 and HY5 HOMOLOGUE (HYH). UVR8 interacts with the E3 ubiquitin ligase COP1 domain, promoting accumulation of HY5/HYH and degradation of GA, leading to suppress elongation growth (Cloix, Kaiserli et al. 2012). UV-B also can inhibit hypocotyl elongation by repressing PIF4 transcript accumulation (Hayes, Sharma et al. 2017). As a consequence, UV-B depleted by neighboring plants absorption under shade condition can de-repress elongation growth and induce SAS.

4. Variety of plant strategies to vegetation proximity

4.1 Different response at seedling stage

Responses to vegetation proximity or plant canopy shade are generally referred to as the SAS and involve different types of growth and development changes. The differences between phenotypic output and photoreceptor signaling determine whether seedlings have adopted a shade-avoidance or shade-tolerance strategy (Gommers, Visser et al. 2013). Hypocotyls, cotyledons and primary leaves have been most commonly studied for checking how plant seedlings respond to shade. By analysis in *A. thaliana*, under simulated shade, plants outgrow the neighbors to avoid light shortages by promoting elongation of organs, like hypocotyls, which is regulated in part by the interaction of active phytochromes with the PIFs, then resulting in rapid changes in the expression of *PAR* genes to implement of the SAS responses (Martinez-Garcia, Galstyan et al. 2010). For example, when shading, phytochromes conversion from active Pfr to inactive Pr, PIF4 and PIF5 are rapidly degraded. Analysis of *A. thaliana pif4pif5* double mutant found that

under low R:FR the hypocotyl elongation was reduced compared to wild-type seedlings, suggesting a functional overlap between these two PIFs. Similarly, under shade condition, the photostable PIF7 transcription factor is dephosphorylated and regulates auxin biosynthesis, thereby promoting hypocotyl elongation (Hersch, Lorrain et al. 2014). On the contrary, shade-tolerant species usually lack the promotion of elongation growth in response to shade, their hypocotyls do not elongate and have developed a variety of traits to acclimate to low R:FR conditions. Both types of species perceive shade in the same way and there is even overlap in some aspects of the response, it is conceivable that some regulatory components are shared between shade avoidance and shade tolerance (Gommers 2016), like PIFs, which were identified as positive players of the hypocotyl SAS response. In addition, proteins of the bHLH family also known to play important roles in regulating SAS responses, such as HFR1, which is a putative bHLH class transcription factor involved in light signaling, but identified as negative players of the hypocotyl SAS response (Sessa, Carabelli et al. 2005). In *C. hirsuta*, higher activity and stability of HFR1 protein interaction with PIF7 results in reduced elongation responses in hypocotyls when exposed to low R:FR (Paulišić, Qin et al. 2021). If these SAS antagonizing proteins are more strongly induced in shade tolerant plants compared with shade avoiders, this would indeed suppress SAS. Those strong factors in shade-tolerant species would mean that a relatively large pool of PIF proteins would be kept from binding to their target promoters, which would suppress shade avoidance (Gommers, Visser et al. 2013). PhyA is another negative regulator of the SAS response, which represses shade-induced elongation growth in seedlings under very low R:FR conditions, causing *A. thaliana phyA* mutant seedlings to show exaggerated hypocotyl elongation in low R:FR (Martínez-García, Gallemí et al. 2014). Consequently, elevated levels of phyA protein would inhibit shade-avoidance

responses. In the shade-tolerant *C. hirsuta*, it has been shown that phyA signaling was enhanced when compared with *A. thaliana*, which caused by an increase in *PHYA* expression (Molina-Contreras, Paulišić et al. 2019).

Moreover, different strategies of plants in response to shade also lead to differences in chlorophyll fluorescence parameters, which can also reflect the degree of environmental influence on plant photosynthetic apparatus. Fv/Fm is an indicator of damage in the photosynthetic apparatus or abiotic stress in leaves (Rascher, Liebig et al. 2000). Shade avoiders, like *A. thaliana* seedlings, usually induce the levels of photosynthetic pigments in order to increase light absorption and to cope the light shortage (Lichtenthaler, Kuhn et al. 1982).

4.2 Different response in adult plants

Flowering time, petiole elongation and leaf expansion have been most commonly studied for checking how adult plants respond to shade. Shade avoiders, usually accelerate flowering, elongate stems and petioles, promote apical dominance and hyponasty (upward movement of the leaves) and reduce branching (Botto and Smith 2002) to ensure species survival. By contrast, some species, which we will refer to as shade-tolerant, have adapted to cope permanently with shaded environments, such as canopy shade, where it is impossible to outgrow the tall neighboring trees. Therefore, typical shade-tolerant species suppress several typical shade-avoidance traits (for instance, shade-induced promotion of elongation growth).

The suppression of the shade-induced elongation response in shade-tolerant species may be caused through by the interaction between several hormones, like auxin, GAs and BRs, they are all important in the regulation of SAS. The growth-related pathways which are induced by shade might be affected by the activity of components in different species. For example, a lack of PIN-FORMED 3 (PIN3)-mediated auxin transport pathway specifically in the hypocotyl would prevent auxin accumulation and hypocotyl elongation under

low R:FR conditions (Keuskamp, Pollmann et al. 2010). In addition, differences in targets will lead to altered induction or repression of hormonal responses, as PIF4 and PIF5 can modify promoters by modulating the expression of auxin signaling components, which then regulate auxin responsiveness (Hornitschek, Kohnen et al. 2012). Alao, GA is another hormone required to promote SAS (Kamiya and García-Martínez 1999). GA regulates leaf changes and maintains them unfolding, which is also suppressed in shade-tolerant species, however, enhancing GA alone did not improve petiole elongation in *A. thaliana*, suggesting that there may be other factors in GA regulation that determine its ability to induce SAS (Djakovic-Petrovic, Wit et al. 2007, De Lucas, Daviere et al. 2008).

5. Additional conditions related with shade signaling

5.1 Dark-Induced Senescence (DIS) on leaves

Leaves are specialized photosynthetic organs, and plants invest a lot of energy and nutrients in the production of leaves. After a period of photosynthetic production, the leaf's photosynthetic contribution to the plant decreases, and the leaf then enters the final stage of its development: senescence (Quirino, Noh et al. 2000). Leaf senescence is an active developmental program in which large metabolic shifts occur aimed at ensuring nutrient remobilization from dying leaves to sink tissues. The senescing programmed is sustained by sequential changes in gene expression (Buchanan-Wollaston et al., 2005). Thereby, the degradation and recycling of nutrients from senescent leaves is a highly regulated process. The onset and timing of leaf senescence are affected not only by endogenous factors (i.e., ageing) but also by environmental cues (i.e., biotic or abiotic stresses) that are sensed and integrated by plants to reprogram their development (Munné-Bosch, 2008). Ultimately, leaf senescence culminates in the degradation of cellular

components, starting by the chloroplasts, where 70% of the leaf proteins are located and which configures the largest reservoir of recoverable nitrogen (Kamranfar et al., 2018).

As mentioned above, environmental changes can also trigger leaf senescence. One of these changes is light-deprivation that, in *A. thaliana*, results in leaf dark-induced senescence (DIS) of the leaf or the whole seedlings. DIS depends on the intensity and wavelength of the available light. As leaves constitute the photosynthetic factories of the plant, darkening them leads to accelerated senescence, which is considered an adaptive response towards extreme shading to secure reproduction (Trejo-Arellano et al., 2020). While darkening individual leaves leads to DIS only to the affected organ, darkening young seedlings might also lead them to enter in DIS (Brouwer, Ziolkowska et al. 2012). DIS is known to be a PIF-dependent process, where PIF4 and PIF5 are its main executors (Liebsch and Keech, 2016). Consistently, *A. thaliana pifq* mutants (deficient in the PIF quartet, PIFQ - PIF1, PIF3, PIF4, and PIF5) present a delayed DIS phenotype (Sakuraba et al., 2014). It is known that PIFs accumulate upon darkness, due to the inactivation of phyB, which is the major suppressor of DIS in *A. thaliana* (Sakuraba et al., 2014). This connection between DIS and PIF activity led to the finding that shade-tolerant plants (in contrast with shade-avoider ones) can extend their survival upon total darkness for several days, likely because of their attenuated PIF activity (Paulišić, Qin et al. 2021) (**Fig 3**).

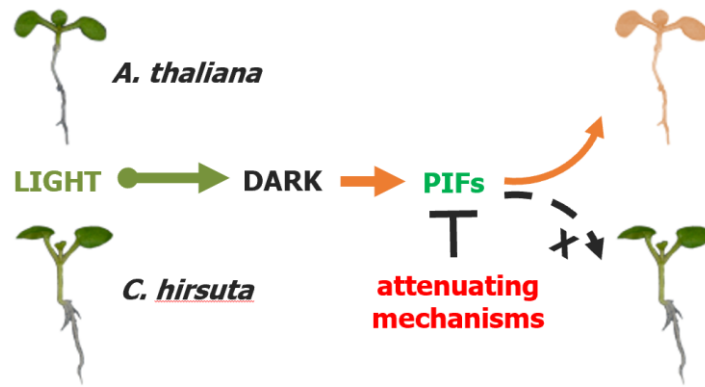


Figure 3. Comparison of PIF-modulated DIS responses in *A. thaliana* and *C. hirsuta* seedlings (Paulišić, Qin et al. 2021).

5.2 Thermal-Induced Morphogenesis (TIM)

Temperature is a major environmental cue that influences the distribution and seasonal responses of plants. Thermal-Induced Morphogenesis (TIM) refers to the effect of warm temperature, which means the temperature increases of over 5 °C above the normal temperatures. The regulation of plant structure is one of the most prominent thermos adaptive features. Plants grown in warm temperatures exhibited accelerated flowering, elongated stems and leaf hyponasty. Hypocotyl elongation is a key morphogenetic trait that is strongly influenced by light and temperature conditions. It has reported that the hypocotyl elongation in response to warm temperature and low R:FR both share regulatory mechanisms in *A. thaliana*. These environmental cues also result in elongated petioles, narrow leaves and early flowering (Koini, Alvey et al. 2009, Stavang, Gallego-Bartolomé et al. 2009). And PIFs, including PIF4, PIF5 and PIF7 are also identified as master regulators in regulating warm-temperature induced hypocotyl elongation (Quint, Delker et al. 2016, Paik, Kathare et al. 2017, Paulišić, Qin et al. 2021), deduced from the hypocotyl unresponsiveness to warm temperature of *pif4*, *pif5* and *pif7* mutant plants.

OBJECTIVES

OBJECTIVES

Plants have evolved different strategies to respond to vegetation proximity: avoidance or tolerance. While many aspects of shade avoidance syndrome (SAS) regulation have been described, we are still far from understanding shade-tolerance. The general objective is to understand how shade tolerance regulates genetically and works molecularly. For this purpose, we have focused on two specific objectives:

1. Comparative genetic and molecular analyses of *A. thaliana* and *C. hirsuta*, two closely related species with differing elongation responses to shade. Our goal is to expand the genetic map of the components that regulate the shade tolerance strategy. Specifically, we will explore the molecular basis that sustains the differences in HFR1 activity from these two species. In addition, we will produce HY5 and PIF7 loss-of-function mutants in *C. hirsuta* to explore next how these components work in different species to either regulate avoidance or tolerance to shade.
2. Identification of novel molecular components involved in the control of PIF-based shade avoidance or shade tolerance habit. To this goal, we will first analyze the association between SAS, Thermal-Induced Morphogenesis (TIM) and Dark-Induced Senescence (DIS), three PIF-regulated processes. Using this information, we next will establish a genetic screening to identify and characterize *A. thaliana* mutant plants with a shade tolerance phenotype.

CHAPTER I

Title: Molecular basis of shade tolerance: the role of PIF7 and HY5 in *Cardamine hirsuta*

Wenting Qin^{1,2}, Sandi Paulisic², Jaime F. Martinez-Garcia^{1,2}

¹Institute for Plant Molecular and Cell Biology (IBMCP), CSIC-UPV, 46022-València, Spain

²Centre for Research in Agricultural Genomics (CRAG), CSIC-IRTA-UAB-UB, Cerdanyola del Vallès, 08193-Barcelona, Spain.

1. Introduction

Arabidopsis thaliana is a shade avoider species. As such, it typically displays a suite of traits and responses to adapt growth and development as a way to “escape” from shade, so-called globally the shade avoidance syndrome (SAS), a set of acclimation responses triggered upon low R:FR exposure. In this species, SAS responses include a delayed germination, the stimulation of plant elongation to overgrow neighbors, an accelerated flowering to ensure the next generation, a reduction of the levels of the photosynthetic pigment to adjust the photosynthetic rate as well as an upward leaf movement (hyponasty) to gain as much light as possible and the inhibition of branching to save more resources for reproductive growth (Ballaré and Pierik 2017). Consequently, resources are reallocated away from leaves and into promoting growth, to position leaves in higher, better-lit strata of the canopy. This physiological stress state intends to optimize light absorption, however, it inevitably limits plant yield and modifies plant architecture as it carries within a decrease in the photosynthetic capacity and in the biomass generation (Murchie, Pinto et al. 2009). Moreover, when high R:FR is detected by phytochromes (i.e., when the shading has ceased), there is a very fast response targeted towards suppressing the SAS, which is altering plant development to ensure survival in resource-limiting conditions. Thus, phytochromes have a main role in the shade response signaling and allow to rapidly switch plant growth according to light cues: they implement a coordinated response to divert resources from biomass production into improve resilience.

From the five phytochromes existing in *A. thaliana*, phyA and phyB are the most important ones in controlling SAS plant responses. Also, those shade-responses can be easily studied at the seedling stage by examining hypocotyl elongation. *Cardamine hirsuta*, an *A. thaliana* relative, is a shade-tolerant species whose hypocotyls are unresponsive to plant shade (Molina-Contreras, Paulišić et al. 2019). Besides, it adopts other physiological and metabolic responses to be able to thrive under limiting light conditions, such as an attenuated reduction of the photosynthetic pigment levels and, very likely, a highly conservative resource utilization. These responses configure additional

shade-tolerance mechanisms in *C. hirsuta* to optimize the net carbon gain, consistent in an efficient balance between CO₂ assimilation, accumulation in the form of organic molecules, and employment of these generated resources (Molina-Contreras, Paulišić et al. 2019). We use *C. hirsuta* as a model to study divergent hypocotyl responses to shade by performing comparative analysis with *A. thaliana*.

Previous research in our group has focused on understanding the molecular and genetic differences that cause the divergent shade-induced elongation between *A. thaliana* and *C. hirsuta*. This led to the conclusion that the lack of shade-induced elongation in *C. hirsuta* is caused by increased levels and/or activity of phyA and HFR1, two SAS regulators known to repress shade-induced elongation in *A. thaliana*, attenuated activity of the repressor of SAS in high R:FR phyB, and an attenuated activity of the SAS positive regulators PHYTOCHROME INTERACTING FACTORS (Molina-Contreras, Paulišić et al. 2019, Paulišić, Qin et al. 2021). In addition, we have also established that an enhanced HFR1 activity further reduces the already lower PIF molecular activity. Therefore, our working hypothesis is that the acquisition of suppressing mechanisms of the SAS is partly due to the enhanced action of repressive components and the reduction of positive components. Thus, other responses regulated by PIFs might be accordingly associated with shade tolerance, such as HY5 or PIF7.

2. Result

2.1 The increased HFR1 abundance in *C. hirsuta* is due to differences in interaction with COP1

2.1.1 ChHFR1 VP peptide had a weaker interaction with COP1 than AtHFR1

By utilizing stably transgenic plants producing ChHFR1 and AtHFR1 at comparable levels under the control of the same promoter (from AtHFR1, pAtHFR1), we observed that the ChHFR1 protein was more stable than AtHFR1, resulting in a higher activity of ChHFR1 compared to its orthologue

AtHFR1. In addition, ChHFR1 protein is more abundant than AtHFR1 also when transiently expressed to comparable levels in *Nicotiana benthamiana* leaves, which indicates that the higher abundance of ChHFR1 is an intrinsic property of the protein that resides in its primary structure (Paulišić, Qin et al. 2021). As known, light- and shade-regulated degradation of AtHFR1 requires binding to COP1 and the associated E3 ubiquitin ligase activity, this binding results in protein ubiquitination, which directs HFR1 for degradation via the 26S proteasome (Jang, Yang et al. 2005, Pacín, Semmoloni et al. 2016). Hence, we wanted to know whether the increased stability of ChHFR1 was due to differences in interaction with COP1 compared with AtHFR1. COP1-interacting proteins harbor sequence-divergent Val-Pro (VP) motifs that bind the COP1 WD40 domain with different affinities (Lau, Podolec et al. 2019). After checking the COP1 WD40 – AtHFR1 complex structure (Lau, Podolec et al. 2019) and compared the primary structure of both HFR1 proteins, we concluded that sequence differences in the COP1 interaction domain between AtHFR1 and ChHFR1 likely map to their N-terminus (VP domain) (**Fig 1A**). We hypothesized that the sequence variations between the VP domain of these HFR1 species may result in different COP1 binding affinities, affecting targeting and subsequent degradation of the two HFR1 orthologues. We thus quantified the interaction of synthetic AtHFR1 and ChHFR1 VP peptides with COP1 WD40 domain by estimating the dissociation constant (k_D) using microscale thermophoresis (MST). We are in collaboration with the group of Michael Hothorn (Geneva University, Switzerland) for this experiment. The k_D is a measure of the affinity between two partners in the binding equilibrium and also describes the interaction between them. Comparing the binding strength of various ligands to a binding partner is an important metric of the interaction strength. Binding curves (concentrations of bound ligand vs ligand concentration) (**Fig 1B**) help to calculate k_D : the lower the k_D the higher the affinity between the interacting partners (Eble 2018). The results showed that AtHFR1 VP peptide bound the COP1 WD40 domain with a k_D of $\sim 120 \mu\text{M}$ (**Fig 1B and Fig 2 AB**). The ChHFR1 VP peptide showed a weak binding to COP1 WD40, with a k_D of $\sim 2 \text{mM}$ (**Fig 1B and Fig 2 CD**). A second potential VP

domain present in both HFR1 proteins (that was identical between them) did not bind to COP1 WD40, indicating that the differences in k_D values are mostly due to the varied sequences of the VP peptide. By contrast, the previously identified *A. thaliana* cryptochrome 1 (AtCRY1) and human HsTRIB1 VP sequences did bind to COP1 WD40 domain with a binding affinity in the 1 μ M range, in agreement with previous data obtained using isothermal titration calorimetry binding assays (**Fig 1B and Fig 2 EF**) (Lau, Podolec et al. 2019). Taken together, AtHFR1 VP peptide had a stronger interaction with COP1 WD40 than ChHFR1, implying that AtHFR1 may be a better substrate for COP1 than ChHFR1.

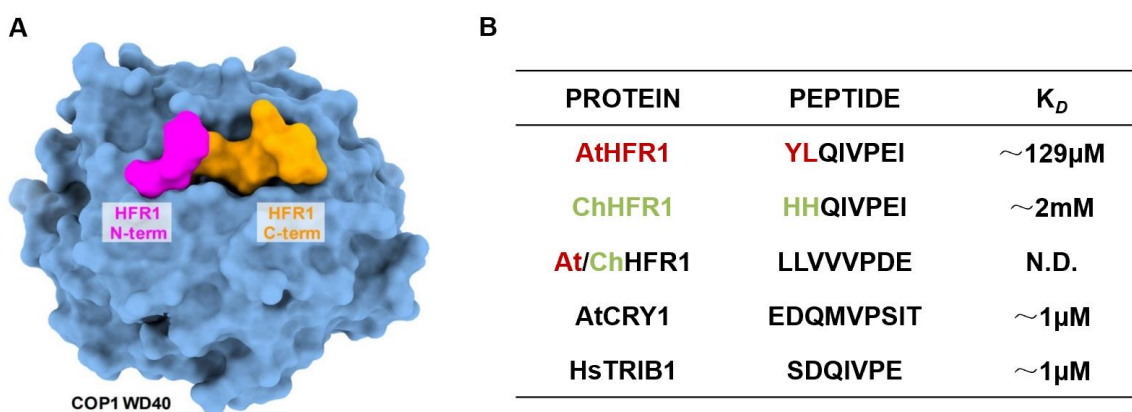


Figure 1. AtHFR1 interacts more strongly than ChHFR1 with the WD40 domain of COP1. **(A)** Overview of the COP1 WD40-AtHFR1 complex. The COP1 WD40 domain and the AtHFR1 VP peptide are shown in surface representation and colored in blue and orange, respectively. The N-terminus of HFR1 VP peptide, the amino acid of which differs between AtHFR1 and ChHFR1, is highlighted in magenta. **(B)** Table summaries of the microscale thermophoresis binding assay. The sequence of the respective synthetic peptides is indicated.

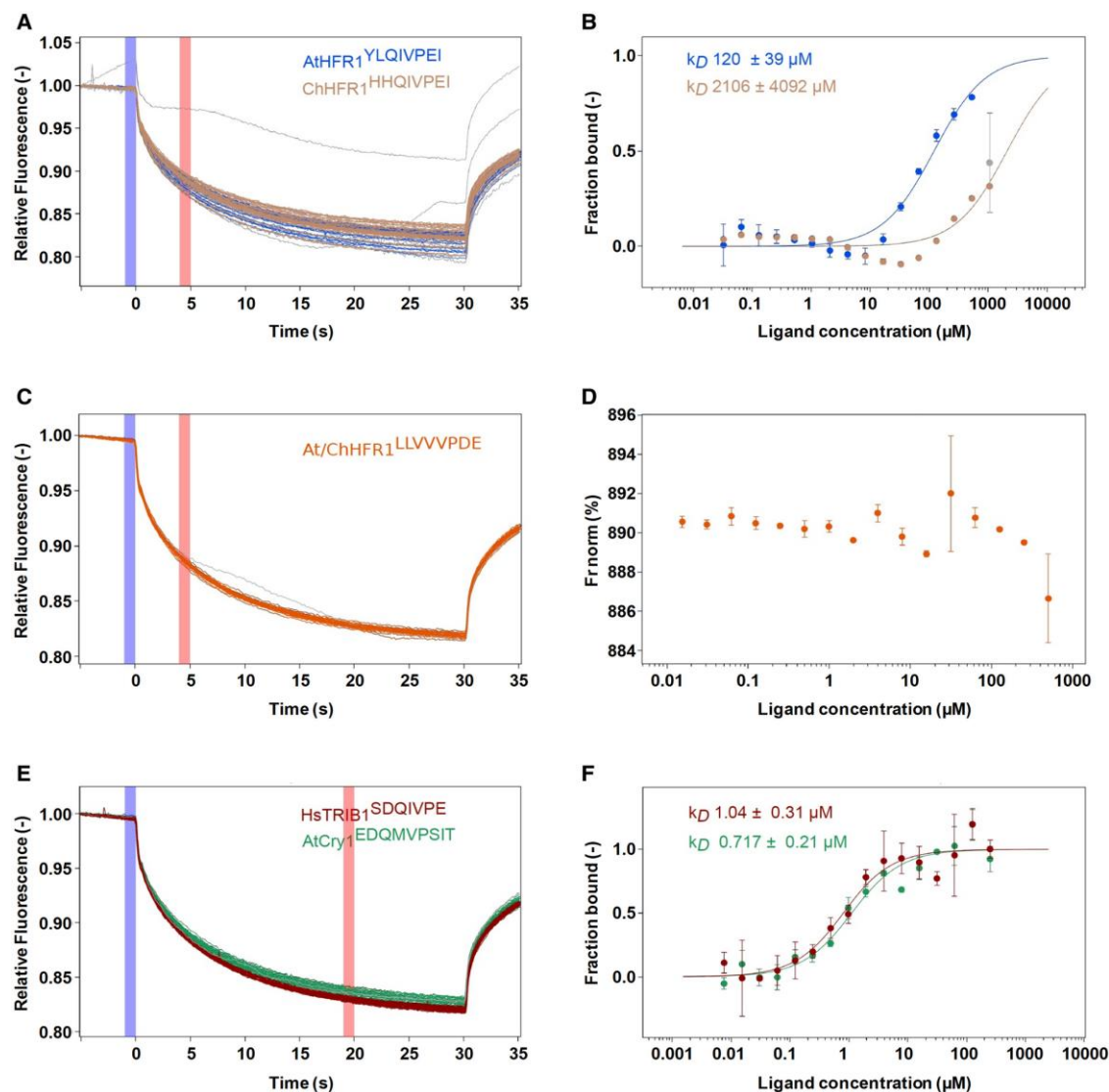


Figure 2. Microscale thermophoresis (MST) experimental traces and analysis. The concentration of AtCOP1 WD40 is fixed at 0.15 μM mixed with 16 serially diluted peptide concentrations at 1:1 ratio. **(A)**, **(C)**, and **(E)** show the normalized MST traces. The blue box area illustrates the fluorescence before activation of the infrared (IR) laser and red box area illustrates average fluorescence after activation of the IR laser. Average values \pm SD (error bars) were subsequently used for fluorescence normalization. k_D fit displaying fraction bound as a function of ligand concentration is shown in adjacent right panels **(B)**, **(D)**, and **(F)**. **(A)** Raw MST traces for AtHFR1 (in blue) and ChHFR1 (in light-brown) VP peptides. Individual concentrations that showed slight aggregation or precipitation are shown in gray and were excluded from the k_D fit calculation. **(B)** Fitted data over a concentration range from 0.032 to 500 μM

for AtHFR1 VP (blue dots) and 0.032 to 1,000 μM for ChHFR1 VP (light-brown dots) were used to derive the corresponding dissociation constant k_D . **(C)** Raw MST traces for At/ChHFR1 VP peptide (in orange). One concentration that showed slight precipitation or aggregation is shown in gray. A concentration range of 0.0154 to 506 μM was used for the At/ChHFR1 VP. **(D)** No k_D was determined, as no binding between COP1 WD40 and the At/ChHFR1 VP peptide (orange dots) was detected. **(E)** A concentration range from 0.0076 to 250 μM for HsTRIB1 (in red) and AtCRY1 (in green) peptides was used. Raw MST traces show no aggregation or precipitation effects during this binding. One AtCRY1 VP outlier is shown in gray. **(F)** The k_D for HsTRIB1 (brown dots) and AtCRY1 (green dots) VP peptides was calculated using the normalized traces.

2.1.2 VP regions determine the different stability of HFR1 orthologue proteins

The results of the last section revealed that changes in the interactions AtHFR1-COP1 and ChHFR1-COP1 could contribute to explain the observed differences in abundance (Paulišić, Qin et al. 2021). Following that, we wanted to see if the changes in COP1 affinity had an impact on the subsequent accumulation of the AtHFR1 and ChHFR1 proteins. To investigate this possibility, we created chimeric *HFR1* genes in which the VP region was swapped, which we designated as *ChHFR1** and *AtHFR1** (**Fig 3A**). *ChHFR1** differed from *ChHFR1* in the VP region, that was substituted for the AtHFR1-VP region. Reciprocally, *AtHFR1** contained the ChHFR1-VP region. All these *HFR1* derivatives were fused to the 3x Hemagglutinin (3xHA) tag and placed under the control of the 35S promoter. In addition, a *GREEN FLUORESCENT PROTEIN (GFP)* gene, which was driven by another 35S promoter, located after the 3xHA tag and was used for normalization (**Fig 3A**). We agroinfiltrated *N. benthamiana* leaves to transiently overexpress these genes in leaves. Following agroinfiltration, the plants were then grown under long-day photoperiods. Samples (leaf circles collected from infiltrated regions) were harvested 3 days later. The results showed that ChHFR1 protein was more stable than AtHFR1, as reported (Paulišić, Qin et al. 2021). When the VP

regions were exchanged, ChHFR1* was now significantly less abundant than ChHFR1. Conversely, AtHFR1* was significantly abundant than AtHFR1. These results indicated that the VP regions contain enough information to determine the stability of the resulting HFR1 protein (**Fig 3B**). Because AtHFR1-VP domain binds to COP1 WD40 domain with higher affinity than ChHFR1-VP domain, these results indicate a negative correlation of the binding affinity to COP1 with the protein accumulation (the higher the affinity with COP1 WD40 domain, the lower the accumulation). Hence, we concluded that in the HFR1 context, a stronger binding to COP1 results in lower abundance.

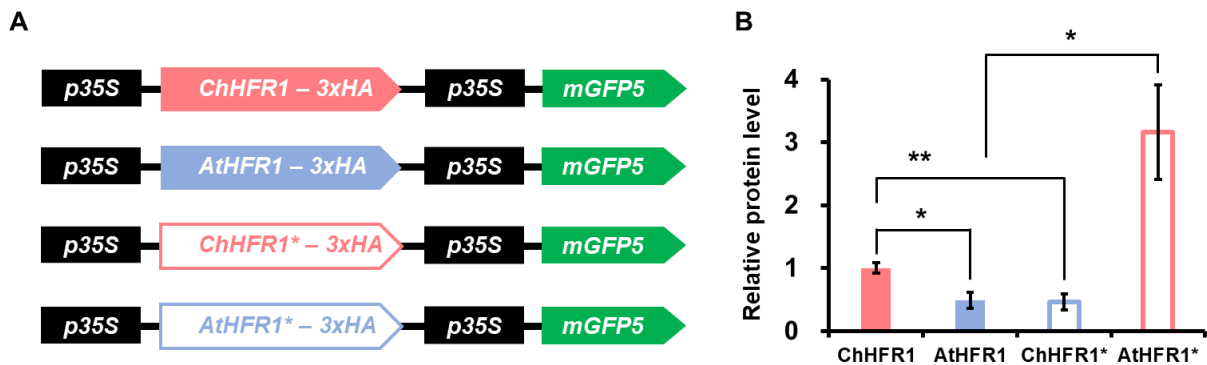


Figure 3. VP regions determine the stability of HFR1 protein. **(A)** Cartoon of constructs containing ChHFR1, AtHFR1, ChHFR1* and AtHFR1* derivatives under the 35S promoter used for transient expression of transgenes in tobacco leaves. A 35S:*GFP* gene cassette was also included to normalize HFR1 levels. **(B)** Relative HFR1 protein levels, normalized to the GFP levels, are the means \pm SE of four independent biological replicates. Asterisks mark significant differences (student's t-test: *P-value < 0.05, **P-value < 0.01) between the indicated pairs.

2.1.3 Other regions participate in conferring differences in HFR1 stability

The very high abundance of AtHFR1* protein in our assays (**Fig 3B**) suggested that other parts of the HFR1 proteins (in addition to the COP1-interacting domain) participate in conferring differences in stability between these two proteins. To further study this possibility, we prepared new HFR1

derivatives in which we exchanged the whole N-terminal domains between AtHFR1 and ChHFR1, which we designated as *ChHFR1* Δ and *AtHFR1* Δ (**Fig 4A**). *ChHFR1* Δ differed from *ChHFR1* in the C-terminal domain, that was substituted for the AtHFR1 C-terminal region. Reciprocally, *AtHFR1* Δ contained the ChHFR1 C-terminal region, all of which were fused to the 3xHA tag, placed under the control of the 35S promoter and subcloned into a binary vector, as in the previous experiment (**Fig 4A**). As before, we transiently express these constructs in *N. benthamiana* leaves. The quantification results showed that, as expected, ChHFR1 is more abundant than AtHFR1. However, the ChHFR1 Δ chimeric protein (the one with the N-terminal region of ChHFR1 fused to the C-terminal half of AtHFR1) was not detected; in contrast, the AtHFR1 Δ protein (with the N-terminal region of AtHFR1 and the C-terminal region of ChHFR1) was easily detected and even more abundant than ChHFR1 (**Fig 4B**). These results suggested that, in addition to the VP domain in the N-terminal region of HFR1, there are other residues and/or motives in the rest of the protein (N-terminal or C-terminal regions) that have a strong impact in the stability of HFR1 protein.

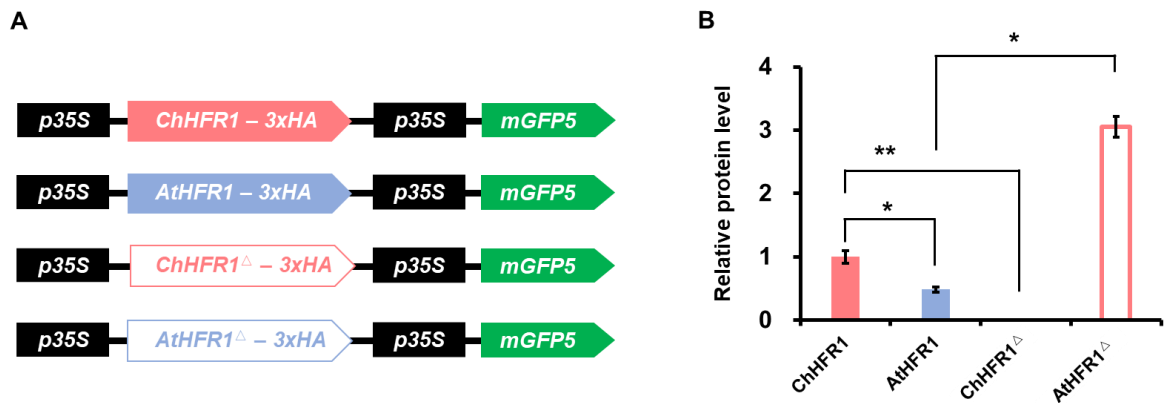


Figure 4. Other regions participate in conferring differences in HFR1 protein stability. **(A)** Cartoon of constructs containing ChHFR1, AtHFR1, ChHFR1 Δ and AtHFR1 Δ derivatives under the 35S promoter used for transient expression of transgenes in *N. benthamiana* leaves. A 35S:*GFP* gene cassette was also included to normalize HFR1 levels. **(B)** Relative HFR1 protein levels,

normalized to the GFP levels, are the means \pm SE of four independent biological replicates. Asterisks mark significant differences (student's t-test: *P-value < 0.05, **P-value < 0.01) between the indicated pairs.

2.2 HY5 and PIF7 both are required for shade tolerance habit of *C.*

hirsuta

2.2.1 Plasmid construction and mutant identification

Plasmids to edit *ChHY5* and *ChPIF7* genes were prepared by CRISPR (Clustered Regularly Interspaced Short Palindromic Repeat)-Cas9 (CRISPR-associated) system. First, we selected two different short RNA molecules (20 bp sequence) to act as guide RNAs for the associated endonuclease Cas9 in both genes (*ChHY5* and *ChPIF7*). Each plasmid targets two different but close sites within each gene, one under the control of the U3 promoter and the other the U6 promoter (**Fig 5A**). In both genes, one of the target sequences is unique for *C. hirsuta* whereas the other one is identical in both *C. hirsuta* and *A. thaliana* genes (**Fig 5B**). These gene cassettes were finally placed in a binary vector containing also the information to express them in plants together with the associated endonuclease Cas9. The resulting plasmids (already available in the laboratory when I joined the project) were named pSP106 and pSEP4, targeting *ChPIF7* and *ChHY5*, respectively. These plasmids were used to transform *Agrobacterium tumefaciens* strain C₅₈C₁ (pGV2260) to proceed with the transformation of *C. hirsuta* plants via floral dipping.

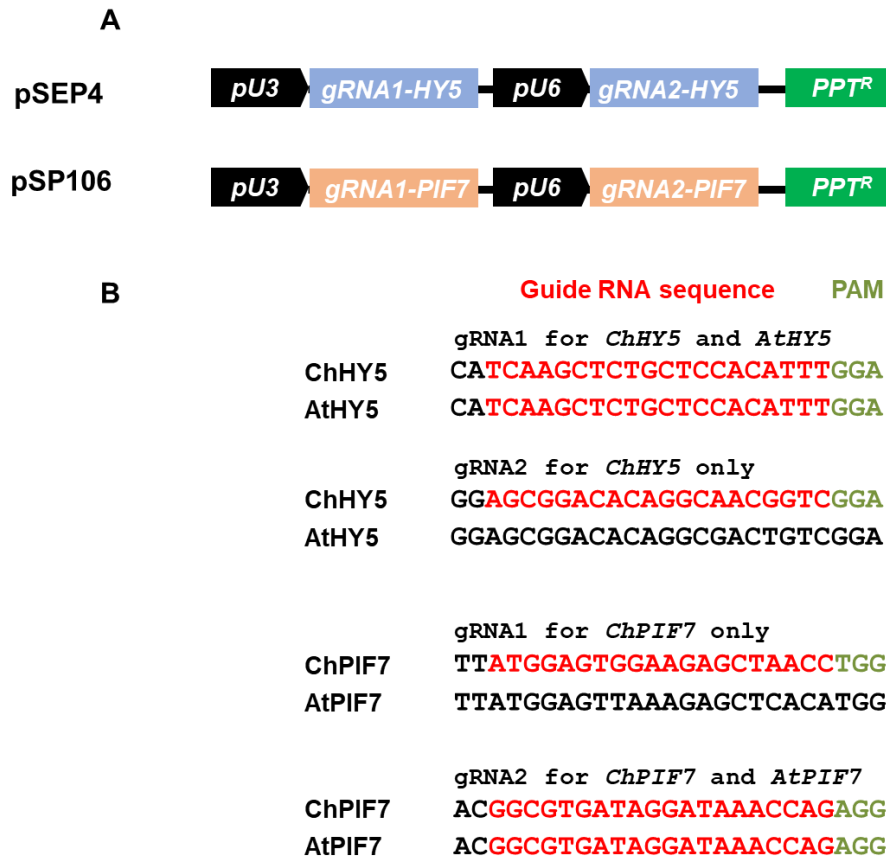


Figure 5. CRISPR/Cas9 system-induced mutation detection in *C. hirsuta* and *A. thaliana*. **(A)** Plasmids pSP106 and pSEP4 were obtained to knock out *ChPIF7* and *ChHY5* genes, respectively. The gRNA1 is under the control of the U3 promoter and gRNA2 is the U6 promoter. Both are L-phosphinothricin (PPT) resistant. **(B)** Targeted mutagenesis with gRNA1 and gRNA2 for *ChHY5* (top) and *ChPIF7* (bottom). The target sequences are indicated in red and the protospacer adjacent motif (PAM) sites are shown in green. The corresponding sequence in the *A. thaliana* orthologue gene is shown below.

As wild-type *C. hirsuta* seedlings are unresponsive to W+FR, we decided to transform *sis1* (phyA deficient) mutant plants, whose hypocotyls strongly elongate in response to W+FR (Molina-Contreras, Paulišić et al. 2019). In this background, we expected that seedlings deficient in *PIF7* would displayed an attenuated hypocotyl elongation under W+FR. Therefore, we transformed *C. hirsuta sis1-1* plants with pSP106 plasmid. After identifying several T1

transgenic seedlings based on their resistance to (PPT), we next selected in the T2 generation which have only 1 T-DNA insertion. We searched in the descendants of these lines individuals that showed a certain level of suppression of the *sis1* phenotype when grown under simulated shade (**Fig 6**). As expected, wild-type seedlings did not elongate in response to W+FR, whereas *sis1-1* seedlings showed a strong elongation under W+FR. Seedlings of the various selected lines showed a wild-type (#041), mild (e.g., line #031) or strong (e.g., line #032) reduction in their shade-induced hypocotyl elongation. This phenotype is consistent with our expectations.

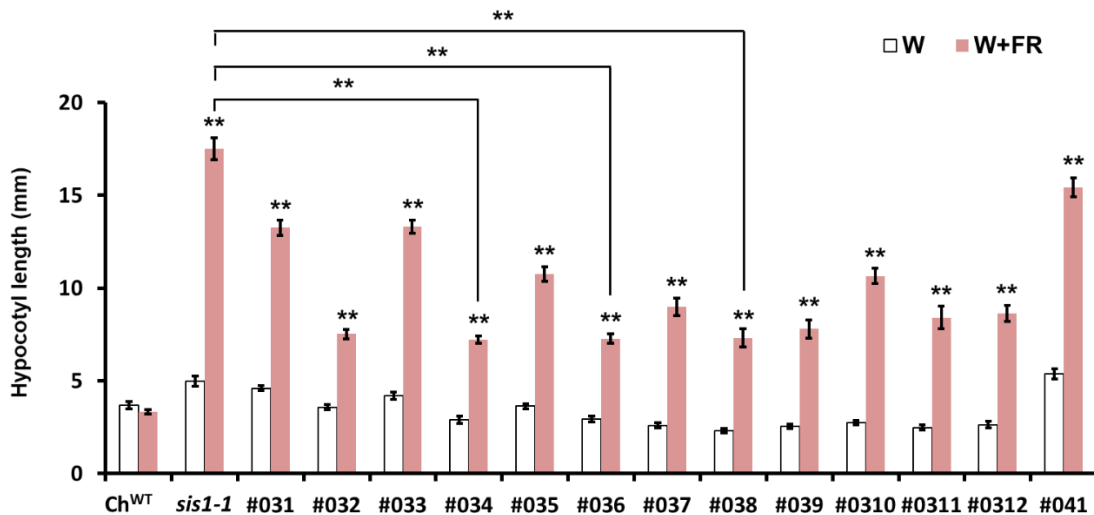


Figure 6. Measurements of length hypocotyls of *chpif7sis1-1* double mutant lines in W light and in W+FR. Seedlings were grown 3 days in W, then transferred to W+FR for 4 days more. Values are the means \pm SE of four independent biological replicates. Asterisks mark significant differences (student's t-test: *P-value < 0.05, **P-value < 0.01) between W light and W+FR, or the indicated pairs in W+FR.

Next, using specific oligos (**Table S3**) we PCR amplified the genomic *ChPIF7* of some of the #03 lines showing the most attenuated response to W+FR (lines #032, #034, #035, #036 and #038) and sequenced them. We

observed that all these lines had a mutation in the *ChPIF7* gene either an insertion in the gRNA1 region (lines #032, #034 and #035) or a deletion in the gRNA2 region (lines #032, #035, #036 and #038) (**Fig S1**), which confirms that these plants are *ChPIF7* mutants. In view of these results, we finally selected 3 different lines (#034, #036 and #038), which include 3 different mutations of PIF7 and have clear suppression of hypocotyls in shade condition in *sis1-1* background. We renamed these mutant lines as *chpif7-1* (#036, 7 nucleotides deletion in gRNA2), *chpif7-2* (#038, 1 nucleotide deletion in gRNA2) and *chpif7-3* (#034, an A nucleotide insertion in gRNA1) (**Fig 7A**). These lines were crossed with Ch^{WT} to get single mutants of *ChPIF7* in a wild-type *SIS1* background. None of the three single *chpif7* mutant seedlings responded to simulated shade (**Fig 7B**). When comparing the deduced protein sequence of all three mutant lines with that of wild-type PIF7, the frame shifts introduced resulted in the loss of the nuclear localization signal (NLS), the bHLH (basic helix-loop-helix) and Q-rich (glutamine-rich) domains. These regions have been shown as necessary for nuclear localization, dimerization and DNA binding, and to modulate the transcriptional activity of PIF7 in vivo (Leivar, Monte et al. 2008). The *chpif7-3* allele is the only one that has changed the APB (active phyB binding) domain, which does mediate the binding of PIF7 to phyB Pfr (Khanna, Huq et al. 2004) (**Fig 8**).

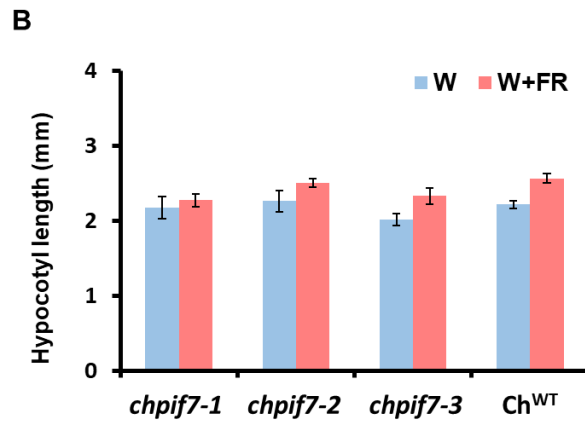


Figure 7. Molecular characterization and length hypocotyls of *chpif7* mutants in *C. hirsuta*. **(A)** The sequences of three identified *chpif7-1*, *chpif7-2* and *chpif7-3* mutants; *chpif7-1* has 7 nucleotides deletion at the position 557 of the ChPIF7 ORF (from the start codon ATG); *chpif7-2* has 1 nucleotide deletion at the position 558 of the ChPIF7 ORF; *chpif7-3* has an insertion of 1 nucleotide at the position 30 of the ChPIF7 ORF. These changes lead to a frame shift and a premature stop codon. **(B)** Measurements of length hypocotyls of *chpif7* mutant lines in W light and in W+FR. Seedlings were grown 3 days in W, then transferred to W+FR for 4 days more. Values are the means \pm SE of three independent biological replicates. Asterisks mark significant differences (student's t-test: *P-value < 0.05, **P-value < 0.01) between W light and W+FR.


```

                APB domain
Ch_PIF7 MSNYGVEELTWENGQLTVHGLGDEVVPTTSNNPIWTQSLNGCETLESVVHQALQQPSKL
chpif7-1 MSNYGVEELTWENGQLTVHGLGDEVVPTTSNNPIWTQSLNGCETLESVVHQALQQPSKL
chpif7-2 MSNYGVEELTWENGQLTVHGLGDEVVPTTSNNPIWTQSLNGCETLESVVHQALQQPSKL
chpif7-3 MSNYGVEELNLGKWAINSWSRR-----

Ch_PIF7 QQLQQNPNGPNHNYETKDGSCSRKRGYPQEMDRWFSVQEDSHRVGHSVTASASGTNMSWA
chpif7-1 QQLQQNPNGPNHNYETKDGSCSRKRGYPQEMDRWFSVQEDSHRVGHSVTASASGTNMSWA
chpif7-2 QQLQQNPNGPNHNYETKDGSCSRKRGYPQEMDRWFSVQEDSHRVGHSVTASASGTNMSWA
chpif7-3 -----

Ch_PIF7 SFESGRSLKTARTGDRDYIRSGSETQDTEGDEQETRGEGRSNGRRGRAAAIHNESERKR
chpif7-1 SFESGRSLKTARTGDRDYIRSGSETQDTEGDEQETRGEGRSNGRRGRAAAIHNESERKR
chpif7-2 SFESGRSLKTARTGDRDYIRSGSETQDTEGDEQETRGEGRSNGRRGRAAAIHNESERKR
chpif7-3 -----

                NLS/bHLH domain
Ch_PIF7 RDRINQRMRTLQKLLPTATKADKVSILDDVIEHLKQLQAQVQFMSLRANLPQQQMMIPQL
chpif7-1 RDRINK-----
chpif7-2 RDRINNRG-----
chpif7-3 -----

                Q-rich domain
Ch_PIF7 PPPQSVLTIQQHQQQQQQQQQQQFQMSLFATMARMGMGGGNAFGGLVPTPPPPPLMVP
chpif7-1 -----
chpif7-2 -----
chpif7-3 -----

Ch_PIF7 SLPNRDCTNGSSADPYSVFLAQTMNMDLYNKMAAAIYRQQSDQNTKVNTGMPSSSSNHEK
chpif7-1 -----
chpif7-2 -----
chpif7-3 -----

Ch_PIF7 RD-----
chpif7-1 -----
chpif7-2 -----
chpif7-3 -----

```

Figure 8. Multiple sequence alignments of ChPIF7 proteins from wild-type and the three *chpif7* mutant lines identified in this work. Yellow highlight: the amino acid residue related to APB domain. Green highlight: the amino acid residue related to NLS/bHLH domain. Grey highlight: the amino acid residue related to Q-rich domain. The amino acid residue with red color is not exactly the same as in wildtype sequences.

To get the mutant lines deficient in *HY5*, *C. hirsuta* wild-type plants were transformed with the pSEP4 plasmid. As before, after identifying several T1 transgenic seedlings (as PPT resistant, that were named pWQ1 lines), we next selected lines in the T2 generation which have only 1 T-DNA insertion. Based on the phenotype of *A. thaliana hy5* mutant seedlings (slightly longer hypocotyls in W and much longer hypocotyls under W+FR than Ch^{WT}), we screened and

selected in the descendants of these lines, which seedlings showing long hypocotyl phenotypes when grown under simulated shade. After propagating these plants, we analyzed the hypocotyl elongation response of shade. The wild-type seedlings elongated as we expected in W and W+FR, whereas some seedlings of pWQ1 lines, such as pWQ1.01 to pWQ1.09, showed very long hypocotyls in both W and W+FR conditions (**Fig S2**). These seedlings were selected, then using specific oligos (**Table S3**) we PCR amplified the genomic *ChHY5* of some of the those lines showing the most enhanced response to W and W+FR (lines pWQ1.01, pWQ1.02, pWQ1.03, pWQ1.05, pWQ1.06, pWQ1.07) and sequenced them. As a result, we found that all the selected lines had mutations in the *ChHY5* (**Fig 9A**).

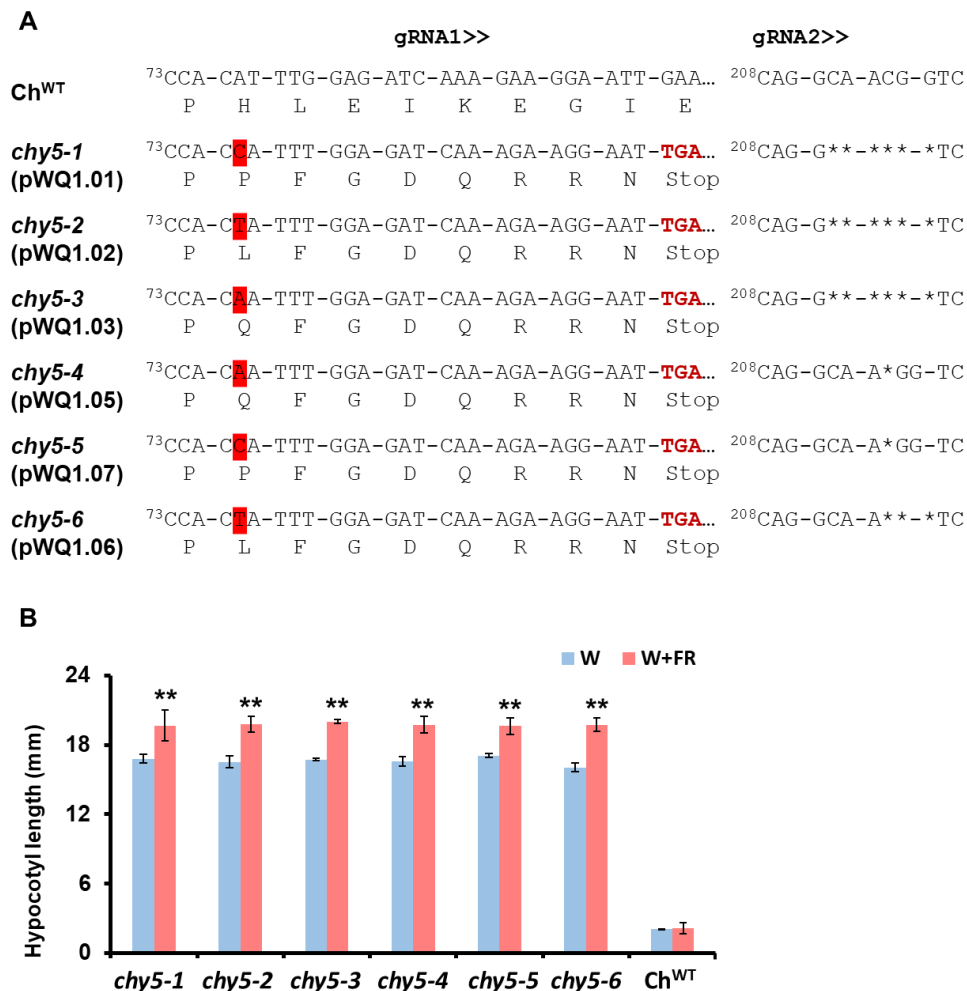


Figure 9. Molecular characterization and length hypocotyls of *chy5* mutants in *C. hirsuta*. **(A)** The sequences of six identified *chy5-1*, *chy5-2*, *chy5-3*, *chy5-4*,

chy5-5 and *chy5-6* mutants; *chy5-1*, *chy5-2* and *chy5-3* have an insertion of 1 nucleotide (*chy5-1* has a C insertion, *chy5-2* has a T insertion and *chy5-3* has an A insertion) at the position 77, and 6 nucleotides deletion at the position 212 of the ChHY5 ORF; *chy5-4* and *chy5-5* have an insertion of 1 nucleotide (*chy5-4* has an A insertion and *chy5-5* has a C insertion) at the position 77, and 1 nucleotide deletion at the position 215 of the ChHY5 ORF; *chy5-6* have a T insertion at the position 77, and 3 nucleotides deletion at the position 215 of the ChHY5 ORF. These changes lead to a frame shift and a premature stop codon. **(B)** Measurements of length hypocotyls of *chy5* mutant lines in W light and in W+FR. Seedlings were grown 3 days in W, then transferred to W+FR for 4 days more. Values are the means \pm SE of three independent biological replicates. Asterisks mark significant differences (student's t-test: *P-value < 0.05, **P-value < 0.01) between W light and W+FR.

Sequencing revealed that we got 6 different mutant alleles of *ChHY5*, that had 1 nucleotide (nct) insertion in the gRNA1 region and 1-6 nct deletion in the gRNA2 region. These alleles were named *chy5-1* to *chy5-6* (**Fig 9A**). When we checked their phenotypes in shade, we observed that all *chy5* mutants have very long hypocotyls in both W and W+FR conditions when compared to Ch^{WT} (**Fig 9B**). Then by checking the protein sequence, there only 3 differences in amino acid composition between these six mutant alleles of *ChHY5* (**Fig 10**). The insertion in the gRNA1 region causes a frameshift that introduces an early stop codon in all cases, making all the likely loss-of-function mutations. Among these lines, these changes result in the loss of the COP1-interaction domain (**Fig 10**), that has been reported is essential for HY5 degradation in the dark in *A. thaliana* (Hardtke, Gohda et al. 2000), and the basic and ZIP domains, important for their DNA-binding activity, loss of function of these domains results in an inability to mediate protein translocation and dimerization (Sib ril, Doireau et al. 2001). Together, these results indicate that *C. hirsuta* HY5 has a role in maintaining short hypocotyls in W and W+FR. In addition, it also participates in repressing the shade-induction of the hypocotyl in this species. ChPIF7 attenuates the shade-induced hypocotyl elongation in a phyA-deficient (*sis1*) background but not in a wild-type background.

	COP1-interaction domain	
ChHY5	MQEQATSSLAASSLPSSSERSSSS	APHLEIKEGIESDEEIRRVPFEGGEAAGKETSGRES
<i>chy5-1</i>	MQEQATSSLAASSLPSSSERSSSS	SAPFPFGDQRRN -----
<i>chy5-2</i>	MQEQATSSLAASSLPSSSERSSSS	SAPLFGDQRRN -----
<i>chy5-3</i>	MQEQATSSLAASSLPSSSERSSSS	SAPQFGDQRRN -----
<i>chy5-4</i>	MQEQATSSLAASSLPSSSERSSSS	SAPQFGDQRRN -----
<i>chy5-5</i>	MQEQATSSLAASSLPSSSERSSSS	SAPFPFGDQRRN -----
<i>chy5-6</i>	MQEQATSSLAASSLPSSSERSSSS	SAPLFGDQRRN -----
	Basic domain	
ChHY5	GSATGQERTQATVGETQ	RKRGRTPAEKENKRLKRLLRNRVSAQQARERKKAYLSELENRV
<i>chy5-1</i>	-----	-----
<i>chy5-2</i>	-----	-----
<i>chy5-3</i>	-----	-----
<i>chy5-4</i>	-----	-----
<i>chy5-5</i>	-----	-----
<i>chy5-6</i>	-----	-----
	Zip domain	
ChHY5	KDLENKNSELEEKLSTLQENQMLRHI	LKNTTGNKRGGGGGSNADASL
<i>chy5-1</i>	-----	-----
<i>chy5-2</i>	-----	-----
<i>chy5-3</i>	-----	-----
<i>chy5-4</i>	-----	-----
<i>chy5-5</i>	-----	-----
<i>chy5-6</i>	-----	-----

Figure 10. Multiple sequence alignments of ChHY5 proteins from wild-type and the six *chy5* mutant lines identified in this work. Yellow highlight: the amino acid residue related to COP1 interaction domain. Green highlight: the amino acid residue related to Basic domain. Grey highlight: the amino acid residue related to Zip domain. The amino acid residue with red color is not exactly the same as in wildtype sequences.

According to the phenotypes, *chy5* seedlings got a dramatic elongation even in W light condition (**Fig 9B**). As a first step in investigating ChHY5 function in *C. hirsuta*, we examined the de-etiolation response of *C. hirsuta* wild-type and *chy5* seedlings in the darkness, phytochromes-absorbing red (R) and far-red (FR) light and cryptochromes-absorbing blue (B) light (**Fig 11A**). As controls, we also included *A. thaliana* wild-type and *hy5* mutant seedlings. When analyzing the *C. hirsuta* de-etiolation response, we observed that the response of Ch^{WT} seedlings to B (**Fig 11B**) and FR (**Fig 11D**) were comparable to that of At^{WT}, whereas significantly less sensitive to R (**Fig 11C**), as it was previously noted (Molina-Contreras, Paulišić et al. 2019). In addition, we noticed that *chy5* seedlings were clearly hyposensitive to all three light

conditions when compared to Ch^{WT}, in agreement with published information for *A. thaliana hy5*. However, *chy5* seedlings were much more hyposensitive to all three lights than *hy5*, as in the lowest intensity of B and R (**Fig 11B and C**), and both FR intensities mutant *chy5* hypocotyls were not significantly shorter to those of dark-grown seedlings (**Fig 11D**), in clear contrast with *A. thaliana hy5* seedlings. It is noteworthy that the cotyledons of *chy5* seedlings are completely open in response to FR (**Fig S3**), indicating that *chy5* seedlings are not completely blind to these wavelengths. These results suggested that light response was affected in *chy5*, and the attenuated cry/phyB/phyA activities or signaling happened in *chy5* seedlings when compared with Ch^{WT}. In addition, HY5-deficiency results in a stronger hyposensitivity to all three monochromatic lights than in wild-type in both *C. hirsuta* and *A. thaliana* although in *C. hirsuta* the HY5 activity is stronger.

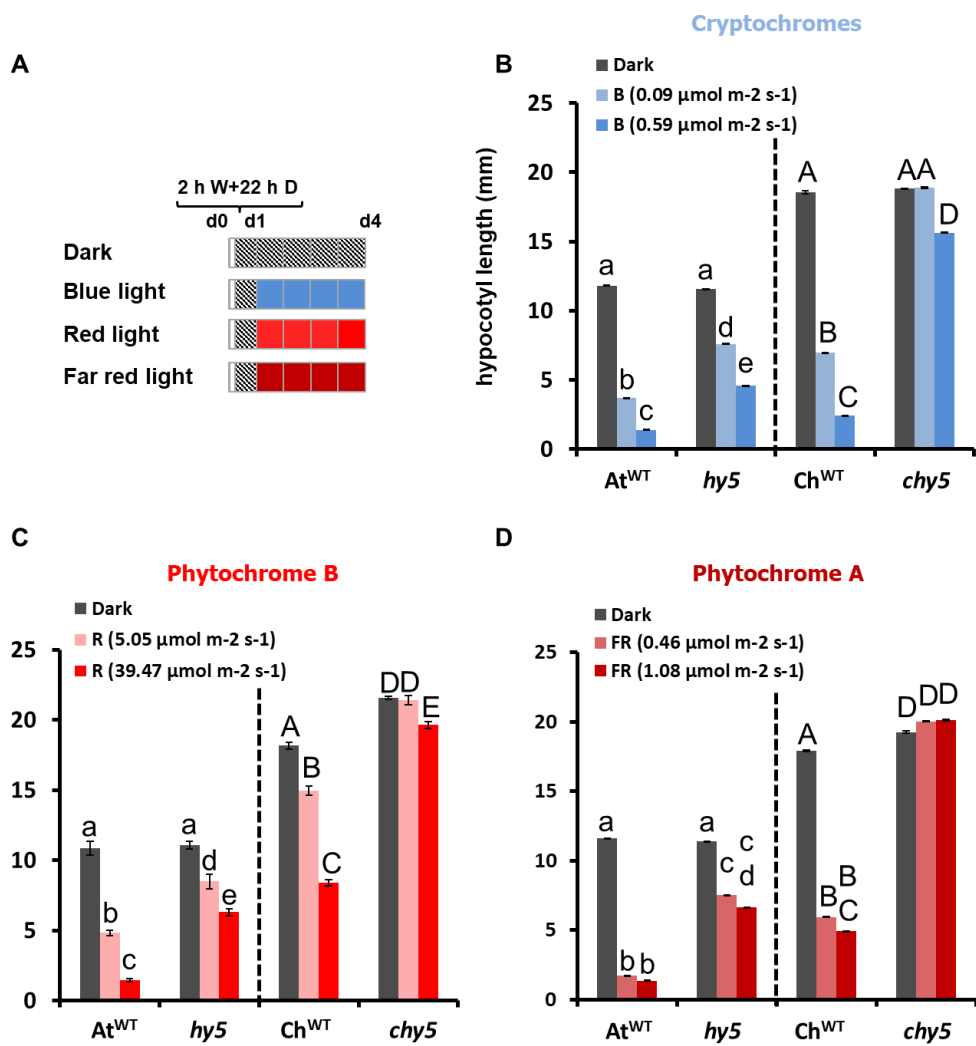


Figure 11. Hypocotyl length of *At*^{WT}, *A. thaliana hy5* (*hy5*), *Ch*^{WT} and *C. hirsuta hy5* (*chy5*) lines in darkness or under different monochromatic lights. **(A)** Cartoon describing the experiment sets up; **(B)** Hypocotyl length under dark and monochromatic blue light (with the light intensity 0.09 $\mu\text{mol m}^{-2} \text{s}^{-1}$ and 0.59 $\mu\text{mol m}^{-2} \text{s}^{-1}$, respectively); **(C)** Hypocotyl length under dark and monochromatic R light (with the light intensity 5.05 $\mu\text{mol m}^{-2} \text{s}^{-1}$ and 39.47 $\mu\text{mol m}^{-2} \text{s}^{-1}$, respectively); **(D)** Hypocotyl length under dark and monochromatic FR light (with the light intensity 0.46 $\mu\text{mol m}^{-2} \text{s}^{-1}$ and 1.08 $\mu\text{mol m}^{-2} \text{s}^{-1}$, respectively). Statistical significance **(B)**, **(C)** and **(D)** were determined using one-way analysis of variance (a-nova) multiple comparisons. Different letters, such as a, b, c, d or A, B, C, D indicate a significant difference (Tukey's multiple comparison test, $P < 0.05$).

2.2.2 ChHY5 protein is more stable than AtHY5

Genetic data suggested that *ChHY5* is more active in repressing elongation growth than *AtHY5*. The amino acid sequence (primary structure) of these two proteins (that have the same number of residues) is very similar, and there are only 3 differences in amino acid composition between them (**Fig 12A**). Although all three are conservative (V-A, S-T and R-K), we aimed to explore if these variations were associated with the observed differences in their biological activities. Next, we sought to see if these differences resulted in changes in protein abundance or stability in the same condition and whether they were affected by shade (i.e., W or W+FR). To do so, we constructed plasmids to transiently express *AtHY5* and *ChHY5* fused to the 3xHA tag, and placed under the control of the 35S promoter. In addition, GFP gene, which was driven by another 35S promoter, located after the 3xHA tag and was used for normalization (**Fig 12B**). We agroinfiltrated *N. benthamiana* leaves, harvested samples, and protein extracts were prepared for quantifying HY5 levels by immunoblot analyses. Protein levels were normalized to the GFP abundance (Paulišić, Qin et al. 2021). In W light, *ChHY5* accumulated at significantly lower levels than *AtHY5*. After W+FR treatment, *ChHY5* abundance was unaffected. By contrast, *AtHY5* levels decreased significantly to those of *ChHY5* (**Fig 12C**). These results suggested that *AtHY5* stability is reduced by shade, whereas that of *ChHY5* is stable in both W light and W+FR conditions. These differences seem to be intrinsic of protein sequence.

Altogether, HY5 and PIF7 have roles in shade-tolerant species. Negative regulator HY5 has higher activity and stability in shade-tolerant species which may help to implement lack of hypocotyl elongation.

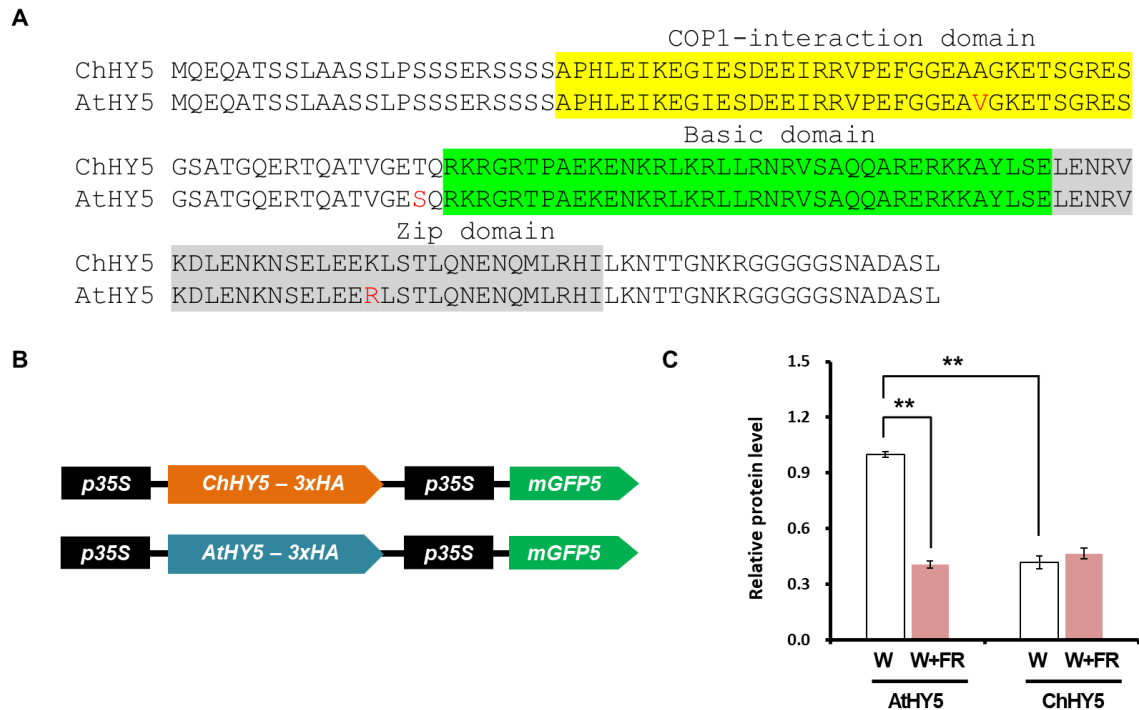


Figure 12. ChHY5 and AtHY5 proteins show different stability in W and W+FR. **(A)** Alignment of ChHY5 and AtHY5 protein sequences. Yellow highlight: the amino acid residue related to COP1 interaction domain. Green highlight: the amino acid residue related to Basic domain. Grey highlight: the amino acid residue related to Zip domain. The amino acid residue with red color in AtHY5 is not exactly the same as in ChHY5 sequences. **(B)** Cartoon representing constructs to transiently express *ChHY5* and *AtHY5* derivatives fused to a 3xHA tag under the 35S promoter in *N. benthamiana* leaves. **(C)** Relative HY5-3xHA protein levels, normalized to GFP protein levels. Values are the means \pm SE of four independent biological replicates. Asterisks mark significant differences (student's t-test: *P-value < 0.05, **P-value < 0.01) between the indicated pairs.

2.2.3 HY5 and PIF7 have less effect on shade-regulated gene expression in *C. hirsuta*

To further investigate the role of HY5 and PIF7 in controlling the shade-induced alterations in gene transcription in *C. hirsuta*, we next conducted RNA sequencing (RNA-seq) experiments. We sequenced the transcriptomes of Ch^{WT}, *chy5-4* and *chpif7-3* seedlings exposed for 0, 1 and 8 h to W+FR (**Fig S1A**). We expected to learn about the transcriptome dynamics on two aspects:

early (0 h vs. 1 h) and late (0 h vs. 8 h) changes after shade treatment and genotype-dependent (Ch^{WT} vs. *chy5* and Ch^{WT} vs. *chpif7* both at 0 h) changes. In addition, the availability of RNA-seq analyses of *A. thaliana* in At^{WT} and *hy5* at the same time points (0, 1, and 8 h) after shade exposure in our laboratory (PhD of Pastor-Andreu 2021) (**Fig 13**) as well as of published *pif7* and the corresponding At^{WT} at 0 and 1 h after shade exposure (Li, Ljung et al. 2012) would also allow us to compare the transcriptomic shade-induced changes between *C. hirsuta* and *A. thaliana* seedlings.

Differentially expressed genes (DEGs) were identified as up- (fold change \geq 1.5, $P < 0.05$) and down-regulated (fold change < 1.5 , $P < 0.05$) after 1 and 8 h of shade treatment compared with 0 h for all three genotypes analyzed. In Ch^{WT} seedlings, 344 and 501 genes were induced after 1 and 8 h of W+FR, respectively. In *chy5* seedlings, 315 genes were induced after 1 h, that rose to 671 after 8 h of W+FR; and for *chpif7* seedlings, 191 genes were induced after 1 h, that rose to 566 after 8 h of W+FR (**Fig 13A**). All together, these results indicated that the number of DEGs in response to simulated shade grew with the time of exposure in the three genotypes analyzed. Regarding the repressed genes, in Ch^{WT} seedlings, 477 and 476 DEGs were repressed after 1 and 8 h of W+FR, respectively. In *chy5* seedlings, 169 genes were repressed after 1 h, that increased to 566 after 8 h of W+FR; and for *chpif7* seedlings, 187 genes were repressed after 1 h, that increased to 486 after 8 h of W+FR (**Fig 13A**). The lower number of rapidly (1 h) repressed DEGs in *chy5* (169) and *chpif7* (187) compared to Ch^{WT} (477) suggested that these two factors have an important role in the rapid shade-modulated repression of gene expression in this species. When comparing our RNA-seq data of *C. hirsuta* with those of *A. thaliana* DEGs (PhD of Pastor-Andreu 2021), the reduced number of DEGs identified in *C. hirsuta* indicated that shade-modulated changes in gene expression are attenuated in this species compared to *A. thaliana* (**Fig 13A**). Overall, shade-modulated changes in gene expression are attenuated in *C. hirsuta* when compared to *A. thaliana*.

Next, we explored the transcriptomic relationships of the different genotypes preparing Venn diagrams of the up- and down-regulated DEGs at 1

and 8 h of W+FR treatment. After 1 h of W+FR, 139 up-regulated genes were shared between Ch^{WT} (out of 344 genes, 71.2 %), *chy5* (out of 315 genes, 77.8 %) and *chpif7* (out of 191, 72.8 %) (**Fig 13B**); and 40 down-regulated genes were shared between them (Ch^{WT} is out of 477 genes, 21.4 %; *chy5* is out of 169 genes, 60.4 % and *chpif7* is out of 187 genes, 21.4 %) (**Fig 13C**). After 8 h of W+FR, 218 up-regulated genes were shared between Ch^{WT} (out of 501 genes, 43.5 %), *chy5* (out of 671 genes, 32.5 %) and *chpif7* (out of 566, 38.5 %) (**Fig 13D**); and 144 down-regulated genes were shared between them (Ch^{WT} is out of 476 genes, 30.3 %; *chy5* is out of 566 genes, 25.4 % and *chpif7* is out of 486 genes, 29.6 %) (**Fig 13E**). More shared genes appear in 8 h of W+FR treatment. These findings suggest that although HY5 and PIF7 have a significant impact on the early shade-regulated changes in gene expression, after 8 hours of W+FR treatment, the transcriptional responses diverge and the influence of HY5 and PIF7 become less important than 1 hour.

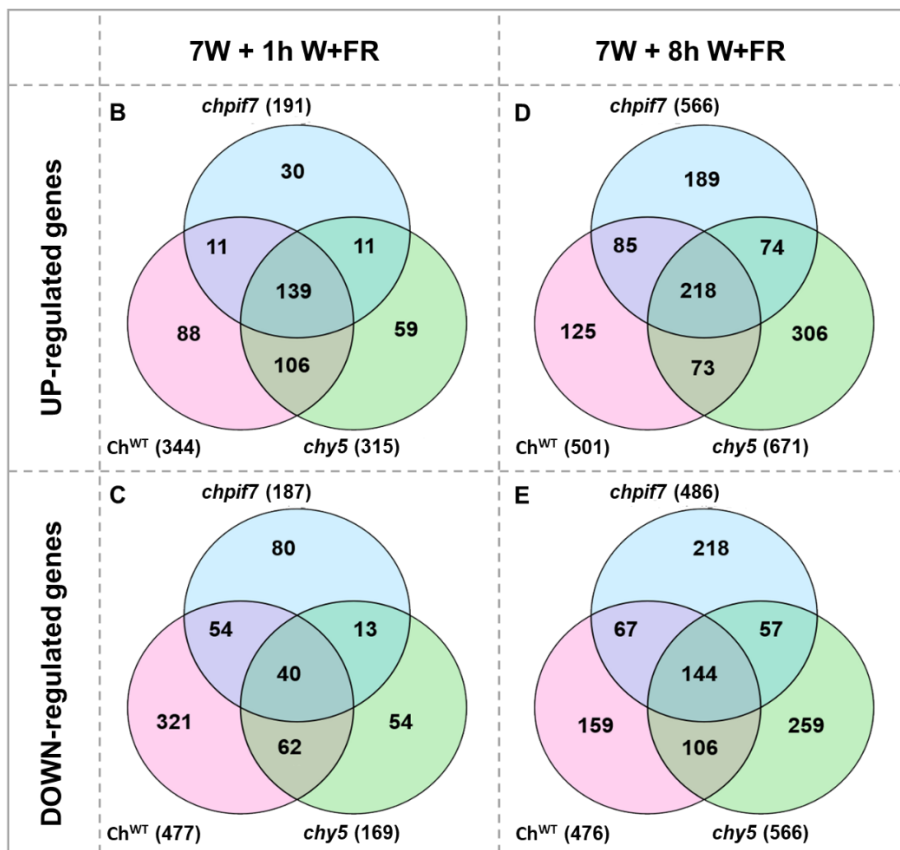
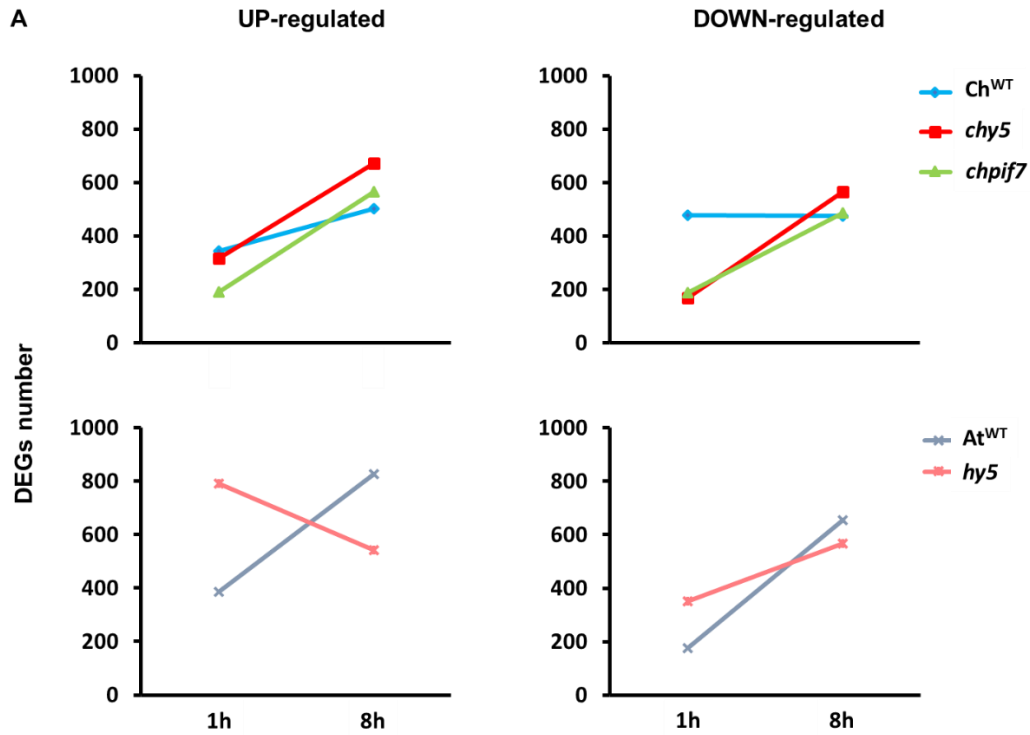


Figure 13. RNA sequencing results show the possible connection between HY5 and PIF7 regulating the shade-induced changes in gene expression. **(A)** Evolution with time (1 and 8 h) of the number of up- and down-regulated DEGs for each genotype. Venn diagram of up- **(B)** and down-regulated **(C)** DEGs at 1 h in each genotype (in parenthesis). Venn diagram of up- **(D)** and down-regulated **(E)** DEGs at 8 h in each genotype.

To make the data comparable with those available in *A. thaliana*, we focused only on those *C. hirsuta* DEGs that have a homologous gene in *A. thaliana* (Hay, Pieper et al. 2014). From a total of 29,458 protein-coding genes (Gan, Hay et al. 2016), only 20,284 (68,85 %) have been found to have an ortholog in *A. thaliana*. In our RNA-seq analyses, between 79.0-89.0 % of the DEGs identified in all genotypes and treatments had an ortholog in *A. thaliana* **(Table 1)**. Because of the high number of orthologous genes found in all samples (at least 79%), we proceeded to do functional GO analysis with them.

Table 1. Number of DEGs in *C. hirsuta* and their homologues in *A. thaliana*.

Name	Shade time	Number of DEGs	Homologous genes	Homologous rate (%)		
UP-regulated genes	Ch ^{WT}	1h	344	302	87.8	
		8h	501	402	80.2	
	<i>chy5</i>	1h	315	279	88.6	
		8h	671	578	86.1	
	<i>chpif7</i>	1h	191	170	89.0	
		8h	566	447	79.0	
	DOWN-regulated genes	Ch ^{WT}	1h	477	402	84.3
			8h	476	392	82.4
<i>chy5</i>		1h	169	144	85.2	
		8h	566	494	87.3	
<i>chpif7</i>		1h	187	164	87.7	
		8h	486	422	86.8	

Regarding the functional predictions, GO terms enrichments were obtained by using agriGO online analyses tool. We observed that DEGs belonged to similar GO terms categories in all genotypes. GO terms from the *light&shade* and *growth* (13 terms), *auxin*, *gibberellin*, *ethylene* and *brassinosteroid* (18 terms) groups were described as enriched in the shade-up-regulated genes in At^{WT} seedlings exposed to 1 or 8 h of W+FR (PhD of Pastor-Andreu 2021). Next, we focused on the p-values obtained from the GO enrichment analyses as an indication of the number of genes found in each genotype that are involved in a biological process: the lower the p-value, the higher the significance of the enrichment.

All 13 GO terms related to *light&shade* and *growth* were found as significantly enriched in Ch^{WT} seedlings after 1 h in shade (**Table 2**). Most of them were also found in At^{WT}, and in *HY5*-deficient seedlings of *A. thaliana* (*hy5*) or *C. hirsuta* (*chy5*) grown in the same conditions. In all cases, the slightly higher p-values indicated that less genes contributed to these GO terms in these various genotypes. In the case of functional predictions involving the 18 hormones-related GO terms (*auxin*, *gibberellin*, *ethylene* and *brassinosteroid*), just 3 appeared as enriched in Ch^{WT} seedlings after 1 h of shade treatment (response to auxin stimulus, GO:0009733; response to gibberellin stimulus, GO:0009739; response to brassinosteroid stimulus, GO:0009741), in contrast with 12 GO terms of the same group that appeared as enriched in At^{WT}. These results indicate that both species are similarly sensitive to shade, whereas *A. thaliana* has stronger response to this condition than *C. hirsuta*. Deficiency of *HY5* had little impact in both species, with similar p-values to those found in the corresponding wild-type seedlings, suggesting that *HY5* likely has a minor role in these functional groups after 1 h of shade exposure in both plant species. Deficiency of *PIF7* had almost no impact on the enrichment of *light&shade* and *growth* related GO terms in *C. hirsuta* (*chpif7*); it had however a strong impact on GO terms associated with hormones, that were significantly enriched only in Ch^{WT} seedlings (**Table 2**). This suggested that *PIF7* is important for responsive to shade condition in *C. hirsuta*. For the comparative analyses with *A. thaliana*, data were taken from other authors, that only analyzed transcriptomic changes (by microarray analyses) after 1 h of W+FR (Li, Ljung et al. 2012). Using these data, less GO terms of these groups (*light&shade*, *growth*, *auxin*, *gibberellin*, *ethylene* and *brassinosteroid*) appeared as significantly enriched in At^{WT}. In *pif7* seedlings, only one term (response to light stimulus, GO:0009416) appeared as significantly enriched, indicating that *PIF7* in *A. thaliana* is may factor to promote growth.

After 8 h of shade treatment, 6 GO terms related to *light&shade* and *growth* were found as significantly enriched in Ch^{WT} seedlings, all of them were also found in At^{WT}, *hy5*, *chy5* and *chpif7*, whereas the functional *growth* related process in early shade exposure only appeared in *A. thaliana*, dissipates after

8 h shade in *C.hirsuta* (**Table 2**), suggesting that only *A. thaliana* grows in response to shade after longer periods of simulated shade. In the case of functional predictions involving the 18 hormones-related GO terms (*auxin*, *gibberellin*, *ethylene* and *brassinosteroid*), just 2 appeared as enriched in Ch^{WT} seedlings after 8 h of shade treatment (response to auxin stimulus, GO:0009733; response to gibberellin stimulus), in contrast with 16 GO terms of the same group that appeared as enriched in At^{WT}. These results indicate that *A. thaliana* has stronger response to this condition than *C. hirsuta*. Deficiency of *HY5* and *PIF7* had little impact in both species or only in *C. hirsuta*, suggesting that all these growth-related processes not rely on the presence of *HY5* and *PIF7* genes to be activated after 1 h and 8 h of shade in both species.

Table 2. Shade-up-regulated genes on the significant GO processes (p-value < 0.05) at short- (1 h) and later- times (8 h) in shade.

		1h shade vs 0h shade						8h shade vs 0h shade					
		Ch ^{WT}	<i>chy5</i>	<i>chpif7</i>	At ^{WT}	<i>hy5</i>	At ^{WT} (<i>Li et al 2012</i>)	<i>pif7</i> (<i>Li et al 2012</i>)	Ch ^{WT}	<i>chy5</i>	<i>chpif7</i>	At ^{WT}	<i>hy5</i>
<i>Light & shade</i>	GO:0009416 response to light stimulus	1.90E-20	4.90E-18	5.20E-18	1.30E-14	9.60E-09		1.10E-09	1.70E-04				
	GO:0009642 response to light intensity	5.30E-15	1.80E-10	6.20E-10	2.70E-03								4.10E-04
	GO:0009637 response to blue light	1.70E-07	8.50E-08	1.90E-09	6.90E-09	2.70E-05							1.10E-10
	GO:0010017 red or far-red light signaling pathway	1.80E-06	1.10E-06	4.60E-11	4.90E-07	4.60E-05							1.80E-09
	GO:0009639 response to red or far red light	3.60E-13	7.70E-14	9.80E-14	2.70E-13	2.20E-09		9.80E-09					5.60E-17
	GO:0010114 response to red light	4.70E-04	3.10E-04										2.40E-05
	GO:0010218 response to far red light	7.10E-07	3.90E-07	3.70E-07	3.60E-06	2.90E-04							3.10E-07
	GO:0009641 shade avoidance	3.10E-11	1.60E-11	5.10E-11	7.00E-09	2.10E-08		1.70E-11					4.80E-08
<i>Growth</i>	GO:0040007 growth	5.10E-06	2.40E-04	4.40E-03	5.10E-09	5.10E-06		4.60E-05				2.50E-07	7.90E-07
	GO:0048589 developmental growth	5.80E-06	1.50E-05	8.40E-04	2.40E-11	4.20E-07		4.00E-05				1.90E-07	7.50E-07
	GO:0060560 developmental growth involved in morphogenesis	2.60E-05	5.10E-04	1.60E-03	2.20E-09	1.50E-05		8.00E-05				1.40E-06	2.30E-05
	GO:0016049 cell growth	1.30E-05	8.40E-04	1.30E-03	3.00E-08	5.70E-06		8.10E-06				7.50E-07	2.30E-06
	GO:0009826 unidimensional cell growth	2.60E-05	5.10E-04	1.60E-03	2.20E-09	1.50E-05		8.00E-05				1.40E-06	2.30E-05
<i>Auxins</i>	GO:0010252 auxin homeostasis				5.40E-06	1.50E-04						1.10E-05	4.00E-06
	GO:0060918 auxin transport				4.80E-05							1.00E-05	3.60E-06
	GO:0009926 auxin polar transport				4.40E-05							2.90E-03	
	GO:0009734 auxin mediated signalling pathway											2.90E-03	
	GO:0009733 response to auxin stimulus	1.40E-29	5.70E-22	1.20E-12	3.50E-48	1.00E-34		2.50E-32				6.20E-33	2.00E-22
<i>Gibberellin</i>	GO:0009685 gibberellin metabolic process				8.50E-05	3.00E-04						3.70E-05	5.30E-05
	GO:0010476 gibberellin mediated signaling pathway				8.50E-05	3.00E-04						2.40E-03	3.80E-04
	GO:0009740 gibberellic acid mediated signaling pathway				2.90E-04	2.30E-03						2.40E-03	3.80E-04
	GO:0009739 response to gibberellin stimulus	7.80E-06	2.90E-05		2.90E-04	2.30E-03			1.70E-03			2.60E-04	1.50E-07
<i>Ethylene</i>	GO:0009693 ethylene biosynthetic process				1.80E-05	4.80E-04						6.60E-06	
	GO:0009692 ethylene metabolic process				1.80E-05	4.80E-04						6.60E-06	
	GO:0009873 ethylene mediated signaling pathway											1.50E-06	1.80E-05
	GO:0010104 regulation of ethylene mediated signaling pathway											2.50E-05	2.40E-06
	GO:0010105 negative regulation of ethylene mediated signaling pathway											1.70E-06	1.60E-07
GO:0009723 response to ethylene stimulus				2.70E-04							8.00E-07	4.20E-05	
<i>Brassinosteroid</i>	GO:0016131 brassinosteroid metabolic process				3.00E-07	1.80E-04						2.40E-03	
	GO:0009742 brassinosteroid mediated signaling pathway											5.30E-05	
	GO:0009741 response to brassinosteroid stimulus	9.30E-06	7.70E-05		3.20E-06	1.50E-03							

Regarding the functional predictions of down-regulated DEGs, we found enrichment in a small number of processes related with *light&shade*, *growth* and *hormones* (**Table 3**). In here, no terms enriched in Ch^{WT}, *chy5* and *chpif7* seedlings after 1 h of shade treatment, in contrast with 5 GO terms that appeared as enriched in At^{WT} and *hy5*. In 8 h shade treatment, there are 2 GO terms enriched in Ch^{WT} and 1 term in At^{WT}; for *chy5*, *chpif7* and *hy5* seedlings, no terms were enriched (**Table 3**). Because of the lower number of GO terms enriched in *C. hirsuta*, it's difficult to get conclusions in general about the specific functions of HY5 and PIF7.

In comparison to Ch^{WT} and its two mutant lines without shade, from the total of GO-terms considered, only 1 GO terms are significantly induced (response to auxin stimulus, GO:0009733) and 3 terms are significantly repressed (response to light stimulus, GO:0009416; response to red light, GO:0010114; response to gibberellin stimulus, GO:0009739) between *chy5* and Ch^{WT}; no terms are induced but also 3 terms are significantly repressed (response to light stimulus, GO:0009416; response to red or far red light, GO:0009639; response to auxin stimulus, GO:0009733) between *chpif7* and Ch^{WT}, still the lower number of GO terms are enriched, so it's difficult to get conclusions in general about the specific functions of these two genes (**Table 4**).

Table 3. Shade-down-regulated genes on the significant GO processes (p-value < 0.05) at short- (1 h) and later- times (8 h) in shade.

		1h shade vs 0h shade					8h shade vs 0h shade				
		Ch ^{WT}	chy5	chpif7	At ^{WT}	hy5	Ch ^{WT}	chy5	chpif7	At ^{WT}	hy5
<i>Light & shade</i>	GO:0009416 response to light stimulus				1.60E-03	1.60E-08					
	GO:0009642 response to light intensity										
	GO:0009637 response to blue light										
	GO:0010017 red or far-red light signaling pathway										
	GO:0009639 response to red or far redlight				2.80E-03	3.70E-05					
	GO:0010114 response to red light						2.00E-04				
	GO:0010218 response to far red light										
GO:0009641 shade avoidance											
<i>Growth</i>	GO:0040007 growth										
	GO:0048589 developmental growth										
	GO:0060560 developmental growth involved in morphogenesis										
	GO:0016049 cell growth										
GO:0009826 unidimensional cell growth											
<i>Auxins</i>	GO:0010252 auxin homeostasis										
	GO:0060918 auxin transport										
	GO:0009926 auxin polar transport										
	GO:0009734 auxin mediated signalling pathway										
GO:0009733 response to auxin stimullus				2.50E-04	2.20E-03						
<i>Gibberellin</i>	GO:0009685 gibberellin metabolic process										
	GO:0010476 gibberellin mediated signaling pathway										
	GO:0009740 gibberellic acid mediated signaling pathway										
	GO:0009739 response to gibberellin stimulus				9.90E-05	8.50E-04	3.10E-04				
<i>Ethylene</i>	GO:0009693 ethylene biosynthetic process										
	GO:0009692 ethylene metabolic process										
	GO:0009873 ethylene mediated signaling pathway										
	GO:0010104 regulation of ethylene mediated signaling pathway										
	GO:0010105 negative regulation of ethylene mediated signaling pathway										
GO:0009723 response to ethylene stimulus				4.00E-05	4.00E-06				1.90E-04		
<i>Brassinosteroid</i>	GO:0016131 brassisteroid metabolic process										
	GO:0009742 brassisteroid mediated signaling pathway										
	GO:0009741 response to brassisteroid stimulus										

Table 4. Up- and down-regulated genes on the significant GO processes (p-value < 0.05) in W light.

		no shade-UP		no shade-DOWN	
		<i>chy5</i> vs Ch ^{WT}	<i>chpif7</i> vs Ch ^{WT}	<i>chy5</i> vs Ch ^{WT}	<i>chpif7</i> vs Ch ^{WT}
<i>Light and shade</i>	GO:0009416 response to light stimulus			1.60E-04	6.10E-08
	GO:0009642 response to light intensity				
	GO:0009637 response to blue light				
	GO:0010017 red or far-red light signaling pathway				
	GO:0009639 response to red or far redlight				3.2E-10
	GO:0010114 response to red light			1.80E-04	
	GO:0010218 response to far red light				
	GO:0009641 shade avoidance				
<i>Growth</i>	GO:0040007 growth				
	GO:0048589 developmental growth				
	GO:0060560 developmental growth involved in morphogenesis				
	GO:0016049 cell growth				
	GO:0009826 unidimensional cell growth				
<i>Auxins</i>	GO:0010252 auxin homeostasis				
	GO:0060918 auxin transport				
	GO:0009926 auxin polar transport				
	GO:0009734 auxin mediated signalling pathway				
	GO:0009733 response to auxin stimullus	6.70E-05			2.9E-15
<i>Gibberellin</i>	GO:0009685 gibberellin metabolic process				
	GO:0010476 gibberellin mediated signaling pathway				
	GO:0009740 gibberellic acid mediated signaling pathway				
	GO:0009739 response to gibberellin stimulus			1.00E-04	
<i>Ethylene</i>	GO:0009693 ethylene biosynthetic process				
	GO:0009692 ethylene metabolic process				
	GO:0009873 ethylene mediated signaling pathway				
	GO:0010104 regulation of ethylene mediated signaling pathway				
	GO:0010105 negative regulation of ethylene mediated signaling pathway				
	GO:0009723 response to ethylene stimulus				
<i>Brassinosteroid</i>	GO:0016131 brassisteroid metabolic process				
	GO:0009742 brassisteroid mediated signaling pathway				
	GO:0009741 response to brassisteroid stimulus				

3. Discussion

Plants have evolved two main strategies to respond to plant shade: avoidance or tolerance (Gommers, Visser et al. 2013). While many aspects of shade-avoidance regulation have been described (Gallemí, Galstyan et al. 2016), we are still far from understanding shade-tolerance. In order to understand how shade tolerance molecularly works, the generation of a range of mutants of the shade-tolerant species *C. hirsuta* has been particularly helpful. In the past, we have identified mutant lines deficient in *ChPHYA* (*sis1* lines), a component shown to negatively regulate this adaptive strategy (Molina-Contreras, Paulišić et al. 2019). As *phyA* was also known to regulate SAS in the shade-avoider *A. thaliana*, we have got a better understanding on how this component works in these two different species to either regulate shade-avoidance or -tolerance: *ChPHYA* has higher activity than *AtPHYA*, and this is achieved by increased *ChPHYA* expression and protein accumulation combined with a stronger specific intrinsic repressor activity (Molina-Contreras, Paulišić et al. 2019).

In the *A. thaliana*, *HFR1* and *HY5* (together with *phyA*) act as SAS negative regulators, whereas *PIF7* acts as a positive regulator of the shade-induced hypocotyl elongation response (Fraser, Hayes et al. 2016). Our genetic and molecular analyses showed that in addition to *phyA*, *HFR1* is also required for implementing shade tolerance in *C. hirsuta* (Paulišić, Qin et al. 2021). We hypothesize that other *A. thaliana* SAS regulators, such as *HY5* and *PIF7*, might also have a role in implementing shade tolerance in *C. hirsuta*. To address this possibility, we produced and characterize *C. hirsuta* mutant plants deficient in *HY5* or *PIF7*. We aimed to test whether *HY5* and *PIF7* can also participate in implementing shade tolerance in this species and explore the mechanisms by which why *ChHFR1* has higher stability and activity than *AtHFR1*.

3.1 COP1-interacting domain controls *At/ChHFR1* stability

Usually light-exposure and COP1-dependent phosphorylation and ubiquitination of the *AtHFR1* protein alters its abundance (Jang, Yang et al. 2005, Yang, Lin et al. 2005, Park, Ding et al. 2008). Shade enhances the

nuclear accumulation of COP1, which is able to directly interact with and polyubiquitinate AtHFR1, causing it to be degraded by the 26S proteasome (Pacín, Legris et al. 2013, Huang, Ouyang et al. 2014, Pacín, Semmoloni et al. 2016). The N-terminal (Nt) half of AtHFR1 possesses two putative COP1 binding sites (VP motifs) (**Fig 1**), but only one of these sites is shown to bind COP1 (Lau, Podolec et al. 2019). Deletion of AtHFR1-Nt resulted in the protein stabilization in both the dark and light conditions (Duek, Elmer et al. 2004), as well as increased biological activity (Jang, Yang et al. 2005, Yang, Lin et al. 2005, Galstyan, Cifuentes-Esquivel et al. 2011), demonstrating the relevance of the COP1-interacting domain in the light-control of AtHFR1 stability. Except 30 amino acids extra in the ChHFR1-Nt and a 9-amino acid insertion in the AtHFR1-C-terminal, the fundamental primary structures of AtHFR1 (Jang, Yang et al. 2005) and ChHFR1, including the putative COP1-interacting domain, are almost identical (Paulišić, Qin et al. 2021). Using peptides corresponding to the VP motif, our MST binding experiment results revealed that ChHFR1 interacts with COP1 weakly than AtHFR1 (**Fig 2A and B**). Importantly, the weak interaction of COP1 and ChHFR1 seems to contribute to its increased stability (and hence biological activity) and ChHFR1 and AtHFR1 proteins change their stabilities when the VP region of both proteins is swapped (**Fig 2C and D**). This suggests that the binding affinity of COP1 for its substrates is a major factor in the stability of the two HFR1 orthologues. However, changes in protein sequences or structures other than the VP motifs might also contribute to the stability of HFR1 orthologues, because the resulting protein AtHFR1* is much more abundant than ChHFR1 (**Fig 2C and Fig 3**). In addition to the VP domain in the N-terminal region of HFR1, there are other residues and/or motives in the rest of the protein (N-terminal or C-terminal regions) also are relevant in the stability of HFR1 protein, because the resulting protein AtHFR1^Δ is much more abundant than AtHFR1, whereas ChHFR1^Δ has no detected levers (**Fig 4**). Altogether, our findings suggest that the stability of HFR1 is influenced by the control of COP1 affinity and it will serve as a mechanism to control global HFR1 activity to modify the adaptability of various plant species to vegetation

proximity and shade. In addition, there still are other parts in the remaining proteins that greatly affect the stability of the HFR1 protein.

3.2 ChPIF7 and ChHY5 have roles in shade tolerance in *C. hirsuta*

C. hirsuta mutant seedlings defective in PIF7 (*chpif7*) showed comparable growth characteristics to wild type plants in both W and shade conditions (**Fig 7B**), but they were able to reduce shade-induced hypocotyl elongation when grown in the *sis1* (phyA-deficient) background rather than in the wild-type background (**Fig 6**). This observation suggests that PIF7 has a negative role in implementing a shade tolerant habit in *C. hirsuta* seedlings, at least in the *sis1* background. In contrast, Loss of HY5 function in *C. hirsuta* (*chy5*) results in a very exaggerated long hypocotyl phenotype, comparable to that of plants defective in the phyB photoreceptor (Molina-Contreras, Paulišić et al. 2019). These lines also show an attenuated response to simulated shade, giving genetic support for the involvement of HY5 in restricting the elongation of the *C. hirsuta* hypocotyls under both W and W+FR conditions (**Fig 9B**). This indicates that HY5 seems to be a component of the process that results in the development of a shade tolerant habit in *C. hirsuta* seedlings.

We already knew that in *A. thaliana*, under shade condition, the inactivation of phyB resulted in enhanced activity of GA biosynthetic enzymes, such as oxidases and ent-kaurenoic acid oxidase (KAO) (De Lucas, Daviere et al. 2008). Furthermore, when phyB is deactivated, the expression of genes encoding GA inactivating enzymes were downregulated, which is a result of the decreased activity of the COP1/SPA substrate HY5 (Feng, Martinez et al. 2008). Thus, the concentrations of bioactive GAs rise, causing the ubiquitination and subsequent proteasomal degradation of DELLA proteins, which in turn promotes PIF activity and eventually increases the length of the hypocotyls (Li, Yu et al. 2016). In *C. hirsuta*, it was previously reported that the decreased phyB activity was associated with increased repressor activity of phyA, which resulted in a significant reduction in the elongation of hypocotyls when wildtype seedlings grown in shade (Molina-Contreras, Paulišić et al. 2019). Based on these observations, it is possible that when HY5 is deficient, the levels of bioactive

GAs are elevated; at the same time, the PIF activity may be boosted by the degradation of DELLA proteins, which results in elongated hypocotyls. It is however unclear why in *C. hirsuta*, HY5 deficiency (*chy5*) results in such a stronger long hypocotyl even in *W*. Analyses of our RNAseq data however, did not provide clues about the molecular causes of these differences, because of the lower number of GO terms enriched (**Table 4**). However, the attenuated phyB activity may still induce other growth-related genes or hormones, such as HY5 and GAs, resulting in no significant change in hypocotyl length in PIF7 deficient seedlings. Moreover, when PIF7 is deficient, the shade-induced auxin levels are lowered, which may attenuate the hypocotyl length in the *chpif7* seedlings in a phyA-deficient (*sis1*) background in shade, resulting in a substantial reduction of the elongation suppression observed in *sis1*.

3.3 ChHY5 and ChPIF7 are less affected by shade

ChHY5 seems to make wild-type *C. hirsuta* seedlings more sensitive to *W* and shade, which is based on the fact that *chy5* seedlings have a very strong long hypocotyl (shade-like) phenotype (**Fig 9B**). In contrast, the role of ChPIF7 promoting shade-induced growth is only visible in a phyA-deficient background (**Fig 6 and 7B**). These results are in contrast with what is observed in *hy5* and *pif7* seedlings in *A. thaliana* (Roig-Villanova, Bou et al. 2006, Paulišić, Qin et al. 2021). Our results led us to postulate that protein activities of HY5 and PIF7 are different in *C. hirsuta* and *A. thaliana*: HY5 activity is higher in *C. hirsuta* than in *A. thaliana*, whereas PIF7 activity is lower in *C. hirsuta* than in *A. thaliana*. The different activity could be caused by several interdependent and non-excluding factors, such as the different biological functions encoded by these genes, and the post-translational regulation which affects their protein stability and degradation (Paulišić, Qin et al. 2021).

We performed transcriptome analysis to investigate how the biological functions encoded by DEGs varied in *C. hirsuta* and *A. thaliana*. We found that the total DEG numbers of up- and down-regulated genes increased with the time of shade exposure (**Fig 13A**), which is consistent with an amplification of the non-primary transcriptional effects with time. In contrast with *ChHY5*,

absence of *ChPIF7* had a greater impact on the early (1 h) DEGs, in agreement with the early role for this PIF in the modulation of shade-regulated changes in gene expression (Pastor-Andreu PhD thesis 2021). PIF7 influence become less important after 8 h of shade exposure. This finding agrees with the strong impact that lack of PIF457 has on the early and rapid changes in gene expression compared to *At*^{WT} (Pastor-Andreu PhD thesis 2021). However, the relatively mild impact of absence of *ChHY5* contrasts to what was observed in *A. thaliana*, where the lack of HY5 had a very strong influence on the DEGs than what was seen in *At*^{WT}, particularly at 1 h (PhD of Pastor-Andreu 2021). Independently on the number of DEGs identified, absence of these two factors had a clear impact on the identity of the DEGs, as observed in the Venn diagrams (**Fig 13B-E**).

Moreover, both external (environment) and internal (hormones) signals influence plant growth and development (Gray 2004). In the selected GO terms, which related with “*auxins, gibberellin, ethylene and brassinosteroid*” appeared and enriched only in *A. thaliana* in both 1h and 8h shade (**Tables 2**), up-regulated levels of auxin and gibberellin may be the result of induction of gibberellin biosynthesis-related gene expression (Bou-Torrent, Galstyan et al. 2014), these genes are also known to be controlled by auxin, implying that rapid and transient IAA synthesis caused by shade may lead to GA accumulation, (Frigerio, Alabadí et al. 2006). which is something we would want to investigate more in the future. In addition, it has been shown that ethylene affects HY5 degradation and activity in *A. thaliana* via an indirect regulatory mechanism (Yu, Wang et al. 2013, Yu and Huang 2017). Our data reveal that there are no substantial modifications in *C. hirsuta*, which is in contrast to the results for *A. thaliana* (**Table 2 and 3**). The findings from *A. thaliana* showed that AtHY5 could be involved in a feedback loop that affects ethylene production and metabolism in the plant. In the case of *C. hirsuta*, this procedure may not take place. When we performed comparative studies between *chy5* and *Ch*^{WT} or *chpif7* and *Ch*^{WT}, it's difficult to get conclusions from the lower number of GO terms enriched in general about the specific functions of HY5 and PIF7 (**Table 4**). In conclusion, the differences in transcriptomes between these two mustard

species support the hypothesis that they use same system but different strategies to adapt to shade, as evidenced by their different responses to growth-related hormones, which differ from the manipulation of elongation growth.

4. Materials and method

4.1 Plant material and growth conditions

Mutants of the *A. thaliana hy5-2* and *pif7-1* (in the Col-0 background) as well as *C. hirsuta* (Oxford ecotype, OX) plants have previously been reported (Yang, Lin et al. 2005, Leivar, Monte et al. 2008, Galstyan, Cifuentes-Esquivel et al. 2011, Hay, Pieper et al. 2014). These *A. thaliana* and *C. hirsuta* plants were cultivated in the greenhouse under long-day photoperiods (16 hours of light and 8 hours of darkness) in order to yield seeds (Martínez-García, Gallemí et al. 2014, Gallemí, Galstyan et al. 2016, Gallemí, Molina-Contreras et al. 2017). For hypocotyl measuring, these experiments were performed using seeds that had been surface-sterilized and sowed on half strength Murashige and Skoog solid growth medium without sucrose (0.5xMS⁻). For gene expression analyses and RNA-seq experiments, seeds were sowed on a sterilized nylon membrane placed on top of the solid 0.5xMS⁻ medium. To break dormancy and synchronize germination, plates containing seeds were incubated at 22°C under continuous white light (W) for 7 days after stratification in the dark at 4°C for 4 days, then transferred those plates to shade 1h and 8h, respectively (Paulišić, Molina-Contreras et al. 2017, Roig-Villanova, Paulišić et al. 2019). For transient expression studies, *N. benthamiana* plants were also cultivated in a greenhouse under long-day photoperiods. Cool fluorescent tubes were used for all those experiments to produce white light (W) with a red (R) to far-red light (FR) ratio (R:FR) ranging from 1.3 to 3.3, and the photosynthetically active radiation (PAR) is between 20 and 100 $\mu\text{mol m}^{-2} \text{s}^{-1}$. In order to achieve the various simulated shade effects, varying concentrations of fluorescent far-red light were added to the W (W+FR). An LED module from Philips' GreenPower LED HF far-red (HF) emits FR light with a R:FR ratio of between 0.02-0.09, using Spectrosense2 meter (Skye Instruments Ltd) to measure the

light fluence rates (Martínez-García, Gallemí et al. 2014). For the de-etiolation experiments, using a short (2 h) W treatment to activate the germination process, they should be kept in darkness at 22 °C for up to 24 hours when germination was started. Thereafter, one plate should be kept in complete darkness at 22 °C for the duration of the treatment, while the other plates should be exposed to various monochromatic light conditions (Blue light (B), Red light (R), or Far red light (FR)).

4.2 Generation of constructs for transient expression

To generate constructs overexpressing ChHY5 and AtHY5, we used cDNA from *A. thaliana* and *C. hirsuta* wildtype plants as a template, a fragment of 516 bp was amplified with WQO31, which introduced a *Xho*I site at the C-terminal site, and WQO32, which removed the stop codon and introduced a *Xho*I site at the N-terminal site for both species, respectively. The resulting fragment was subcloned into pJET1.2 (Thermo Fisher) to generate pWQ8 (AtHY5) and pWQ9 (ChHY5), which were confirmed by sequencing. A *Bam*HI-*Xho*I fragment of pSP55 (Paulišić, Qin et al. 2021) was subcloned into pENTRTM3C (Thermo Fisher) digested to generate pWQ18 (attL1<3xHA<attL2). Then, A *Xho*I fragment of pWQ8 and pWQ9 were subcloned into pWQ18 digested with *Sal*I to get pWQ19 (attL1< AtHY5-3xHA<attL2) and pWQ20 (attL1< ChHY5-3xHA<attL2). Recombination of pWQ19 and pWQ20 with the binary vector pSP135 (35S:attR1<ccdB<attR2, 35S:mGFP5), which was constructed by the host lab (Paulišić, Qin et al. 2021), using Gateway LR Clonase II gave pWQ21 (35S:attB1<AtHY5-3xHA<attB2, 35S:mGFP5) and pWQ22 (35S:attB1<ChHY5-3xHA<attB2, 35S:mGFP5), respectively. Both vectors also overexpress mGFP5 and confer resistance to Kanamycin in bacteria.

4.3 Construction of transgenic lines

Mutant lines of ChHY5 (*chy5-1* to *chy5-6*) and ChPIF7 (*chpif7-1* to *chpif7-3*), which were produced in *C. hirsuta* Oxford (OX) background, were generated by CRISPR-Cas9 and/or crosses. We used the CRISPR-Cas9 gene editing technique to create mutants (LeBlanc, Zhang et al. 2018) that were deficient in HY5 or PIF7 specific function. The guide RNA targeting sequence of ChHY5

(gRNA1_{ChHY5}, which is for both *A. thaliana* and *C. hirsuta*, 5'-ATC-AAG-CTC-TGC-TCC-ACA-TTT-GG-3'; gRNA2_{ChHY5}, which is only for *C. hirsuta* 5'-GAG-CGG-ACA-CAG-GCA-ACG-GTC-GG3') and ChPIF7 (gRNA1_{ChPIF7}, which is also for both *A. thaliana* and *C. hirsuta*, 5'-ATG-GAG-TGG-AAG-AGC-TAA-CCT-GG-3'; gRNA2_{ChPIF7}, which is only for *C. hirsuta* 5'-GGC-GTG-ATA-GGA-TAA-ACC-AGA-GG-3') were engineered to be under the control of the *A. thaliana* U6 promoter (pU6) and to include the Gateway recombination sites attB1 and attB2 (IDT, eu.idtdna.com/site). Related with HY5, these sequences were recombined with the vector pDONR207, which contains the attP1/attP2 recombination sequences, using Gateway BP Clonase II (Invitrogen) to generate the entry vectors (pSEP1: attL1<pU6:gRNA^{ChHY5}<attL2 and pSEP2: attL1<pU6:gRNA^{ChPIF7}<attL2). Next, the vector pSEP1 was digested with *salI*+*PstI*, to generate open vectors which remove an attL2 site. pSEP2 was digested with *XhoI*+*PstI*, also for getting a fragment that is missing attL2. Then the digested pSEP2 fragment was cloned into the pSEP1 vector digested with *salI*+*PstI*, generating pSEP3 (attL1<pU3:gRNA1^{ChHY5}<pU6:gRNA2^{ChHY5}<attL2). Using the Gateway LR Clonase II (Invitrogen), *in vitro* recombination with pSEP3 and the destination vector pDe-CAS9, which containing attR1 and attR2 sites, generated pSEP4 (attB1<pU3:gRNA1^{ChHY5}<pU6:gRNA2^{ChHY5}<attB2), a binary plasmid that resistant to PPT in plants, Rifampicin, Kanamycin and Spectinomycin in bacteria. The binary plasmid for PIF7 called pSP106, it also confers resistance to PPT in plants, Rifampicin, Kanamycin and Spectinomycin in bacteria. These binary vectors pSEP4 and pSP106 were introduced in *Agrobacterium tumefaciens*, strain C₅₈C₁ (pGV2260) by electroporation and transformed colonies were selected in YEB media supplemented with Rifampicin (100 µg/mL), Kanamycin (25 µg/mL) and Spectinomycin (100 µg/mL). The strains were grown and used to transform *A. thaliana* and *C. hirsuta* plants by floral dipping were harvest, the putative transgenic seedlings would be selected in media containing PPT (30 µg/mL).

4.4 Measurement of hypocotyl length

Hypocotyl length was measured after laying out seedlings flat on agar plates, using the National Institutes of Health ImageJ software (Bethesda, MD, USA) (Roig-Villanova, Bou-Torrent et al. 2007).

4.5 Gene expression analyses

Real-time qPCR studies were carried out in biological triplicates (Gallemí, Molina-Contreras et al. 2017). Reverse transcriptase with Transcriptor First Strand cDNA synthesis Kit (Roche, www.roche.com). The ELONGATION FACTOR 1 α (*EF1a*) gene was used as control *A. thaliana* and *C. hirsuta* for normalizations (Sorin, Salla-Martret et al. 2009). RNA integrity was checked through agarose gel electrophoresis (1%) and the concentration was estimated using an Agilent 2100 Bioanalyzer (Agilent Technologies, Inc., Santa Clara, CA, USA). All primers sequences for qPCR analyses are provided as Supplementary information.

4.6 Floral dip

A. tumefaciens strain C₅₈C₁ (GV2260) transformed with pSEP4 was conducted by electroporation using standard protocols (CHONG 2001). *A. tumefaciens* was cultured at 28°C in 1 L Yeast Extracts Broth media (YEB) (0.5 % (w/v) Beef extract, 0.1% (w/v) Yeast extract, 0.5% (w/v) peptone, 0.5% (w/v) sucrose, 0.048% (w/v) MgSO₄ and 1.5% (w/v) Agar) overnight. Then 1 L cultures were centrifuged by 5000 rpm for 10min at room temperature, the cell pellet was resuspended in 300 mL of 5% (w/v) sucrose supplemented with 0.02% (v/v) of Silwet L77. The floral stems of *A. thaliana* and *C. hirsuta* were dipped in the solution during 3-5 min, then the pots were left horizontally and covered with plastic during 3 days. After this period, plastics were removed and the plants were returned to the greenhouses. Seeds were harvested after 4-5 weeks.

4.7 Agroinfiltration of *N. benthamiana* leaves

Agroinfiltration was performed on *N. benthamiana* plants by agroinfiltrated them with *A. tumefaciens* strains that had been transformed with the plasmids

which expressed the different HFR1 or HY5 derivatives. The plants were then grown in the greenhouse under long-day photoperiods. Following agroinfiltration, samples which are the leaf circles collected from infiltrated regions were gathered 3 days later and stored in liquid nitrogen immediately. Approximately 75 mg of leaf tissue from the same leaf was included in each biological sample.

4.8 RNA-sequencing

As with the RT-qPCR expression study, total RNA was collected for sequencing. Three biological replicates were used to prepare the library, which was sequenced at the Centre Nacional de Anàlisi Genòmica (CNAG – CRG) on an Illumina NovaSeq6000 with 50 bp paired-end reads. The False Discovery Rate (FDR) and the Fold Change (FC) were calculated for each gene by mapping to the TAIR10 genome and comparing it to Limma. When the *p*-value was less than 0.05 and the |FC| was more than 1.5, those genes were picked as differentially expressed genes (DEGs).

4.9 Protein extraction and immunoblotting analyses

For protein detection and quantification, about 75 mg of agroinfiltrated *N. benthamiana* leaves (grown as indicated) were used. Using an SDS-containing extraction buffer, which contains 40 μ M Tris-HCl pH 6.8, 4% SDS (w/v), 5% glycerol, 1 mM EDTA and proteinase inhibitor (P2714; Sigma Chemical Co.) (1.5 μ L per mg of fresh weight) (Gallemí, Molina-Contreras et al. 2017), total proteins were extracted from the plant material, which was frozen in liquid nitrogen and crushed to powder. We used Pierce™ BCA 753 Protein Assay Kit (Thermo Scientific, www.thermofisher.com) to quantify the protein concentration, all proteins should be diluted to the same concentration. Then Anti-HA and anti-GFP monoclonal antibodies were used to immunoblot proteins (50 μ g per lanes) after they had been resolved on a 10% SDS-PAGE gel and transferred to PVDF membranes, we immunoblotted with rat monoclonal anti-HA (1:2000 dilution) or mouse monoclonal anti-GFP (1:2000 dilution). Horseradish peroxidase (HRP) conjugated goat anti-rat and HRP conjugated sheep anti-mouse antibodies were utilized as secondary antibodies (Promega;

1:5000 dilution). Molecular weight markers (prestained SDS molecular weight standard mixture) were from Sigma Chemical Co. ChemiDoc™ Touch Imaging System (Bio-Rad, www.bio-rad.com) was used to develop blots using ECL Prime Western Blotting Detection Reagent (GE Healthcare, RPN2236). Image Lab™ Software was used to measure the relative protein levels

4.10 Protein purification for the MST experiments

Spodoptera frugiperda Sf9 cells (Thermo Fisher) were used to express and purify AtCOP1 WD40, which has residues 349-675 (Lau, Podolec et al. 2019). COP1 WD40 was tagged using the Monolith Protein Labeling Kit RED-NHS 2nd Generation Amine Reactive kit (MO-L011; Nanotemper Technologies, Munich, Germany) for the protein labeling and microscale thermophoresis (MST). This is due to the fact that the labeling technique cannot be performed because of the presence of the toxic end product (TEV) in buffer A with 2 mM β -ME after the COP1 WD40 cleavage. As a result, the buffer was switched with the labeling buffer NHS included with the kit prior to labeling. Excess dye was removed in a final stage by elution with 20 mM HEPES pH 7.5, 150mM NaCl, 2mM TCEP and 0.5% Tween20 in 12-15 portions of the assay buffer. Measurements were made at 280 and 650 nanometers for each sample. The method for calculating the degree of labeling (DOL) was supplied in the instructions. All samples used in the test were flash frozen to ensure that the proteins included in them had an optimal DOL of at least 0.5%. The assay buffer was pre-mixed with the necessary quantities of peptide solutions. We put it in 16 PCR tubes, 10 μ L of peptide solution were serially diluted 1:1 using assay buffer for each independent duplicate. Since 10 μ L of solution was removed from the 16th tube, the peptide solution in each tube was 10 μ L. Each dilution step was combined with 10 μ L of 150 nM COP1 WD40 and put into Monolith NT.115 Premium Capillaries (MO-K025). The Monolith NT.115 instrument was used to test the samples at a 25% LED power and 20% MST power. The MOAffinityAnalysis program was used to examine the thermophoresis data that was obtained (Nanotemper Technologies).

Supplementary information

Table S1. Primers used for gene expression analyses.

Gene	Primers	Sequence (5' – 3')
ChEF1 α	CTO9	GGCCGATTGTGCTGTCCTTA
	CTO10	TCACGGGTCTGACCATCCTTA
ChHY5	JRO13	TCATCAAGCTCTGCTCCAC
	JRO14	CAGCTTCTCCTCCAAACTCC
ChPIF7	SPO72	TGGTCACAGCGTTACTGCAA
	SPO64	TGCTCGTCCCCGTCGTCCAT

Table S2. summarizes information regarding mutant alleles

Name	Mutation in gRNA1	Mutations in gRNA2
chpif7-1	-	7 nucleotide deletion
chpif7-2	-	1 nucleotide deletion
chpif7-3	1 A nucleotide insertion	-
chy5-1	1 C nucleotide insertion	6 nucleotides deletion
chy5-2	1 T nucleotide insertion	6 nucleotides deletion
chy5-3	1 A nucleotide insertion	6 nucleotides deletion
chy5-4	1 A nucleotide insertion	1 nucleotides deletion
chy5-5	1 C nucleotide insertion	1 nucleotides deletion
chy5-6	1 T nucleotide insertion	3 nucleotides deletion

Table S3. Primers used for cloning and genotyping.

Gene	Primers	Sequence (5' – 3')
ChPIF7^{WT} (gRNA1)	WQO17	TGGAGTGGAAGAGCTAACC
	WQO15	CCAACCTCACTCAAGTAAGCC
chpif7-3	QWO18	TGGAGTGGAAGAGCTAAAC
	QWO15	CCAACCTCACTCAAGTAAGCC
ChPIF7^{WT} (gRNA2)	WQO5	GGCGTGATAGGATAAACA
	SEO4	GAATACCATTTTATAAAGTTTACG
chpif7-1	WQO6	GTGATAGGATAAACCAGAG
	SEO4	GAATACCATTTTATAAAGTTTACG
chpif7-2	WQO7	GTGATAGGATAAAATGAGA
	SEO4	GAATACCATTTTATAAAGTTTACG
ChHY5^{WT} (gRNA1)	QWO37	CATCAAGCTCTGCTCCACAT
	JRO14	CAGCTTCTCCTCCAAACTCC
chy5-2 & chy5-6	QWO38	CATCAAGCTCTGCTCCACTA
	JRO14	CAGCTTCTCCTCCAAACTCC
chy5-3 & chy5-4	QWO39	CATCAAGCTCTGCTCCACAA
	JRO14	CAGCTTCTCCTCCAAACTCC
chy5-1 & chy5-5	QWO44	CATCAAGCTCTGCTCCACCA
	JRO14	CAGCTTCTCCTCCAAACTCC
ChHY5^{WT} (gRNA2)	QWO40	CGGACACAGGCAAC CGGT
	QWO16	GGAGATCAAAGGCTTGCATC
chy5-1 & chy5-2 & chy5-3	QWO42	CAGGAGCGGACACAGGT
	QWO16	GGAGATCAAAGGCTTGCATC
chy5-4 chy5-5	QWO43	GCGGACACAGGCAAG GT
	QWO16	GGAGATCAAAGGCTTGCATC
chy5-6	QWO41	GAGCGGACACAGGCCAT
	QWO16	GGAGATCAAAGGCTTGCATC
HY5 + XhoI	QWO31	cc <u>CTCGAGATGCAAGAACAAGCGACTAG</u>
	QWO32	gg <u>CTCGAGAAGGCTTGCATCAGCGTTAG</u>

<i>HY5 + 3xHA</i>	QWO33	CGCCCTTCCGTCGAGATGCAAG
	QWO34	CTCCACCGTCGAGAAGGCTTGC
<i>HY5 + attL / attB</i>	QWO35	CCCTTCCGTCGAGATGCAAGAAC
	QWO36	CGAATTCGCCCTTGGCTCGAG

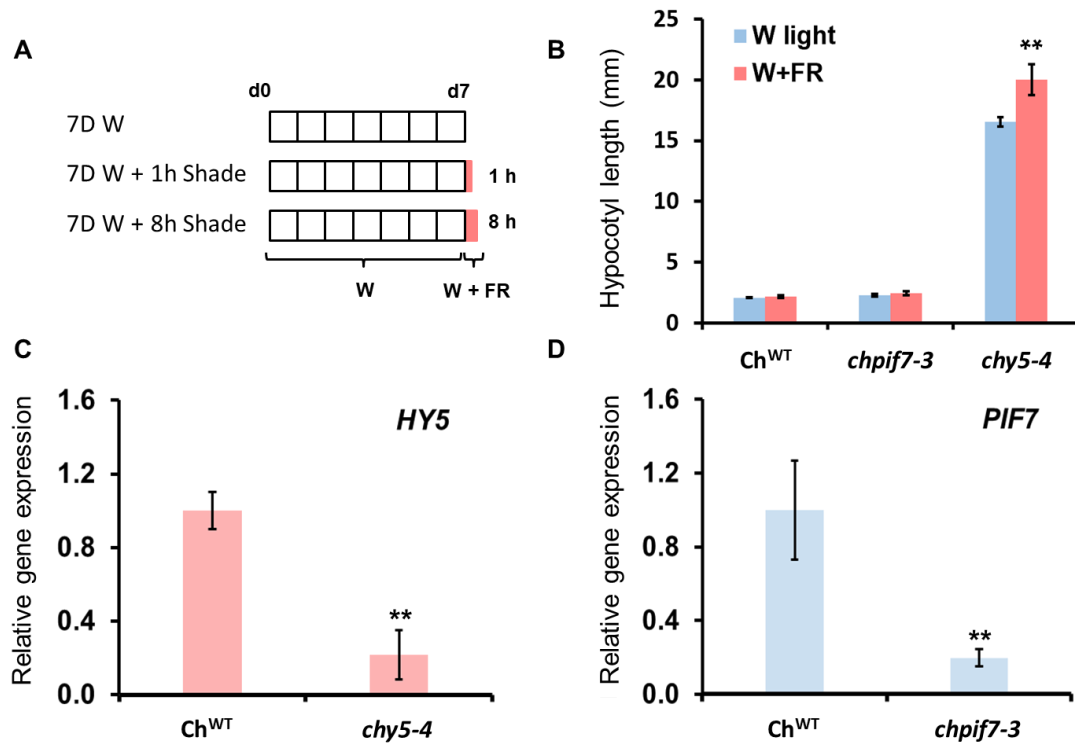


Figure S1. The experiment for RNA-Seq. **(A)** Cartoon describing the experiment sets up; **(B)** Hypocotyl length of testing Ch^{WT}, *chpif7-3* and *chy5-4* lines in W light and in W+FR. The values are the means \pm SE of four independent biological replicates. **(C)** Relative expression levels of ChHY5 genes, normalized to EF1 α ; **(D)** Relative expression levels of ChPIF7 genes, normalized to EF1 α . Expression values are the mean \pm SE of three independent biological replicates. Asterisks mark significant differences (student's t-test: ** P-value <0.01; * P-value <0.05) **(B)** between W light and W+FR or **(C)** **(D)** relative to Ch^{WT} value.

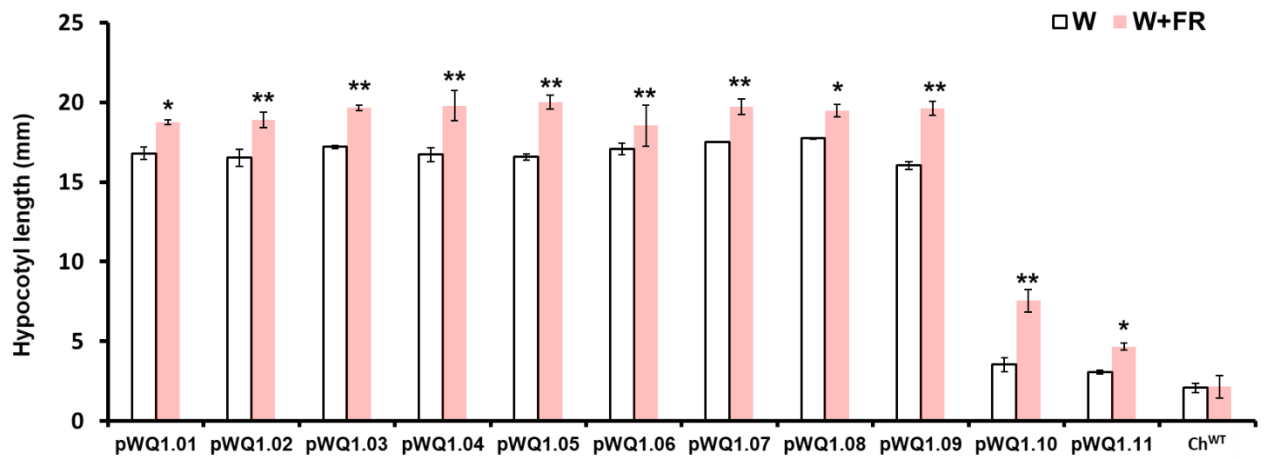


Figure S2. Hypocotyl length of *C. hirsuta* pWQ1 lines in response to simulated shade. The values are the means \pm SE of three independent biological replicates. Asterisks mark significant differences (student's t-test: *P-value < 0.05, **P-value < 0.01) between W light and W+FR.

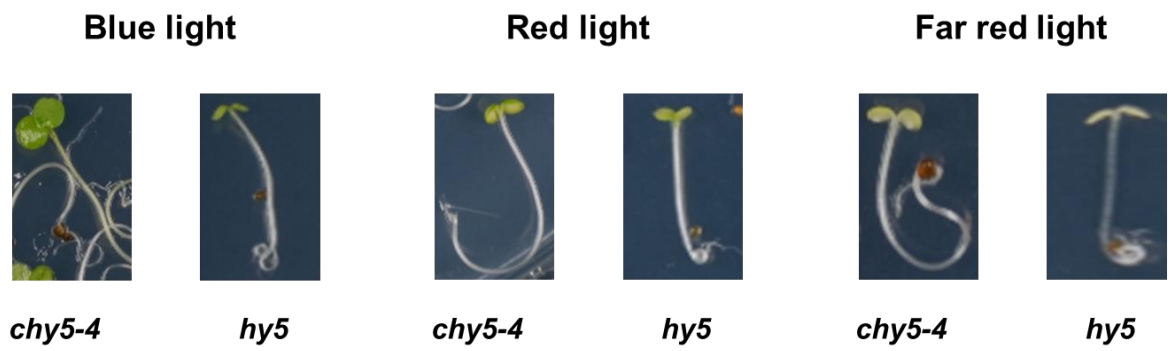


Figure S3. The phenotypes of *C. hirsuta chy5* and *A. thaliana hy5* seedlings grown in the Red, Blue or Far red monochromatic lights.

Reference

Abbas, M., et al. (2015). "Oxygen sensing coordinates photomorphogenesis to facilitate seedling survival." Current Biology **25**(11): 1483-1488.

Alonso, L., et al. (2017). "Diurnal cycle relationships between passive fluorescence, PRI and NPQ of vegetation in a controlled stress experiment." Remote Sensing **9**(8): 770.

Bai, S.-N. (2017). "Reconsideration of plant morphological traits: from a structure-based perspective to a function-based evolutionary perspective." Frontiers in plant science **8**: 345.

Ballaré, C. L. and R. Pierik (2017). "The shade-avoidance syndrome: Multiple signals and ecological consequences." Plant Cell Environ **40**(11): 2530-2543.

Botto, J. and H. Smith (2002). "Differential genetic variation in adaptive strategies to a common environmental signal in Arabidopsis accessions: phytochrome-mediated shade avoidance." Plant Cell Environ **25**(1): 53-63.

Bou-Torrent, J., et al. (2014). "Plant proximity perception dynamically modulates hormone levels and sensitivity in Arabidopsis." Journal of Experimental Botany **65**(11): 2937-2947.

Bou-Torrent, J., et al. (2015). "Regulation of carotenoid biosynthesis by shade relies on specific subsets of antagonistic transcription factors and cofactors." Plant physiology **169**(3): 1584-1594.

Brouwer, B., et al. (2012). "The impact of light intensity on shade-induced leaf senescence." **35**(6): 1084-1098.

Burko, Y., et al. (2020). "Chimeric activators and repressors define HY5 activity and reveal a light-regulated feedback mechanism." The Plant Cell **32**(4): 967-983.

Casal, J. J. (2012). "Shade avoidance." The Arabidopsis book/American Society of Plant Biologists **10**.

Casal, J. J. (2013). "Photoreceptor signaling networks in plant responses to shade." Annual review of plant biology **64**: 403-427.

Casal, J. J. J. A. r. o. p. b. (2013). "Photoreceptor signaling networks in plant responses to shade." Annual review of plant biology **64**: 403-427.

Castillo, M.-C., et al. (2021). "NIN-like protein7 and PROTEOLYSIS6 functional interaction enhances tolerance to sucrose, ABA, and submergence." **187**(4): 2731-2748.

Choi, D.-M., et al. (2021). "Generation and characterization of a specific polyclonal antibody against Arabidopsis thaliana phytochrome-interacting factor 3." Journal of Plant Biology **64**(2): 181-191.

CHONG, L. (2001). "Molecular cloning." Science **292**(5516): 446-446.

Choy, M.-K., et al. (2008). "An Arabidopsis mutant able to green after extended dark periods shows decreased transcripts of seed protein genes and altered sensitivity to abscisic acid." Journal of Experimental Botany **59**(14): 3869-3884.

Choy, M.-K., et al. (2008). "An Arabidopsis mutant able to green after extended dark periods shows decreased transcripts of seed protein genes and altered sensitivity to abscisic acid." Journal of experimental botany **59**(14): 3869-3884.

Cloix, C., et al. (2012). "C-terminal region of the UV-B photoreceptor UVR8 initiates signaling through interaction with the COP1 protein." **109**(40): 16366-16370.

Cochran, W. G. (1952). "The χ^2 test of goodness of fit." The Annals of mathematical statistics: 315-345.

Dannehl, D., et al. (2021). "Increase of yield, lycopene, and lutein content in tomatoes grown under continuous PAR spectrum LED lighting." Frontiers in plant science **12**: 299.

De Lucas, M., et al. (2008). "A molecular framework for light and gibberellin control of cell elongation." Nature **451**(7177): 480-484.

De Marchi, R., et al. (2016). "The N-end rule pathway regulates pathogen responses in plants." Scientific Reports **6**(1): 1-15.

de Wit, M., et al. (2016). "Integration of phytochrome and cryptochrome signals determines plant growth during competition for light." Current Biology **26**(24): 3320-3326.

Djakovic-Petrovic, T., et al. (2007). "DELLA protein function in growth responses to canopy signals." The Plant Journal **51**(1): 117-126.

Duek, P. D., et al. (2004). "The degradation of HFR1, a putative bHLH class transcription factor involved in light signaling, is regulated by phosphorylation and requires COP1." Current Biology **14**(24): 2296-2301.

Eble, J. A. (2018). "Titration ELISA as a method to determine the dissociation constant of receptor ligand interaction." Journal of Visualized Experiments(132): e57334.

Eichers, E., et al. (2004). "Triallelic inheritance: a bridge between Mendelian and multifactorial traits." Annals of medicine **36**(4): 262-272.

Favero, D. S. (2020). "Mechanisms regulating PIF transcription factor activity at the protein level." Physiologia plantarum **169**(3): 325-335.

Feng, S., et al. (2008). "Coordinated regulation of *Arabidopsis thaliana* development by light and gibberellins." Nature **451**(7177): 475-479.

Fernández-Milmanda, G. L. and C. L. Ballaré (2021). "Shade avoidance: Expanding the color and hormone palette." Trends in plant science **26**(5): 509-523.

Fiorucci, A.-S. and C. Fankhauser (2017). "Plant strategies for enhancing access to sunlight." Current Biology **27**(17): R931-R940.

Fiorucci, A.-S., et al. (2020). "PHYTOCHROME INTERACTING FACTOR 7 is important for early responses to elevated temperature in Arabidopsis seedlings." New Phytologist **226**(1): 50-58.

Franklin, K. A. (2008). "Shade avoidance." New Phytologist **179**(4): 930-944.

Franklin, K. A., et al. (2011). "Phytochrome-interacting factor 4 (PIF4) regulates auxin biosynthesis at high temperature." Proceedings of the National Academy of Sciences **108**(50): 20231-20235.

Fraser, D. P., et al. (2016). "Photoreceptor crosstalk in shade avoidance." Current opinion in plant biology **33**: 1-7.

Frigerio, M., et al. (2006). "Transcriptional regulation of gibberellin metabolism genes by auxin signaling in Arabidopsis." Plant physiology **142**(2): 553-563.

Gallemí, M., et al. (2016). "DRACULA2 is a dynamic nucleoporin with a role in regulating the shade avoidance syndrome in Arabidopsis." Development **143**(9): 1623.

Gallemí, M., et al. (2016). "DRACULA2 is a dynamic nucleoporin with a role in regulating the shade avoidance syndrome in Arabidopsis." Development **143**(9): 1623-1631.

Gallemí, M., et al. (2017). "A non - DNA - binding activity for the ATHB 4 transcription factor in the control of vegetation proximity." New Phytologist **216**(3): 798-813.

Gallemí, M., et al. (2017). "A non - DNA - binding activity for the ATHB 4 transcription factor in the control of vegetation proximity." **216**(3): 798-813.

Galstyan, A., et al. (2011). "The shade avoidance syndrome in Arabidopsis: a fundamental role for atypical basic helix–loop–helix proteins as transcriptional cofactors." The Plant Journal **66**(2): 258-267.

Galstyan, A., et al. (2011). "The shade avoidance syndrome in Arabidopsis: a fundamental role for atypical basic helix–loop–helix proteins as transcriptional cofactors." **66**(2): 258-267.

Galvão, V. C., et al. (2019). "PIF transcription factors link a neighbor threat cue to accelerated reproduction in Arabidopsis." Nature communications **10**(1): 1-10.

Gan, X., et al. (2016). "The Cardamine hirsuta genome offers insight into the evolution of morphological diversity." Nature Plants **2**(11): 1-7.

Gommers, C. M. (2016). When growing tall is not an option: contrasting shade avoidance responses in two wild Geranium species, Utrecht University.

Gommers, C. M., et al. (2013). "Shade tolerance: when growing tall is not an option." Trends in plant science **18**(2): 65-71.

Gray, W. M. (2004). "Hormonal regulation of plant growth and development." PLoS biology **2**(9): e311.

Gray, W. M., et al. (1998). "High temperature promotes auxin-mediated hypocotyl elongation in Arabidopsis." Proceedings of the National Academy of Sciences **95**(12): 7197-7202.

Hardtke, C. S., et al. (2000). "HY5 stability and activity in Arabidopsis is regulated by phosphorylation in its COP1 binding domain." The EMBO Journal **19**(18): 4997-5006.

Hauvermale, A. L., et al. (2012). "Gibberellin signaling: a theme and variations on DELLA repression." Plant physiology **160**(1): 83-92.

Hay, A. S., et al. (2014). "Cardamine hirsuta: a versatile genetic system for comparative studies." The Plant Journal **78**(1): 1-15.

Hay, A. S., et al. (2014). "Cardamine hirsuta: a versatile genetic system for comparative studies." **78**(1): 1-15.

Hayes, S., et al. (2017). "UV-B perceived by the UVR8 photoreceptor inhibits plant thermomorphogenesis." **27**(1): 120-127.

Hersch, M., et al. (2014). "Light intensity modulates the regulatory network of the shade avoidance response in Arabidopsis." Proceedings of the National Academy of Sciences **111**(17): 6515-6520.

Hersch, M., et al. (2014). "Light intensity modulates the regulatory network of the shade avoidance response in Arabidopsis." Proceedings of the National Academy of Sciences of the United States of America **111**(17): 6515.

Holman, T. J., et al. (2009). "The N-end rule pathway promotes seed germination and establishment through removal of ABA sensitivity in Arabidopsis." Proceedings of the National Academy of Sciences **106**(11): 4549-4554.

Holtkotte, X., et al. (2017). "The blue light-induced interaction of cryptochrome 1 with COP1 requires SPA proteins during Arabidopsis light signaling." PLoS Genetics **13**(10): e1007044.

Hornitschek, P., et al. (2012). "Phytochrome interacting factors 4 and 5 control seedling growth in changing light conditions by directly controlling auxin signaling." The Plant Journal **71**(5): 699-711.

Hornitschek, P., et al. (2012). "Phytochrome interacting factors 4 and 5 control seedling growth in changing light conditions by directly controlling auxin signaling." **71**(5): 699-711.

Hornitschek, P., et al. (2009). "Inhibition of the shade avoidance response by formation of non-DNA binding bHLH heterodimers." The EMBO Journal **28**(24): 3893-3902.

Huang, X., et al. (2014). "Beyond repression of photomorphogenesis: role switching of COP/DET/FUS in light signaling." Current opinion in plant biology **21**: 96-103.

Iñigo, S., et al. (2012). "Proteasome-mediated turnover of Arabidopsis MED25 is coupled to the activation of FLOWERING LOCUS T transcription." Plant physiology **160**(3): 1662-1673.

Jaillais, Y. and G. Vert (2012). "Brassinosteroids, gibberellins and light-mediated signalling are the three-way controls of plant sprouting." Nature cell biology **14**(8): 788-790.

James, G. V., et al. (2013). "User guide for mapping-by-sequencing in Arabidopsis." **14**(6): 1-13.

Jang, I.-C., et al. (2005). "HFR1 is targeted by COP1 E3 ligase for post-translational proteolysis during phytochrome A signaling." Genes & Development **19**(5): 593-602.

Jang, I.-C., et al. (2005). "HFR1 is targeted by COP1 E3 ligase for post-translational proteolysis during phytochrome A signaling." **19**(5): 593-602.

Jia, Y., et al. (2020). "PIFs coordinate shade avoidance by inhibiting auxin repressor ARF18 and metabolic regulator QQS." New Phytologist **228**(2): 609-621.

Kami, C., et al. (2010). "Light-regulated plant growth and development." Current topics in developmental biology **91**: 29-66.

Kamiya, Y. and J. L. García-Martínez (1999). "Regulation of gibberellin biosynthesis by light." Current opinion in plant biology **2**(5): 398-403.

Keuskamp, D. H. and R. Pierik (2010). Photosensory cues in plant–plant interactions: regulation and functional significance of shade avoidance responses. Plant Communication from an Ecological Perspective, Springer: 159-178.

Keuskamp, D. H., et al. (2010). "Auxin transport through PIN-FORMED 3 (PIN3) controls shade avoidance and fitness during competition." **107**(52): 22740-22744.

Khanna, R., et al. (2004). "A novel molecular recognition motif necessary for targeting photoactivated phytochrome signaling to specific basic helix-loop-helix transcription factors." The Plant Cell **16**(11): 3033-3044.

Klose, C., et al. (2012). "The mediator complex subunit PFT1 interferes with COP1 and HY5 in the regulation of Arabidopsis light signaling." Plant physiology **160**(1): 289-307.

Koch, M. A., et al. (2006). "Three times out of Asia Minor: the phylogeography of *Arabis alpina* L.(Brassicaceae)." Molecular Ecology **15**(3): 825-839.

Koini, M. A., et al. (2009). "High temperature-mediated adaptations in plant architecture require the bHLH transcription factor PIF4." Current Biology **19**(5): 408-413.

Kurepin, L. V., et al. (2007). "Interaction of red to far red light ratio and ethylene in regulating stem elongation of *Helianthus annuus*." Plant Growth Regulation **51**(1): 53-61.

Lau, K., et al. (2019). "Plant photoreceptors and their signaling components compete for COP 1 binding via VP peptide motifs." The EMBO Journal **38**(18): e102140.

Lau, K., et al. (2019). "Plant photoreceptors and their signaling components compete for COP 1 binding via VP peptide motifs." **38**(18): e102140.

LeBlanc, C., et al. (2018). "Increased efficiency of targeted mutagenesis by CRISPR/Cas9 in plants using heat stress." The Plant Journal **93**(2): 377-386.

Lee, J.-H., et al. (2010). "DWA1 and DWA2, two Arabidopsis DWD protein components of CUL4-based E3 ligases, act together as negative regulators in ABA signal transduction." The Plant Cell **22**(6): 1716-1732.

Leivar, P., et al. (2008). "The Arabidopsis phytochrome-interacting factor PIF7, together with PIF3 and PIF4, regulates responses to prolonged red light by modulating phyB levels." The Plant Cell **20**(2): 337-352.

Leivar, P., et al. (2012). "Dynamic antagonism between phytochromes and PIF family basic helix-loop-helix factors induces selective reciprocal responses to light and shade in a rapidly responsive transcriptional network in Arabidopsis." **24**(4): 1398-1419.

Li, K., et al. (2016). "DELLA-mediated PIF degradation contributes to coordination of light and gibberellin signalling in Arabidopsis." Nature communications **7**(1): 1-11.

Li, L., et al. (2012). "Linking photoreceptor excitation to changes in plant architecture." Genes development **26**(8): 785-790.

Lichtenthaler, H., et al. (1982). "Adaptation of chloroplast-ultrastructure and of chlorophyll-protein levels to high-light and low-light growth conditions." **37**(5-6): 464-475.

Liebsch, D. and O. Keech (2016). "Dark-induced leaf senescence: new insights into a complex light-dependent regulatory pathway." New Phytologist **212**(3): 563-570.

Liebsch, D. and O. J. N. P. Keech (2016). "Dark-induced leaf senescence: new insights into a complex light-dependent regulatory pathway." **212**(3): 563-570.

Liu, B., et al. (2011). "Arabidopsis cryptochrome 1 interacts with SPA1 to suppress COP1 activity in response to blue light." Genes & Development **25**(10): 1029-1034.

Lorrain, S., et al. (2008). "Phytochrome-mediated inhibition of shade avoidance involves degradation of growth-promoting bHLH transcription factors." The Plant Journal **53**(2): 312-323.

Lorrain, S., et al. (2008). "Phytochrome-mediated inhibition of shade avoidance involves degradation of growth-promoting bHLH transcription factors." **53**(2): 312-323.

Lu, X.-D., et al. (2015). "Red-light-dependent interaction of phyB with SPA1 promotes COP1–SPA1 dissociation and photomorphogenic development in Arabidopsis." Molecular plant **8**(3): 467-478.

Lup, S. D., et al. (2021). "Easymap: a user-friendly software package for rapid mapping-by-sequencing of point mutations and large insertions." Frontiers in plant science **12**: 655286.

Martínez-García, J. F., et al. (2014). "The shade avoidance syndrome in Arabidopsis: the antagonistic role of phytochrome A and B differentiates vegetation proximity and canopy shade." PloS one **9**(10): e109275.

Martínez-García, J. F., et al. (2014). "The shade avoidance syndrome in Arabidopsis: the antagonistic role of phytochrome A and B differentiates vegetation proximity and canopy shade." **9**(10): e109275.

Martinez-Garcia, J. F., et al. (2010). Regulatory components of shade avoidance syndrome. Advances in botanical research, Elsevier. **53**: 65-116.

Martinez-Garcia, J. F., et al. (2010). "Regulatory components of shade avoidance syndrome." Advances in botanical research **53**: 65-116.

Maxwell, K. and G. N. Johnson (2000). "Chlorophyll fluorescence—a practical guide." Journal of Experimental Botany **51**(345): 659-668.

Molina-Contreras, M. J., et al. (2019). "Photoreceptor activity contributes to contrasting responses to shade in Cardamine and Arabidopsis seedlings." The Plant Cell **31**(11): 2649-2663.

Molina-Contreras, M. J., et al. (2019). "Photoreceptor activity contributes to contrasting responses to shade in Cardamine and Arabidopsis seedlings." **31**(11): 2649-2663.

Morelli, L., et al. (2021). "Light signals generated by vegetation shade facilitate acclimation to low light in shade-avoider plants." Plant physiology **186**(4): 2137-2151.

Morelli, L., et al. (2021). "Light signals generated by vegetation shade facilitate acclimation to low light in shade-avoider plants." Plant physiology **186**(4): 2137-2151.

Morelli, L., et al. (2020). "Light quality signals generated by vegetation shade facilitate acclimation to reduced light quantity in shade-avoider plants." bioRxiv.

Morgan, P. W., et al. (2002). "Opportunities to improve adaptability and yield in grasses: lessons from sorghum." Crop Science **42**(6): 1791-1799.

Müller-Moulé, P., et al. (2016). "YUCCA auxin biosynthetic genes are required for Arabidopsis shade avoidance." **4**: e2574.

Murchie, E., et al. (2009). "Agriculture and the new challenges for photosynthesis research." New Phytologist **181**(3): 532-552.

Murchie, E. H. and T. Lawson (2013). "Chlorophyll fluorescence analysis: a guide to good practice and understanding some new applications." Journal of Experimental Botany **64**(13): 3983-3998.

Murchie, E. H. and T. J. J. o. e. b. Lawson (2013). "Chlorophyll fluorescence analysis: a guide to good practice and understanding some new applications." **64**(13): 3983-3998.

Ortiz-Alcaide, M., et al. (2019). "Chloroplasts modulate elongation responses to canopy shade by retrograde pathways involving HY5 and abscisic acid." The Plant Cell **31**(2): 384-398.

Pacín, M., et al. (2013). "COP 1 re-accumulates in the nucleus under shade." The Plant Journal **75**(4): 631-641.

Pacín, M., et al. (2016). "Convergence of CONSTITUTIVE PHOTOMORPHOGENESIS 1 and PHYTOCHROME INTERACTING FACTOR signalling during shade avoidance." New Phytologist **211**(3): 967-979.

Pacín, M., et al. (2016). "Convergence of CONSTITUTIVE PHOTOMORPHOGENESIS 1 and PHYTOCHROME INTERACTING FACTOR signalling during shade avoidance." **211**(3): 967-979.

Paik, I., et al. (2017). "Expanding roles of PIFs in signal integration from multiple processes." Molecular plant **10**(8): 1035-1046.

Park, H.-J., et al. (2008). "Multisite phosphorylation of Arabidopsis HFR1 by casein kinase II and a plausible role in regulating its degradation rate." Journal of Biological Chemistry **283**(34): 23264-23273.

Paulišić, S., et al. (2017). Approaches to study light effects on brassinosteroid sensitivity. Brassinosteroids, Springer: 39-47.

Paulišić, S., et al. (2021). "Adjustment of the PIF7-HFR1 transcriptional module activity controls plant shade adaptation." The EMBO Journal **40**(1): e104273.

Pedmale, U. V., et al. (2016). "Cryptochromes interact directly with PIFs to control plant growth in limiting blue light." Cell **164**(1-2): 233-245.

Pierik, R. and M. de Wit (2014). "Shade avoidance: phytochrome signalling and other aboveground neighbour detection cues." Journal of Experimental Botany **65**(11): 2815-2824.

Pierik, R. and C. Testerink (2014). "The art of being flexible: how to escape from shade, salt, and drought." Plant physiology **166**(1): 5-22.

Qi, L., et al. (2020). "PHYTOCHROME-INTERACTING FACTORS interact with the ABA receptors PYL8 and PYL9 to orchestrate ABA signaling in darkness." **13**(3): 414-430.

Quint, M., et al. (2016). "Molecular and genetic control of plant thermomorphogenesis." Nature Plants **2**(1): 1-9.

Quirino, B. F., et al. (2000). "Molecular aspects of leaf senescence." **5**(7): 278-282.

Ranade, S. S. and M. R. García-Gil (2021). "Molecular signatures of local adaptation to light in Norway spruce." Planta **253**(2): 1-18.

Rascher, U., et al. (2000). "Evaluation of instant light - response curves of chlorophyll fluorescence parameters obtained with a portable chlorophyll fluorometer on site in the field." Plant Cell Environ **23**(12): 1397-1405.

Riber, W., et al. (2015). "The greening after extended darkness¹ is an N-end rule pathway mutant with high tolerance to submergence and starvation." Plant physiology **167**(4): 1616-1629.

Roig-Villanova, I., et al. (2006). "Identification of primary target genes of phytochrome signaling. Early transcriptional control during shade avoidance responses in Arabidopsis." Plant physiology **141**(1): 85-96.

Roig-Villanova, I. and J. F. Martínez-García (2016). "Plant responses to vegetation proximity: a whole life avoiding shade." Frontiers in plant science **7**: 236.

Roig-Villanova, I. and J. F. J. F. i. P. S. Martínez-García (2016). "Plant responses to vegetation proximity: a whole life avoiding shade." **7**: 236.

Roig-Villanova, I., et al. (2019). Shade avoidance and neighbor detection. Phytochromes, Springer: 157-168.

Roig-Villanova, I., et al. (2007). "Interaction of shade avoidance and auxin responses: a role for two novel atypical bHLH proteins." The EMBO Journal **26**(22): 4756-4767.

Roig-Villanova, I., et al. (2007). "Interaction of shade avoidance and auxin responses: a role for two novel atypical bHLH proteins." Embo Journal **26**(22): 4756-4767.

Ruberti, I., et al. (2012). "Plant adaptation to dynamically changing environment: the shade avoidance response." **30**(5): 1047-1058.

Sagar, S. and A. Singh (2020). "Dark-induced hormonal regulation of plant growth and development." Frontiers in plant science **11**: 1527.

Sairanen, I., et al. (2012). "Soluble carbohydrates regulate auxin biosynthesis via PIF proteins in Arabidopsis." **24**(12): 4907-4916.

Sakuraba, Y., et al. (2014). "Phytochrome-interacting transcription factors PIF4 and PIF5 induce leaf senescence in Arabidopsis." Nature communications **5**(1): 1-13.

Sakuraba, Y., et al. (2014). "Phytochrome-interacting transcription factors PIF4 and PIF5 induce leaf senescence in Arabidopsis." **5**(1): 1-13.

Sasidharan, R., et al. (2008). "The regulation of cell wall extensibility during shade avoidance: a study using two contrasting ecotypes of *Stellaria longipes*." Plant physiology **148**(3): 1557-1569.

Schreiber, U. (2004). "Pulse-amplitude-modulation (PAM) fluorometry and saturation pulse method: an overview." Chlorophyll a fluorescence: 279-319.

Schreiber, U. and C. Klughammer (2008). "Non-photochemical fluorescence quenching and quantum yields in PS I and PS II: analysis of heat-induced limitations using Maxi-Imaging-PAM and Dual-PAM-100." PAM Application Notes 1: 15-18.

Sessa, G., et al. (2005). "A dynamic balance between gene activation and repression regulates the shade avoidance response in Arabidopsis." **19**(23): 2811-2815.

Sheerin, D. J. and A. Hiltbrunner (2017). "Molecular mechanisms and ecological function of far-red light signalling." Plant Cell Environ **40**(11): 2509-2529.

Sibénil, Y., et al. (2001). "Plant bZIP G-box binding factors. Modular structure and activation mechanisms." European Journal of Biochemistry **268**(22): 5655-5666.

Smith, H. (1982). "Light quality, photoperception, and plant strategy." Annual review of plant physiology **33**(1): 481-518.

Smith, H. (2000). "Phytochromes and light signal perception by plants—an emerging synthesis." Nature **407**(6804): 585-591.

Smith, H. and G. Whitelam (1997). "The shade avoidance syndrome: multiple responses mediated by multiple phytochromes." Plant Cell Environ **20**(6): 840-844.

Solovchenko, A., et al. (2013). "Probing the effects of high-light stress on pigment and lipid metabolism in nitrogen-starving microalgae by measuring chlorophyll fluorescence transients: studies with a $\Delta 5$ desaturase mutant of *Parietochloris incisa* (Chlorophyta, Trebouxiophyceae)." Algal Research **2**(3): 175-182.

Sorin, C., et al. (2009). "ATHB4, a regulator of shade avoidance, modulates hormone response in Arabidopsis seedlings." Plant Journal **59**(2): 266-277.

Souter, M., et al. (2002). "hydra mutants of Arabidopsis are defective in sterol profiles and auxin and ethylene signaling." **14**(5): 1017-1031.

Stavang, J. A., et al. (2009). "Hormonal regulation of temperature-induced growth in Arabidopsis." The Plant Journal **60**(4): 589-601.

Straumite, E., et al. (2015). "Pigments in mint leaves and stems." Agronomy research **13**(4): 1104-1111.

Tian, Y., et al. (2017). "Direct impact of the sustained decline in the photosystem II efficiency upon plant productivity at different developmental stages." Journal of plant physiology **212**: 45-53.

Tissot, N. and R. Ulm (2020). "Cryptochrome-mediated blue-light signalling modulates UVR8 photoreceptor activity and contributes to UV-B tolerance in Arabidopsis." Nature communications **11**(1): 1-10.

Toledo-Ortiz, G., et al. (2014). "The HY5-PIF regulatory module coordinates light and temperature control of photosynthetic gene transcription." PLoS Genetics **10**(6): e1004416.

Valladares, F. and Ü. Niinemets (2008). "Shade tolerance, a key plant feature of complex nature and consequences." Annual Review of Ecology, Evolution, Systematics **39**: 237-257.

Wolters, H. and G. J. N. R. G. Jürgens (2009). "Survival of the flexible: hormonal growth control and adaptation in plant development." Nature Reviews Genetics **10**(5): 305-317.

Xie, Y., et al. (2017). "Phytochrome-interacting factors directly suppress MIR156 expression to enhance shade-avoidance syndrome in Arabidopsis." **8**(1): 1-11.

Xu, X., et al. (2014). "PHYTOCHROME INTERACTING FACTOR1 enhances the E3 ligase activity of CONSTITUTIVE PHOTOMORPHOGENIC1 to synergistically repress photomorphogenesis in Arabidopsis." The Plant Cell **26**(5): 1992-2006.

Yang, C. and L. Li (2017). "Hormonal regulation in shade avoidance." Frontiers in plant science **8**: 1527.

Yang, C., et al. (2018). "Phytochrome A negatively regulates the shade avoidance response by increasing auxin/indole acetic acid protein stability." Developmental Cell **44**(1): 29-41. e24.

Yang, J., et al. (2005). "Light regulates COP1-mediated degradation of HFR1, a transcription factor essential for light signaling in Arabidopsis." **17**(3): 804-821.

Yu, Y. and R. Huang (2017). "Integration of ethylene and light signaling affects hypocotyl growth in Arabidopsis." Frontiers in plant science **8**: 57.

Yu, Y., et al. (2013). "Ethylene promotes hypocotyl growth and HY5 degradation by enhancing the movement of COP1 to the nucleus in the light." PLoS Genetics **9**(12): e1004025.

Zhang, H., et al. (2008). "Dolichol biosynthesis and its effects on the unfolded protein response and abiotic stress resistance in Arabidopsis." The Plant Cell **20**(7): 1879-1898.

Zhang, Y., et al. (2013). "A quartet of PIF bHLH factors provides a transcriptionally centered signaling hub that regulates seedling morphogenesis through differential expression-patterning of shared target genes in Arabidopsis." **9**(1): e1003244.

Zhou, Y., et al. (2018). "TCP transcription factors regulate shade avoidance via directly mediating the expression of both PHYTOCHROME INTERACTING FACTOR s and auxin biosynthetic genes." Plant physiology **176**(2): 1850-1861.

CHAPTER II

Identification of novel molecular components involved in controlling the shade avoidance or shade tolerance habit

Wenting Qin^{1,2}, Celia Anton-Sales², Sandi Paulisic¹, Violeta Sánchez-Retuerta¹,
Jaime F. Martinez-Garcia^{1,2}

¹Institute for Plant Molecular and Cell Biology (IBMCP), CSIC-UPV, 46022-València, Spain

²Centre for Research in Agricultural Genomics (CRAG), CSIC-IRTA-UAB-UB, Cerdanyola del Vallès, 08193-Barcelona, Spain.

1. Introduction

Plants have adopted two main strategies to adapt to vegetation proximity and shade: avoidance or tolerance. Shade-avoider species like *Arabidopsis thaliana* (Col-0 accession), *Capsella bursa-pastoris* PHA (Cbu-P), *Capsella bursa-pastoris* SCH (Cbu-S) and *Capsella rubella* (Cru) (Morelli, Paulišić et al. 2021) spend energy promoting elongation in order to outgrow their neighbors at an early stage of growth, a response that is part of a process called the shade avoidance syndrome (SAS). Shade-tolerant plants, such as *Cardamine hirsuta* (Oxford, Ox accession), *Sisymbrium irio* (Sir) and *Arabis alpina* (Aal) (Morelli, Paulišić et al. 2021), by contrast, display often slow growth rates, such as do not involve the stimulation of elongation growth (Valladares and Niinemets 2008). The shade-avoider *A. thaliana* supplied the groundwork for our understanding of the genetic components and regulatory processes involved in the control of the SAS (Martínez-García, Galstyan et al. 2010, Casal 2012, Roig-Villanova and Martínez-García 2016). *A. thaliana* perceives the shade signal via the photoreceptors phytochrome B (phyB) and phytochrome A (phyA), which play important and antagonistic roles in hypocotyl elongation, that is the most noticeable response to low R:FR (Martínez-García, Gallemí et al. 2014). In *A. thaliana* wild-type (At^{WT}) seedlings, exposure to intermediate, low or very low R:FR inactivation of phyB resulted in promotion of hypocotyl elongation. When exposed to very low R:FR, phyA accumulates and becomes active, preventing excessive elongated on hypocotyls and antagonizing phyB inactivation (Martínez-García, Gallemí et al. 2014, Yang, Xie et al. 2018).

In addition, genetic and molecular evidence indicate that PHYTOCHROME INTERACTING FACTORS (PIFs) are main factors promoting shade-stimulated hypocotyl elongation. Under high R:FR (no shade), active phyB interacts with PIFs and inhibits their transcriptional activity. Under low or very low R:FR, removal of active phyB results in PIF-mediated changes in the expression of genes involved in the implementation of the SAS response (Lorrain, Allen et al. 2008). For example, in the model plant *A. thaliana*, At^{WT} and *pifq* seedlings, hypocotyls elongated after simulated shade (W+FR, low R:FR) treatment, whereas *pif7*

seedlings showed a very attenuated elongation response, displaying hypocotyls of a length closer to those grown in white light (W, high R:FR) (**Fig 1A**) (Roig-Villanova and Martínez-García 2016). PIFs are also engaged in the regulation of other signaling pathways, including dark-induced senescence (DIS) and thermal-induced morphogenesis (TIM) (Liebsch and Keech 2016, Galvão, Fiorucci et al. 2019). TIM refers to the effect of warm temperature (28°C) on plant growth and development. In *A. thaliana*, one of the TIM process best characterized is the promotion of hypocotyl length, a phenotype that resembles that of plants growing under simulated shade (Gray, Östin et al. 1998). This induction is in an auxin-dependent way (Koini, Alvey et al. 2009, Stavang, Gallego-Bartolomé et al. 2009).

From published data, among PIFs, PIF4, PIF5 and PIF7 were identified as major regulators of seedling hypocotyl elongation in response to warm temperature, which deduced from the hypocotyl unresponsiveness to warm temperature of the single mutants *pif4*, *pif5* and *pif7* (Quint, Delker et al. 2016, Paik, Kathare et al. 2017, Paulišić, Qin et al. 2021). In our laboratory conditions, *At*^{WT} seedlings elongate in response to warm temperature, whereas *pif7* and *pifq* seedlings display a much attenuated hypocotyl elongation response that is similar to those growing at normal temperature (22°C) (**Fig 1B**). Furthermore, darkness induces senescence in *At*^{WT} and *pif7* seedlings, but *pifq* seedlings maintain green cotyledons after several days under continuous dark conditions (**Fig 1C**). This is consistent with the demonstrated results of an important role for PIFs, especially PIF4, PIF5 and PIF3 (with less contribution) in promoting DIS in *A. thaliana* (Hornitschek, Kohnen et al. 2012). These PIFs were shown to be induced at the transcriptional and protein levels in a phyB-dependent manner during prolonged darkness. Moreover, their overexpression resulted in accelerated DIS, while their mutant combination showed a delay, with the strongest effect observed in the *pifq* mutant. In contrast with *A. thaliana*, seedlings of *C. hirsuta* (wild type, *Ch*^{WT}) exhibit no response to shade and warm temperature. In addition, *Ch*^{WT} seedlings also display a delayed DIS in comparison to the *At*^{WT} when transferred to darkness (**Fig 1**) (Paulišić, Qin et al. 2021).

Altogether, we would like to test if shade-tolerant plants behave similarly to *A.thaliana* PIFs deficient lines in the previously described PIF-mediated processes (**Fig 1**). According to this information, a genetic screening was initiated in our laboratory. This screening was based on characterized mutant or transgenic lines that have delayed DIS and altered hypocotyl length in both shade and warm temperature conditions. We aimed to get the novel molecular components involved in the control of PIF-based shade avoidance or shade tolerance habit.

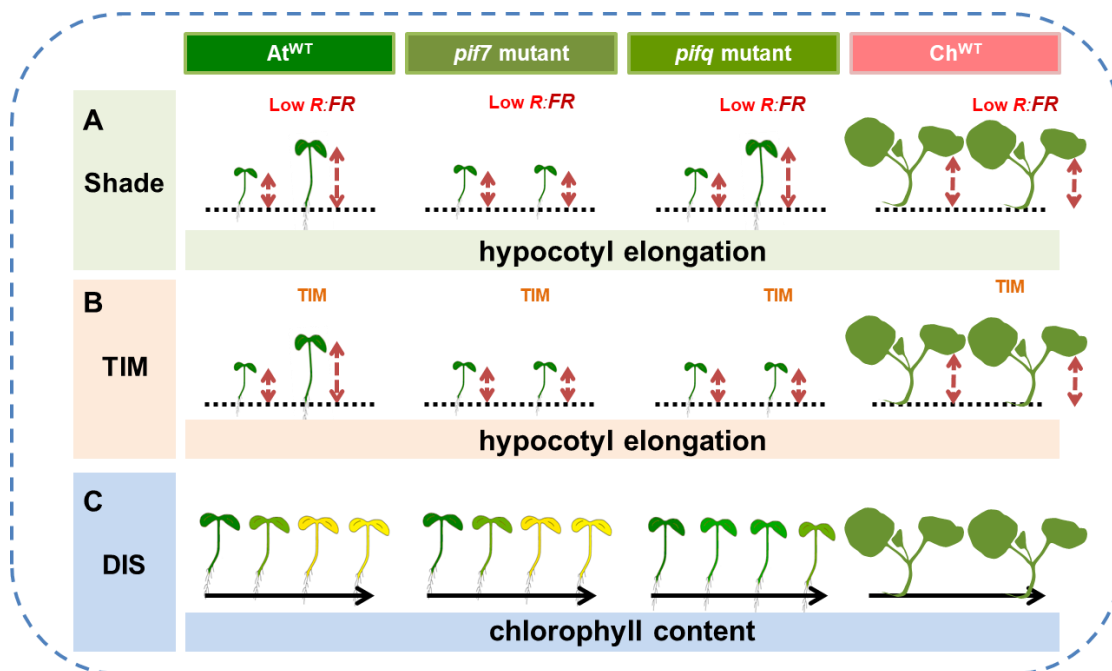


Figure 1. Summary of the PIF-dependent phenotypes described in *A. thaliana* and *C. hirsuta* seedlings. **(A)** Hypocotyl elongation in response to high (left) and low R:FR (right). **(B)** Hypocotyl elongation in response to normal (22°C, left) and warm temperature (28°C, right). **(C)** Chlorophyll content in response to DIS.

2. Result

2.1 Characteristics of shade-tolerant plants

2.1.1 Hypocotyls of shade-tolerant species are unresponsive to warm temperature

The result raised the possibility that PIF activity was lower in shade-tolerant than in shade-avoider species. In order to investigate this idea further, we analyzed a set of PIF-dependent responses in a set of mustards characterized by us as shade-tolerant (*C. hirsuta*, *S. irio* and *A. alpina*) and shade-avoider (*A. thaliana*, *C. bursa-pastoris PHA*, *C. bursa-pastoris SCH* and *C. rubella*) species. Based on published information (Paulišić, Qin et al. 2021), we hypothesized that in *C. hirsuta* or other shade-tolerant species the restrained PIF activity may impair TIM responses. Following that, we explored the effects the thermo-induced hypocotyl elongation in seedlings of the several shade-avoider and shade-tolerant species characterized for the DIS. We analyzed this response by growing seedlings constantly at 22°C, 28°C, or transferred from 22°C to 28°C after day 2 from germination (**Fig 2A**). Whereas warm temperature promoted hypocotyl elongation of *At*^{WT} seedlings compared to those growing at 22°C, *pifq* (loss function of PIF1, PIF3, PIF4 and PIF5) and *pif7 pifq* (loss function of PIF7) mutant seedlings were almost unresponsive to 28°C (**Fig 2B**), in accordance with the role of PIF4, PIF5, and PIF7 in thermomorphogenesis (Stavang, Gallego-Bartolomé et al. 2009, Franklin, Lee et al. 2011, Hay, Pieper et al. 2014, Fiorucci, Galvão et al. 2020). Hypocotyls of the three shade-avoider species (*C. bursa-pastoris PHA*, *C. bursa-pastoris SCH* and *C. rubella*) elongated in response to warm temperatures, similar to *A. thaliana* (**Fig 2C**). When analyzing the group of shade-tolerant species, we observed that the hypocotyls of *Ch*^{WT} and *S. irio* seedlings were unresponsive to warm temperatures. By contrast, *A. alpina* seedlings responded to this treatment, though to a lower extent than *A. thaliana* (**Fig 2D**). Altogether, our results indicated that shade-avoider species respond to warm temperatures by elongating their hypocotyls, whereas shade-tolerant species showed a lack or attenuated TIM response.

(This part was done by Violeta Sanchez Retuerta, Master in Plant Biology, Genomics and Biotechnology 2017).

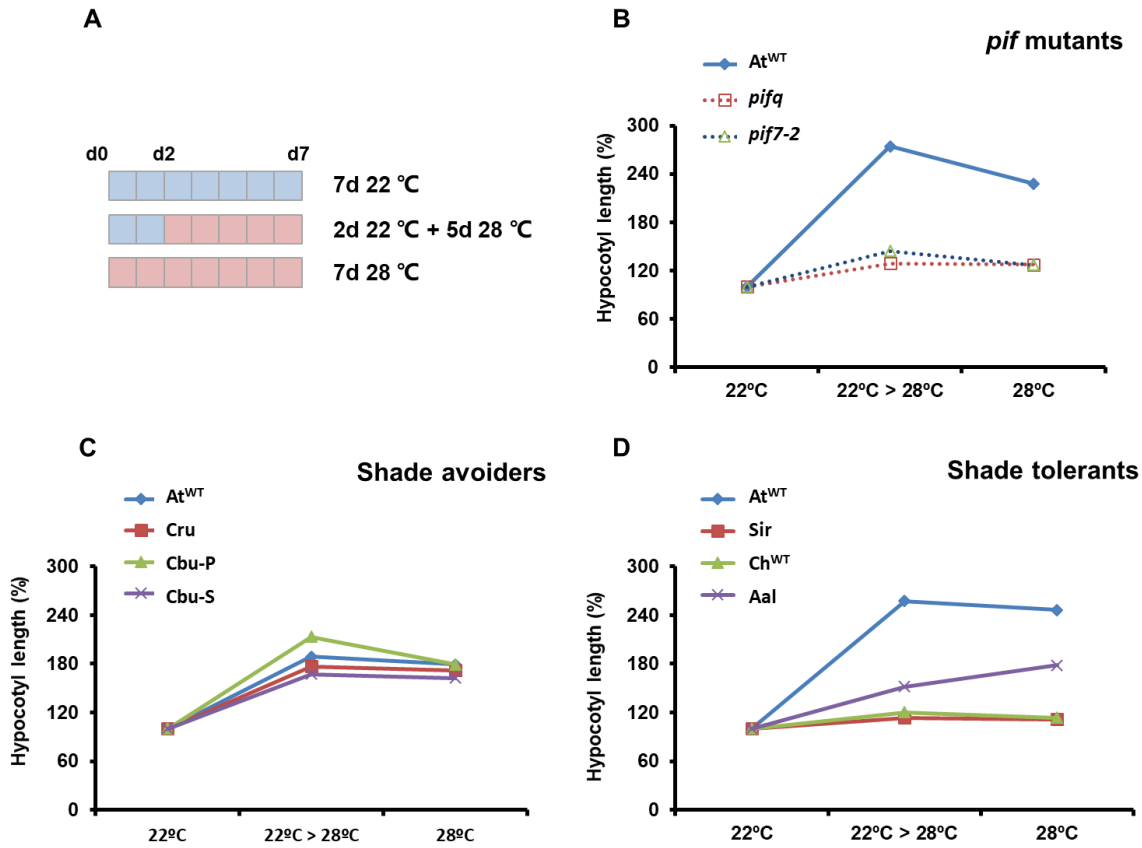


Figure 2: Thermo-induced morphogenesis of seedlings of shade tolerant and shade avoider species compared to *A. thaliana*, *pifq* and *pif7-2* mutants. **(A)** Cartoon describing the experiment set up. **(B-D)** Normalized hypocotyl length of seedlings of **(B)** At^{WT}, *pifq* and *pif7-2* mutants. **(C)** At^{WT}, *C. bursa-pastoris* PHA (Cbu-P), *C. bursa-pastoris* SCH (Cbu-S) and *C. rubella* (Cru). **(D)** Ch^{WT}, *S. irio* (Sir) and *A. alpina* (Aal) grown at different temperatures, as indicated in **A**. The values are the means ± SE of at least 15 seedlings of three independent biological replicates.

2.1.2 Shade-tolerant plants show overall a delayed DIS

Another well-established PIF-dependent response in *A. thaliana* is the DIS (Sakuraba, Jeong et al. 2014). DIS was investigated by transferring 7-day-old seedlings grown in W to darkness for up to 10 days. To determine the senescence progression, chlorophyll content was analyzed before transferring to the dark (0DD) and at various moments throughout the dark incubation (5DD and 10DD) (**Fig 3A**). After 10DD, *At*^{WT} and *pif7* seedlings were pale, indicating that they were senescing; by contrast, *pifq* mutant seedlings still retained its green color (**Fig 3B**). Chlorophyll levels quantification confirmed this view, as their relative levels dropped to about 7% of those at 0DD in both *At*^{WT} and *pif7* seedlings whereas in *pifq* chlorophyll levels stayed at about 45% (**Fig 3E**). These results are consistent with the published results on the central role of PIF4 and PIF5 in promoting DIS in Arabidopsis (Sakuraba, Jeong et al. 2014). Seedlings of the other three shade-avoider species (*C. bursa-pastoris* PHA, *C. bursa-pastoris* SCH and *C. rubella*) became extremely pale and dropped their chlorophyll levels, indicating they entered in senescence as *A. thaliana* (**Fig 3C and F**). Chlorophyll levels of *C. rubella* were not estimated because there were problems with the synchronization of seed germination in this species. We next tested this response in the shade-tolerant species (*C. hirsuta*, *S. irio* and *A. alpina*). After 10DD seedlings of *C. hirsuta* and *S. irio* senesced more slowly and remained greener than *At*^{WT}, similar to those of *pifq* (Paulišić, Qin et al. 2021). Relative levels of chlorophylls in these two species paralleled the slow senescing rate (**Fig 3D**). By contrast, *A. alpina* seedlings began to turn pale after 10 days and their relative chlorophyll levels dropped more dramatically after 10DD (2 %) than *At*^{WT} (7 %) (**Fig 3G**). In summary, the results showed that shade-avoider species got a faster senescence in response to dark (based on CHL levels), whereas shade-tolerant species presented more variation in the delay of this response. An exception to this tendency was *A. alpina*, which behaved like the shade-avoider species. Based on those results, we concluded that the delay DIS and attenuated hypocotyl response in TIM overall associated with the shade tolerant habit, which are all PIF-induced processes. An exception to this observation is *A. alpina*.

(This part was done by Violeta Sanchez Retuerta, Master in Plant Biology, Genomics and Biotechnology 2017).

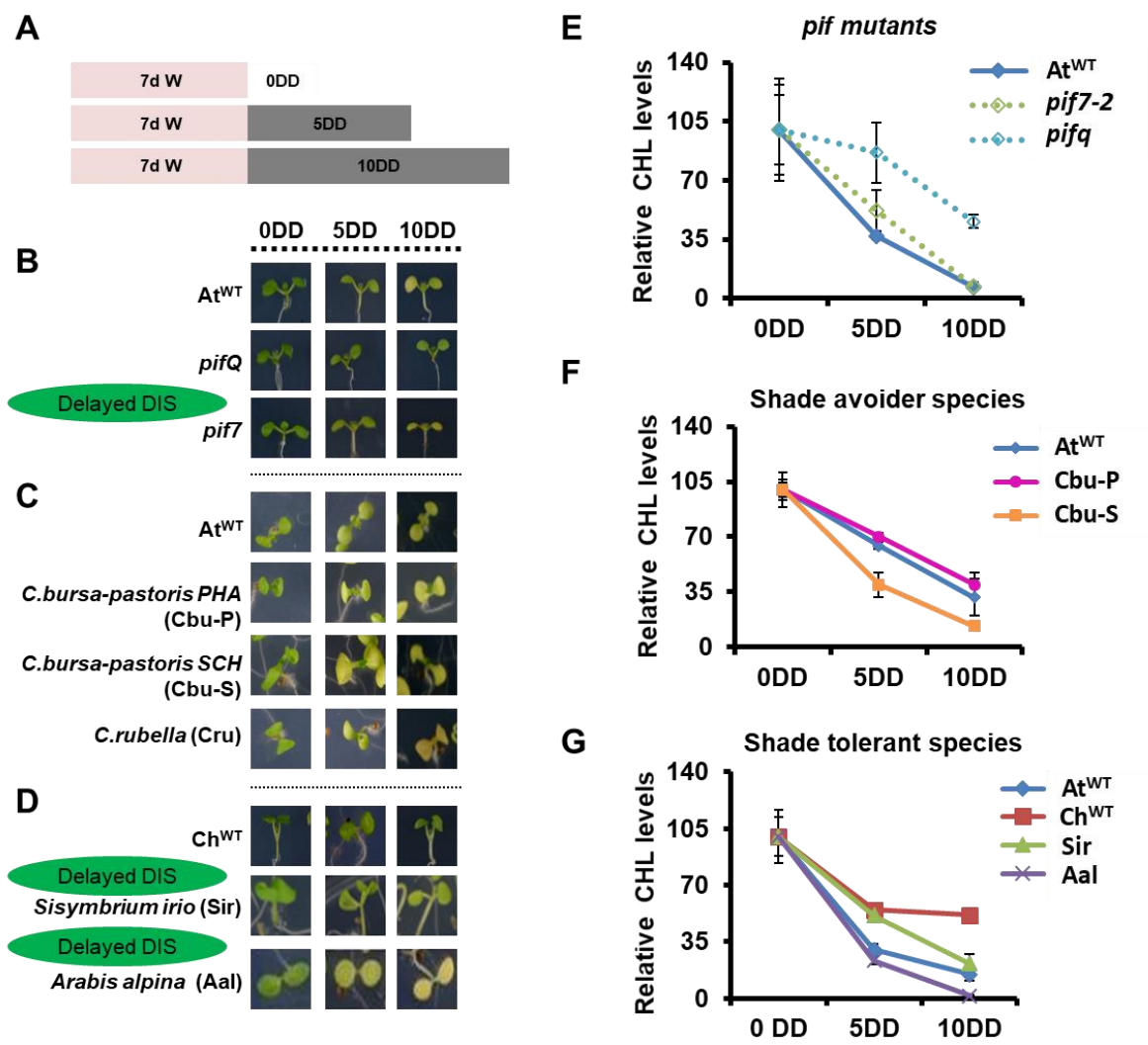


Figure 3. Dark-Induced Senescence (DIS) of shade tolerant and shade avoider species compared to *A. thaliana* wild-type and *pifq* lines. **(A)** Cartoon describing the experiment set up. **(B-D)** Aspect of seedlings of **(B)** At^{WT}, *pifq* and *pif7* mutants; **(C)** At^{WT}, *C. bursa-pastoris* PHA (Cbu-P), *C. bursa-pastoris* SCH (Cbu-S) and *C. rubella* (Cru); **(D)** Ch^{WT}, *S. irio* (Sir) and *A. alpina* (Aal) grown as indicated in the

dark. **(E-G)** Relative chlorophyll (CHL) levels of seedlings of **(E)** *At*^{WT}, *pifq* and *pif7* mutants; **(F)** *At*^{WT}, *Cbu-P* and *Cbu-S*; **(G)** *Ch*^{WT}, *Sir* and *Aal* grown as indicated in **A** after 0DD, 5DD and 10DD. The values are the means \pm SE of four independent biological replicates.

2.1.3 Different early changes in chlorophyll fluorescence levels

The detection of these early senescence-related changes by harvesting dozens of individual seedlings and extracting photosynthetic pigments as described above, these are invasive methods that prevent temporal analysis of individual seedlings, which complicate the establishment of genetic screenings intended to identify potential mutants defective in the DIS process. To overcome these limitations, non-invasive and quantitative strategies need to be developed. One possibility is based on early changes in chlorophyll levels. Therefore, to compare DIS phenotypes of different genotypes quantitatively, we tested the use of non-invasive measurements of photosystem II (PSII) activity using an IMAGING-PAM Chlorophyll Fluorometer machine (Heinz Waltz GmbH, Germany). Early changes in chlorophyll levels are one way to detect early senescence, it is proportionally reflected by changes in chlorophyll fluorescence (CF) measurements (Solovchenko, Solovchenko et al. 2013, Alonso, Van Wittenberghe et al. 2017). The CF measurements essentially include the assessment of the chlorophyll fluorescence yield, in which there are 2 main significant parameters, one is the maximum quantum yield of PSII (F_v/F_m) and the other is the effective quantum yield of PSII (ϕ_{PSII}), which can be calculated by the so-called saturating pulse method (Schreiber 2004, Murchie and Lawson 2013). Specifically, F_v/F_m has been shown theoretically and empirically to be a reliable indicator of the maximum energy conversion yield of PSII reaction centers, which are highly sensitive to abiotic and biotic stresses (Murchie and Lawson 2013). Similarly, ϕ_{PSII} is an important photosynthetic-related parameter that describes the operating efficiency of the PSII photochemistry at a given photosynthetically active photon flux density (PPDF) (Murchie and Lawson 2013).

According to this information, we performed CF measurements of multiple seedling lines which include *At*^{WT} and *Ch*^{WT}, as well as *A. thaliana* mutants with a reduced PIF activity, such as *pifq* and *pif45* (loss function of PIF4 and PIF5); in addition, the mutant line *aba deficient 2 (aba2)*, which has the abscisic acid (ABA) biosynthesis impaired and *HY5ox*, a transgenic lines overexpressing *HY5* fused to the *GFP* marker gene (*35S:HY5-GFP*) were also selected. From the results we found that all these selected *A. thaliana* mutant genotypes presented delayed DIS compared to *At*^{WT} (**Fig 4**), as well as *Ch*^{WT} as a shade-tolerant species that also displayed a delayed DIS phenotype (stays green for longer than *At*^{WT} after transferring them to darkness) (**Fig 4**), which is consistent with our previous works (Paulišić, Qin et al. 2021). Because the line *HY5ox* showed an increased activity in *HY5*, which would also contribute to a reduction in PIFs activity compared to *At*^{WT} (Xu, Paik et al. 2014). Based on this, the results suggest that *Ch*^{WT} like the *A. thaliana* PIFs-deficient mutant ones, showing a delayed DIS in comparison to the *At*^{WT}.

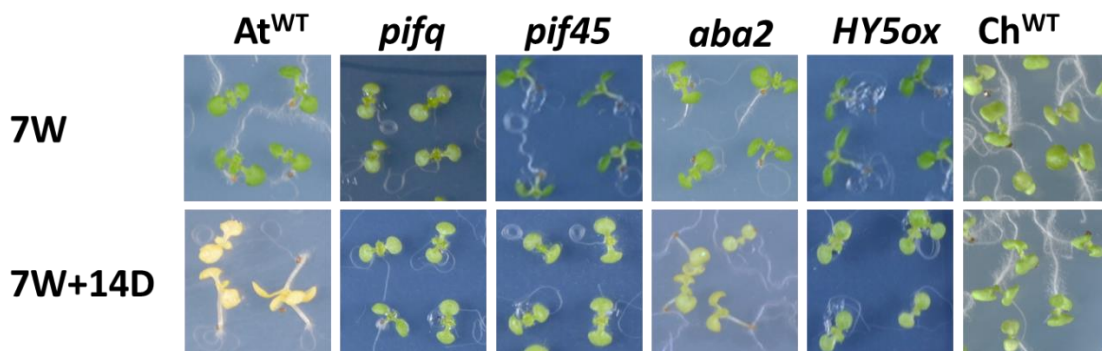


Figure 4. Aspect of *At*^{WT}, *pifq*, *pif45*, *aba2*, *HY5ox* and *Ch*^{WT} seedlings grown for 7 days in continuous W (upper panels) and then transferred to darkness for 14 to induce DIS (lower panels).

Then, we have gathered data of the 2 main CF parameters (F_v/F_m and ϕ_{PSII}) in 4 different time points including 0, 2, 4 and 7 days in the dark (0DD, 2DD, 4DD, and 7DD, respectively) for all the mentioned genotypes (**Fig 5A**). These measurements gave us a good understanding of the *in vivo* photosynthetic

performance of plants upon transference to dark, as reported (Buchanan - Wollaston et al., 2005). The results indicated that under 0DD, all genotypes exhibited similar values of Fv/Fm (around 0.70-0.75) (**Fig 5B**) and ϕ PSII (around 0.65-0.70) (**Fig 5C**). When plants were transferred to the dark, a marked and progressive decrease in both Fv/Fm and ϕ PSII was observed (2DD, 4DD and 7DD). The lowest values were observed after 7DD for all the studied genotypes (**Fig 5B and C**).

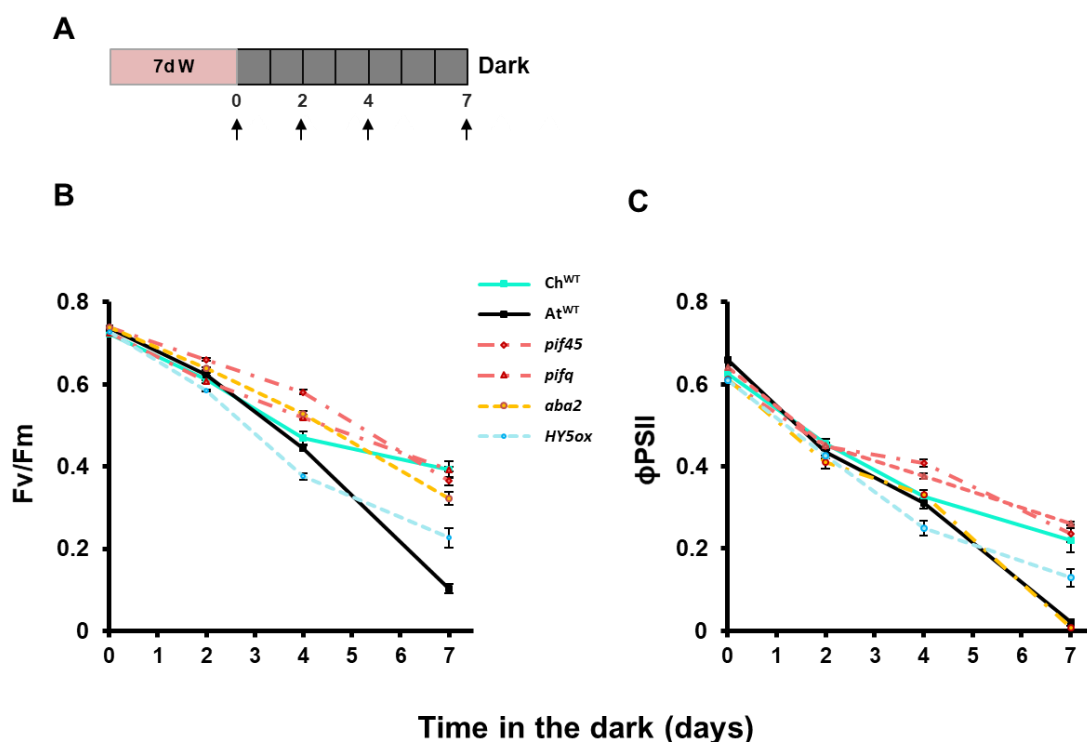


Figure 5. Photosynthetic-related responses of *A. thaliana* and *C. hirsuta* seedlings and *A. thaliana* mutants presenting a delayed DIS after transfer to darkness conditions. **(A)** Cartoon representing growth conditions of seedlings for the chlorophyll fluorescence analysis and photosynthetic-related responses studied by PAM-fluorimetry. Seedlings were germinated and grown for 7 days in white light and transferred to total darkness for 2, 4 and 7 days. **(B)** Maximum photochemical efficiency of PSII in the dark-adapted state (Fv/Fm) and **(C)**

effective quantum yield of PSII (ϕ PSII) are shown at the times indicated in **A**. The values are the means \pm SE of three independent biological replicates.

When comparing the various mutant phenotypes, no significant differences were observed in both parameters for seedlings analyzed at 2DD (**Fig 5B and C**). A turning point was observed after 4DD, at which the Fv/Fm and ϕ PSII values of At^{WT} and Ch^{WT} started to be significantly different ($p < 0.05$) (**Fig 6A and C**). Mutants with a reduced PIF activity (*pifq* and *pif45*) maintained their Fv/Fm and ϕ PSII values higher compared to At^{WT} , in agreement with the key role of PIFs in the DIS (**Fig 6A and C**). The Fv/Fm and ϕ PSII values in *HY5ox* seedlings, that dropped at 2DD and 4DD faster than those of At^{WT} , were stabilized considerably at 7DD and remained higher than in At^{WT} but lower than those of the *pif45* and *pifq* mutants (**Fig 6B and D**); these results suggested that HY5 has the role in improving DIS but weaker than *pifq* and *pif45*. In addition, *aba2* seedlings maintained the Fv/Fm values after 7DD like those of *pifq* and *pif45* (also significantly higher than At^{WT}) (**Fig 6B and D**), which reflects the impaired stress signaling occurring in this mutant line with an impaired ABA biosynthesis. When did the comparison between *aba2* and At^{WT} , the *aba2* mutants exhibiting the lowest ϕ PSII values after 7DD dark treatment, indeed, the ϕ PSII of *aba2* follows a decreasing pattern upon darkness as observed with At^{WT} (**Fig 6D**), meaning that the photosynthesis efficiency is affected by the senescing program in the same way as At^{WT} . In summary, these analyses showed that (1) Ch^{WT} exhibits a phenotype in the dark that resembles that of *pifq* and *pif45* mutants, and (2) PIF-defective mutants and *HY5ox* are senescing differently than *aba2*.

(This part was done by Celia Anton Sales, Master in Plant Biology, Genomics and Biotechnology 2020).

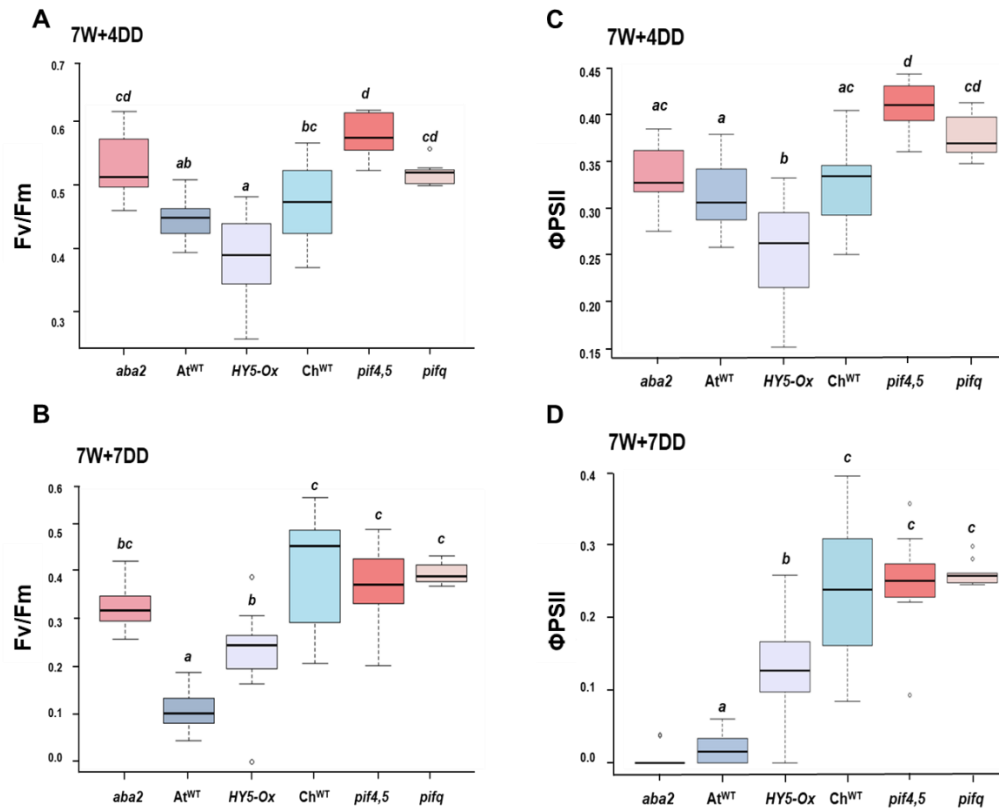


Figure 6. Photosynthetic-related responses in the dark-adapted state of *A. thaliana* and *C. hirsuta* seedlings. Maximum photochemical efficiency of PSII in (A) 4DD and (B) 7DD. Effective quantum yield of PSII (ϕ PSII) in (C) 4DD and (D) 7DD. Values represent mean and standard error of n=10 seedlings per treatment. Different letters indicate a significant difference between genotypes at the indicated time point (Tukey's multiple comparison test, $P < 0.05$).

2.2 Screening from EMS-mutagenized pools

2.2.1 Selection of mutants displaying a delayed DIS phenotype

In order to identify novel molecular components involved in controlling the shade tolerance habit, we aimed to do a genetic screening. Previously (sections 2.1.1 and 2.1.2), our results suggested that the TIM hypocotyl elongation and the DIS response in seedlings were somehow related to the shade tolerant habit. This association of phenotypes led us to hypothesize that all three processes might share some regulatory components, such as PIFs, known to regulate all of them.

Therefore, we have postulated that the shade habit of a plant (avoidance or tolerance) co-regulates with the TIM and DIS responses. Based on this, we devised a screening aimed at identifying seedlings displaying a delayed DIS. We expected that some of these mutants would show also altered (likely attenuated) hypocotyl responses to warm temperature and simulated shade.

As the first step of the screening, we wanted to optimize the induction of the DIS phenotype. To address this, we first explored the effect of the time in which seedlings would grow in W and dark. For testing that, *At*^{WT}, *pifq*, *pif457* (loss function of PIF4, PIF5 and PIF7) and *HFR1*_{ox}, a transgenic lines overexpressing *HFR1* fused to the *GFP* marker gene (*35S:HFR1-GFP*). These seedlings were germinated and grown for 3, 4, 5 or 7 days, respectively, under continuous W before transferring them to dark for 10 or 14 days at 22°C. These three mutant lines were selected because they are PIFs-deficient mutant ones, which showing a delayed DIS in comparison to the *At*^{WT}. *HFR1*_{ox} showed an increased activity in HFR1, which would also contribute to a reduction in PIFs activity compared to *At*^{WT} (Paulišić, Qin et al. 2021). The results indicated that seedlings that were growing in W for 3, 4 or 5 days and then transferred to the dark for 10 or 14 days appeared not to enter in senescence, suggesting these conditions were not adequate for the proposed screening. When seedlings were grown for 7-day in W and then transferred to the dark for 10 or 14 days, only *At*^{WT} seedlings entered in senescence. The senescence phenotype was more clearly distinct from the mutant lines when time in the dark was extended to 14 days (**Fig 7**). These results suggested that *At*^{WT} seedlings growing for 7 days under continuous W and then transferred to darkness for 14 days at 22 °C displaying a delayed DIS phenotype that could be clearly distinguished from that of PIF-related mutants that still retained their green color.

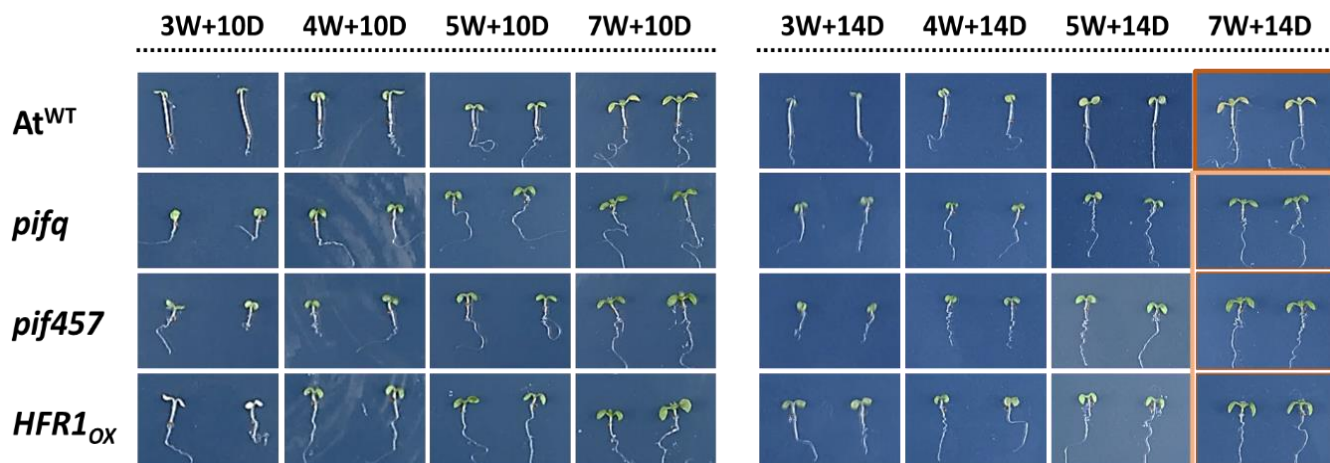


Figure 7. Aspect of *At*^{WT}, *pifq*, *pif457* and *HFR1*_{ox} seedlings grown for 3, 4, 5 or 7 days in continuous W and then transferred to darkness for 10 or 14 to induce DIS.

Based on these results, we established as the screening conditions to germinate and grow seeds at 22°C under continuous W for 7 days and then transfer them to darkness for 14 days to induce DIS. To do so, we employed a collection of *At*^{WT} seeds mutagenized with 0.3% (v/v) ethyl-methanesulfate (EMS), a chemical mutagen that predominantly introduces C to T and G to A changes. After mutagenesis, about 2500 seeds were sown in groups of 5 individuals per pot to germinate and let them grow in the greenhouse until maturity. These plants were considered the M1 generation. The seeds of each pot (M2 generation) were harvested together, conforming a total of 504 independent pools. In summary, we had 504 pools of M2 seeds, each of one originated from 5 different M1 plants.

We screened around 100 seeds for each pool of a total of 320 individual M2 pools. As a result, I isolated more than 60 seedlings that stayed green, which were considered as “putative” mutant seedlings. These mutants belonged to 28 independent pools (i.e., when two mutant seedlings were identified in the same pool, they were considered as non-independent). From those, more than 50% belong to 6 families (a family means they are from the same M2 pool of seeds). We named the individual plant with the pool number (e.g., m45) followed by a number to indicate the number of seedlings that were selected as mutant from the

same family (e.g., m45.1, m45.2, m45.3 and m45.4). The isolated seedlings were transferred to pots to produce seeds. From the resulting M3 seeds, only 31 lines out of the 60 maintained the delayed DIS phenotype, that belong to 23 independent pools. We considered these 31 lines as authentic mutants. An overview of the screening and the name of the generations are shown in **Fig S1**.

2.2.2 Additional sequential screenings of the selected mutants with a delayed DIS

Next, we performed two additional screenings with the M3 seeds of the 31 mutant lines for further selecting: we analyzed the hypocotyl elongation induced by simulated shade or by warm temperature to select these mutant lines showing an altered (attenuated or enhanced) elongation response to simulated shade and/or warm temperature. We first analyzed their shade response by growing seedlings at W 2 days at 22°C, then transferred to low R:FR or very low R:FR conditions for 5 days more. As a result, 16 of the selected lines had an altered hypocotyl elongation in response to low R:FR (m39.3, m45.4, m67.3, m74.3, m74.5, m84.2, m96.3, m119.1, m121.1, m146.2, m148.4, m217.2, m239.1, m254.3, m289.1 and m304.1) and 20 lines to very low R:FR (m39.3, m45.4, m67.3, m74.6, m83.1, m84.2, m96.3, m119.1, m121.1, m135.2, m146.1, m146.2, m148.3, m153.1, m209.1, m239.1, m251.1, m254.3, m289.1 and m304.1) compared to wild type plants (**Fig S2**). Based on these, I found that seedlings of 12 lines have an altered elongation response to both shade conditions compared to the wild-type line. Five of them (m39.3, m96.3, m254.3, m289.1 and m304.1) were displaying an enhanced hypocotyl elongation in response to low R:FR and very low R:FR conditions compared to *At*^{WT}. On the contrary, other 6 lines (m45.4, m67.3, m119.1, m121.1, m146.2 and m239.1) were showing an attenuated hypocotyl elongation in response to these shade conditions. The mutant line m84.2, displayed an enhanced hypocotyl elongation in low R:FR but a slightly attenuated elongation in very low R:FR compared to the wild-type seedlings (**Fig S2**). For the rest of lines identified, some lines only had an altered phenotype in low (m74.3, m74.5, m148.4 and m217.2) or very low (m74.6, m83.1, m135.2, m146.1, m148.3, m153.1, m209.1 and m251.1) R:FR, so at this stage we did not

consider them to work with. In summary, from a total of 31 mutant lines displaying a delayed DIS, 12 presented an alteration in their hypocotyl elongation in response to shade (**Fig S2**). We checked the hypocotyl elongation of the 12 selected lines in the two shade conditions again. The results obtained were similar as before (**Fig 8**), even though some length differences were not statistically significant, they had a similar trend (e.g., lines m146.2 and m239.1).

Next, we explored the response to warm temperature (TIM) of these 12 lines by growing seedlings constantly at 22°C, at 28°C, or transferring them to 28°C after day 2 at 22°C. Seedlings of all the tested lines have an altered elongation response to warm temperature compared to *At*^{WT}. Five of them (m84.2, m96.3, m254.2, m289.1 and m304.1) were displaying longer and 7 lines (m39.3, m45.4, m67.3, m119.1, m121.1, m146.2 and m239.1) showed shorter hypocotyls in response to warm temperature than *At*^{WT} (**Fig 8**). All lines except m39.3 displayed the same trend in hypocotyl elongation alteration as in shade (**Fig 8**). For the mutant line m84.2, which showed an enhanced hypocotyl elongation in low R:FR but a slightly attenuated elongation in very low R:FR compared to the *At*^{WT} at the first shade experiment (**Fig S2**), while at the second time, this line performed an enhanced hypocotyl elongation in both low R:FR and warm temperature, no significantly change in very low R:FR (**Fig 8**), because we made three biological replicates in the second selection, which was more reliable than the first one, so for this line, hypocotyls were enhanced after treatment. In summary, we identified 12 lines showing a delayed DIS and a significantly altered (attenuated or enhanced) elongation response to both simulated shade and warm temperature conditions, and they had a significant change in at least one of the responses (**Fig 8**). Seedlings displaying an attenuated response to shade or warm temperature were named as *ever green and attenuated in shade and TIM* (*eva*) mutants and the second one *attenuated DIS and enhance hypocotyl elongation in shade and TIM* (*adm*) mutants. The mutant line m39.3 was named as *enhanced hypocotyl elongation in both types of shade but attenuated elongation in TIM* (*eden*) mutants. These 12 *A. thaliana* mutant lines were considered as true mutant candidates for identifying components involved in coordinating the regulation of these responses.

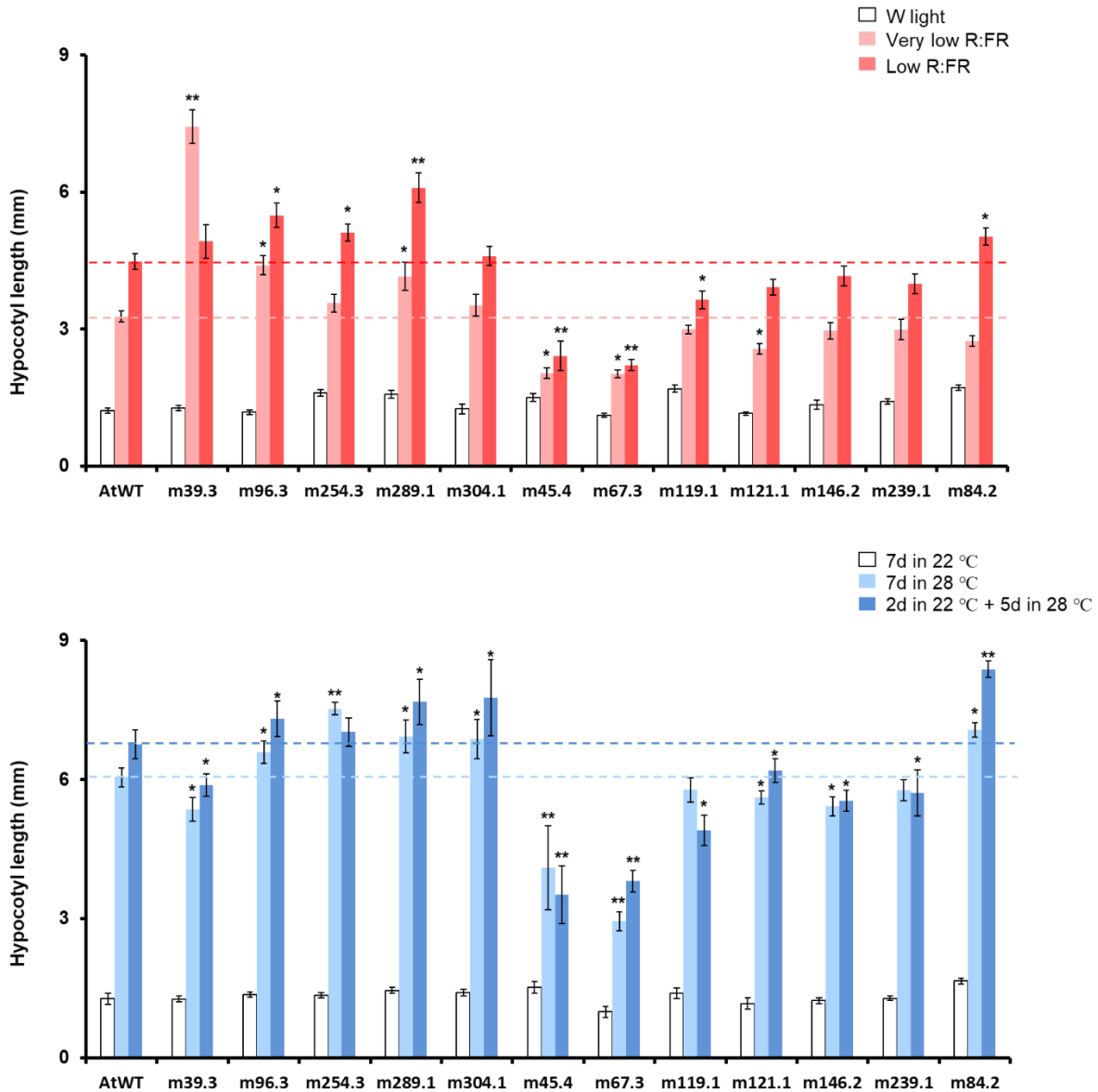


Figure 8. Hypocotyl length of *A. thaliana* seedlings in response to different shade and warm temperature conditions. The values are the means \pm SE of at least 10 seedlings of three independent biological replicates. Asterisks mark significant differences (student's t-test: *P-value < 0.05, **P-value < 0.01) between mutants and At^{WT} in the same light conditions.

2.2.3 Chlorophyll levels dropped slowly in mutants

We next detected chlorophyll fluorescence of the selected mutant lines to evaluate the variations in the senescence degree after different times in the dark.

We grew seeds under continuous W at 22°C for 7 days and then transferred them to darkness for 7-12 days (22-24°C) to induce senescence (**Fig 9A**). *At*^{WT}, *pifq*, m119.1 and m254.3 (from now on m119 and m254, respectively) were analyzed first. The Fv/Fm (around 0.70-0.80) and ϕ PSII (around 0.30-0.60) values were similar in ODD seedlings of all the lines analyzed. When seedlings were exposed to darkness, a progressive decrease in the Fv/Fm and the ϕ PSII was observed with time (7, 10, 12DD), so the lower values were observed after 12DD for all the studied genotypes (**Fig 9B**). However, after 12DD, except *At*^{WT}, the Fv/Fm value of m254 also becomes 0, and the ϕ PSII of all lines is 0, so it is difficult to distinguish them with these two parameters (**Fig 9B**). Based on these results, we found that the differences between *At*^{WT} and the rest of mutant lines analyzed of Fv/Fm and PSII became obvious after 10DD. From the two parameters analyzed, the Fv/Fm value provided more clear differences when compared to *At*^{WT} (The Fv/Fm of only *At*^{WT} is 0, the rest are not.) (**Fig 9B**). Based on this observation, we analyzed the Fv/Fm in the rest 10 mutant lines growing the seedlings for 7 days in W (7W) and then transferring them to darkness for 10 days (7W + 10DD). As a result, we established that the Fv/Fm (around 0.40-0.70) value were similar in ODD seedlings of all the tested lines. When seedlings were exposed to darkness, a gradual decrease in Fv/Fm was observed, with the lowest value from *At*^{WT} at 0. By contrast, the highest value is from *pifq* (around 0.1-0.2). Fv/Fm value of all other lines are between these two values (**Fig 9C**). In summary, these analyses showed that (1) 10DD is a good choice for distinguishing wild-type and mutants with Fv/Fm values and (2) the Fv/Fm values of the PIF-related mutants were between *At*^{WT} and *pifq*.

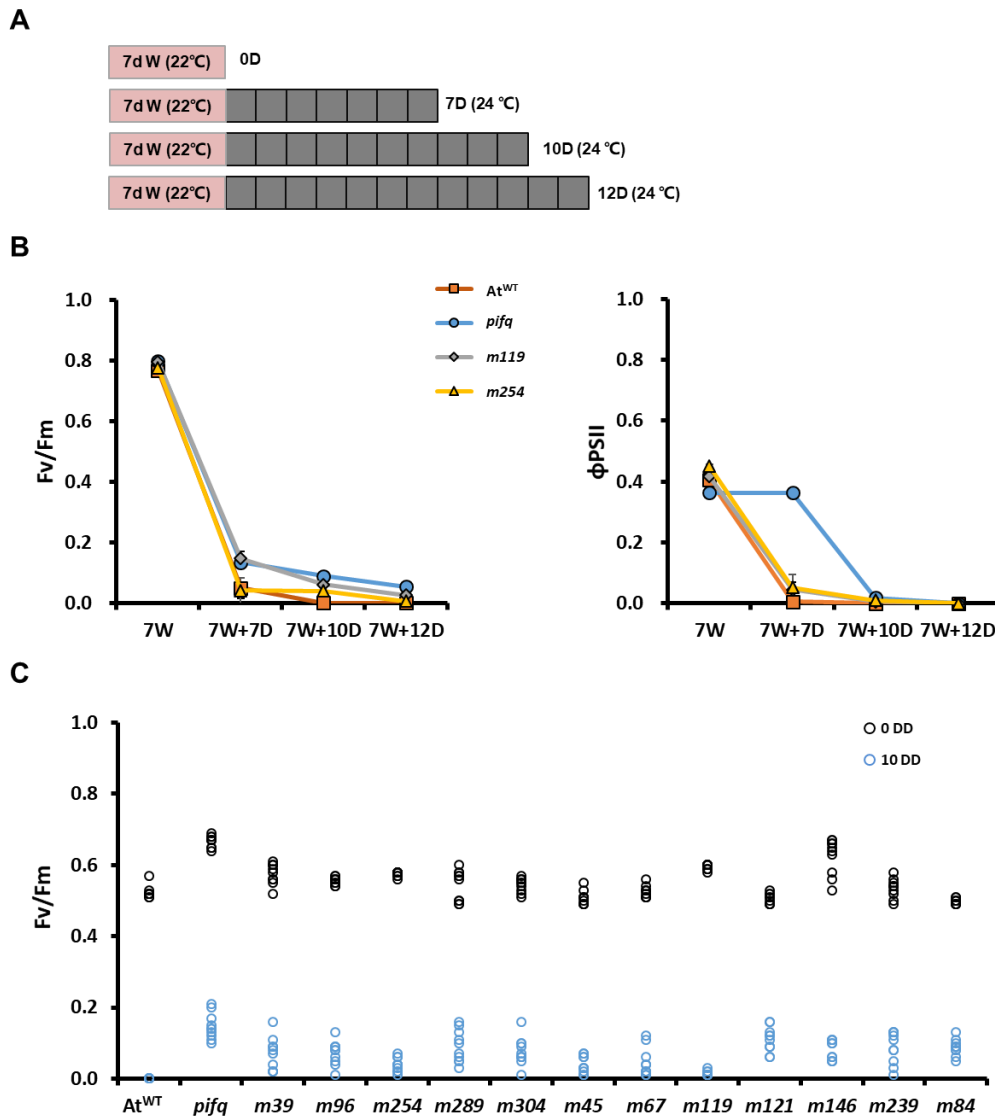


Figure 9. Photosynthetic-related responses of *A. thaliana* and *A. thaliana* mutants presenting an altered hypocotyl elongation after transfer to shade and TIM. **(A)** Cartoon representing growth conditions of seedlings for the chlorophyll fluorescence analysis and photosynthetic-related responses studied by PAM-fluorimetry. Seedlings were germinated and grown for 7 days in white light and transferred to total darkness for 7, 10 and 12 days. **(B)** The maximum photochemical efficiency of PSII (Fv/Fm) and the effective quantum yield of PSII (ϕ PSII) in the 7, 10 or 12 dark-adapted state of At^{WT}, *pifq*, m119 and m254 seedlings. The values are the means \pm SE of three independent biological

replicates. **(C)** Fv/Fm value in other 10 candidate lines. Different colored circles represent different times of darkness, black is 0DD and blue is 12DD. The values are detected 10 seedlings per line.

2.3 Mapping by sequencing to identify the mutated genes

2.3.1 Backcrossing to purify mutants

To proceed with the genetic and molecular characterization of the mutations, we first backcrossed those 12 mutants with At^{WT} (Col-0). In addition, these crosses would clean the mutated lines from unrelated mutations that might have been induced by EMS during the preparation of the mutagenized population. After crossing, I subjected the resulting F₂ segregating populations of those 12 lines (B₁F₂) to a dark treatment to induce senescence. There are two possible phenotypes for these 12 lines, which are green after DIS or pale. We performed a chi-square test to check whether the observed segregation of DIS provided an approximate deviation from the expected value (Cochran 1952). In our cases, the chi-square test statistic values for each mutant line are calculated to prove that the observed number of green seedlings after DIS is a normal distribution at 5% significance level. Then checking the critical table value (**Table S1**) at the 0.05 level, which is 3.841, suggesting that if calculated chi-square is less than 3.841, the null hypothesis will be accepted, which predicts a theoretical segregation ratio of 1:3 for one T-DNA insertion, implying that the tested mutant line is monogenic recessive, which refers to the kind of inheritance whereby a trait is determined by the expression of a single gene or allele, not by several genes as in polygenic inheritance (Eichers, Lewis et al. 2004). By contrast, if calculated chi-square is more than 3.841, the line will be the monogenic dominant. Based on our results, we found that all 12 mutations were monogenic recessive (**Table 1**).

Table 1. The Chi-square analysis of the segregation populations.

Name	Green seedlings	Pale seedlings	Total (green+pale)	Chi square
m39B ₁ F ₂	15	60	75	1.00
m45B ₁ F ₂	12	63	75	3.24
m67B ₁ F ₂	14	61	75	1.60
m84B ₁ F ₂	24	51	75	1.96
m96B ₁ F ₂	12	63	75	3.24
m119B ₁ F ₂	30	70	100	1.33
m121B ₁ F ₂	22	53	75	0.75
m146B ₁ F ₂	15	60	75	1.00
m239B ₁ F ₂	12	63	75	3.24
m254B ₁ F ₂	12	63	75	3.24
m289B ₁ F ₂	17	83	100	3.41
m304B ₁ F ₂	14	61	75	1.60

2.3.2 Mapping by sequence revealed candidate mutations

After that, we chose a few lines to do the chromosome mapping, that was performed in collaboration with Professor Jose Luis Micol (Universidad Miguel Hernandez, Elche, Spain). Using the F₂ segregating population (B₁F₂ or B₂F₂) of lines m45, m84, m119, m121, m146, m239 and m254, we selected at least 100 seedlings that displayed a clear delayed DIS after 10-12 days in the dark (i.e., they were greener than At^{WT} seedlings grown in parallel under the same conditions). The selected seedlings were then transferred to individual pots and grown in greenhouse. For each mutant line, one leaf of each individual plant was harvested and pooled together with those of the more than 100 plants selected, resulting in samples of > 1 g of fresh weight (**Table 2**).

Table 2. The details of samples for mapping by sequence.

Name	Number	Weight
m45B ₂ F ₂	102	1.8 g
m84B ₂ F ₂	174	2.4 g
m119B ₂ F ₂	134	1.4 g
m121B ₂ F ₂	131	6.6 g
m146B ₂ F ₂	124	3.6 g
m239B ₂ F ₂	101	1.9 g
m254B ₂ F ₂	133	9.2 g

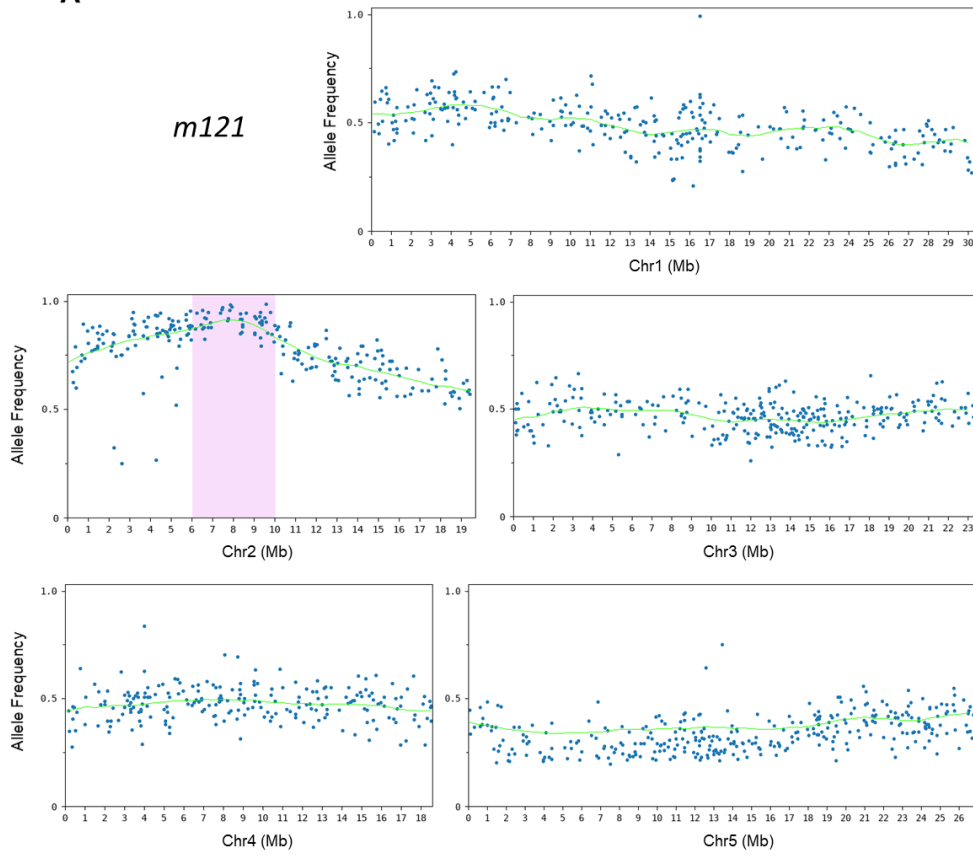
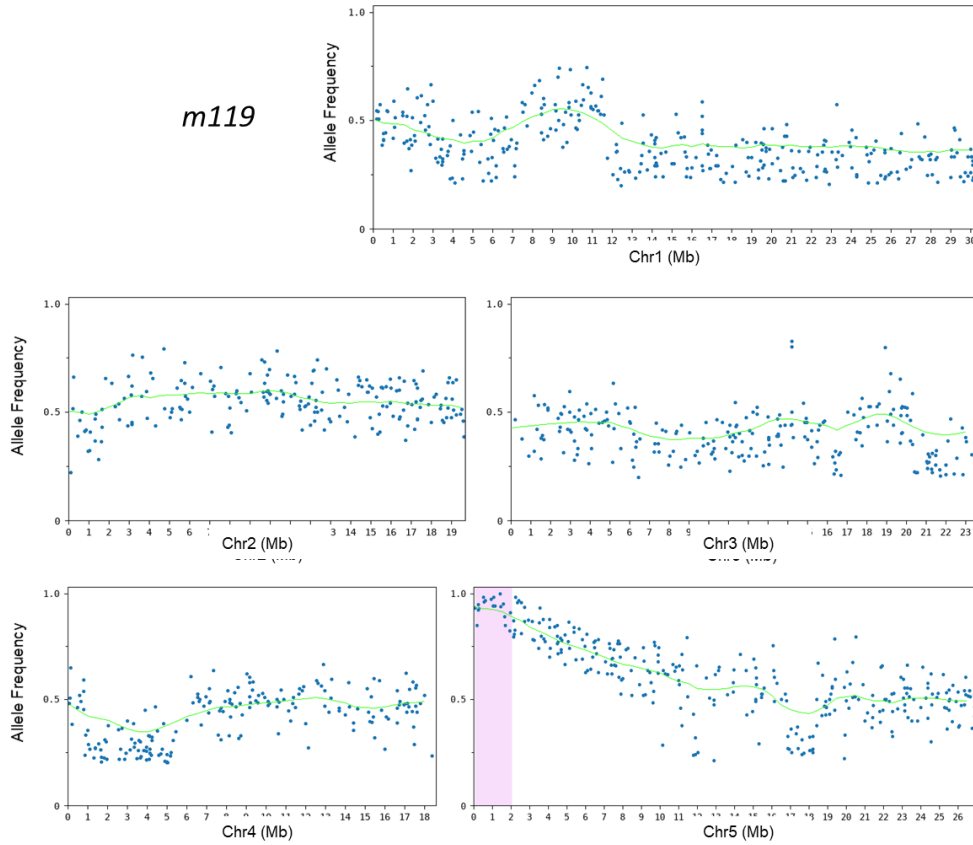
After sampling, genomic DNA was extracted and sequenced by an external company (Novogene) using next generation sequencing (NGS) approaches, that returned high-quality short reads amounting to around 85 times the coverage of the genome. The reads were analyzed using Easymap program, a custom software to ease mapping-by-sequencing data analysis that simplifies the data analysis workflows from raw NGS reads to candidate mutations (Lup, Wilson-Sánchez et al. 2021). This software checks whether a given single nucleotide polymorphism (SNP) affects the sequence of a gene and its protein product, and if it may alter splicing sites, putative promoter regions, or UTRs. The current *At*^{WT} genome assembly (TAIR10.1) was used as reference for the read alignments. In order to distinguish fixed EMS mutations associated with the mutant phenotype in the segregating pool, the resequencing data of the F₂ short-read analysis was performed to identify all mutations with an allele frequency (AF) higher than 80% and that affects a transcription unit.

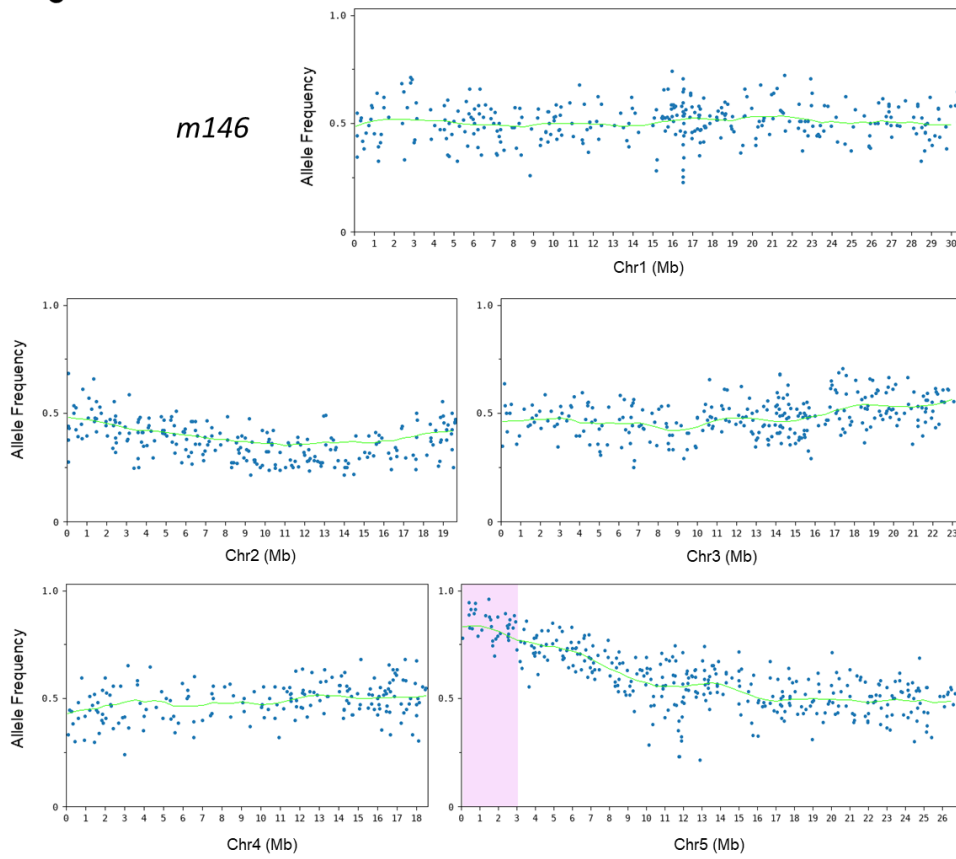
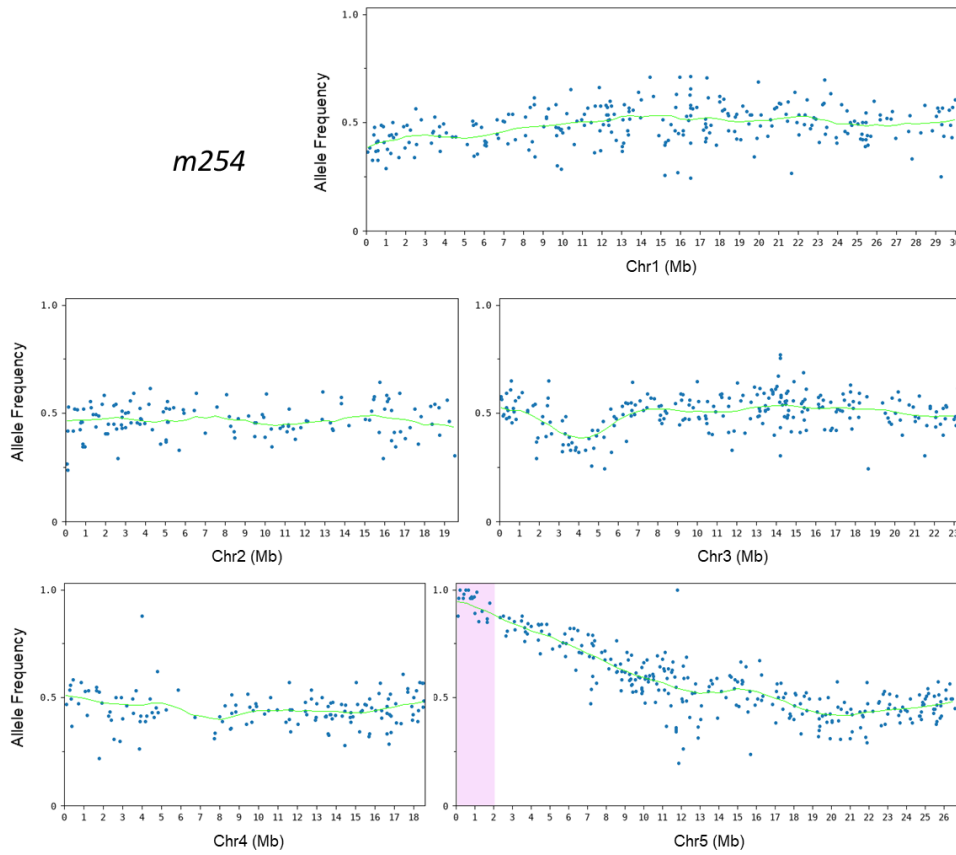
As a result, we got candidate regions from five of the tested lines (**Fig 10**): m119, m121, m146 (all three are *eva* mutants), m254 and m84 (both are *adm* mutant). The mapping-by-sequencing results of m45 and m239 did not yield clear candidate mutations, likely because the selection process was not good enough

(Fig S3). From the five lines that resulted in candidate regions, m121 identified a region in the middle of chromosome 2 (**Fig 10A**), and the other four lines pointed to the same region on top of chromosome 5 (**Fig 10B-E**). In these regions, the mapping-by-sequencing analyses identified a set of EMS-induced changes that affected to different genes in the various lines (**Table S2**). As indicated, we only considered as good candidates those mutations that affected a transcription unit (changing the sequence of a gene and its protein product, or altered splicing sites, putative promoter regions, or UTRs) and did not consider mutations that affecting introns (unless they are predicted to affect the splicing), those that affected a CDS (coding sequence) but produced synonym changes in the protein and the one found in intergenic regions (James, Patel et al. 2013). Based on these filters, we identified a limited number of candidate mutations in the various mutants: 13 mutation in m121, 8 mutations in m119, 13 mutations in m146, 10 mutations in m254 and 9 mutations in m84 (**Table 3**).

Next, in order to get the truly candidates involved in shade phenotypes faster and more accurately, we check if the list of these candidate genes is related with our selected processes, which include senescence induced by dark, shade and warm temperature responses, as well as whether the gene product could interact with proteins involved in any of these of the gene products are also related with any of these processes. As shown in **Table 3**, first, we checked the description of the candidate genes. In the case of m121, no gene emerged as an obvious candidate based on their described function. In the case of m119, m146, m254 and m84, that identified SNPs in the same region on top of chromosome 5, we observed that the only gene that had a mutation in all four lines was *AT5G02310* (**Table 3**). This gene receives different names, one of which is *GREENING AFTER EXTENDED DARKNESS 1 (GED1)*, as it was previously identified in a screening showing an altered ability to green on illumination after extended periods of darkness (Choy, Sullivan et al. 2008). In summary, we have done mapping by sequence of 7 of the 12 mutant lines identified. From those we identified a candidate region only in 5 cases: m119, m121, m146, m254 and m84. All of them but m121 located in the same region (top of chromosome 5).

Comparison of the mutated genes in these candidate regions identified *AT5g02310* (*GED1*) as the only gene being mutated in all four lines.

A**B**

C**D**

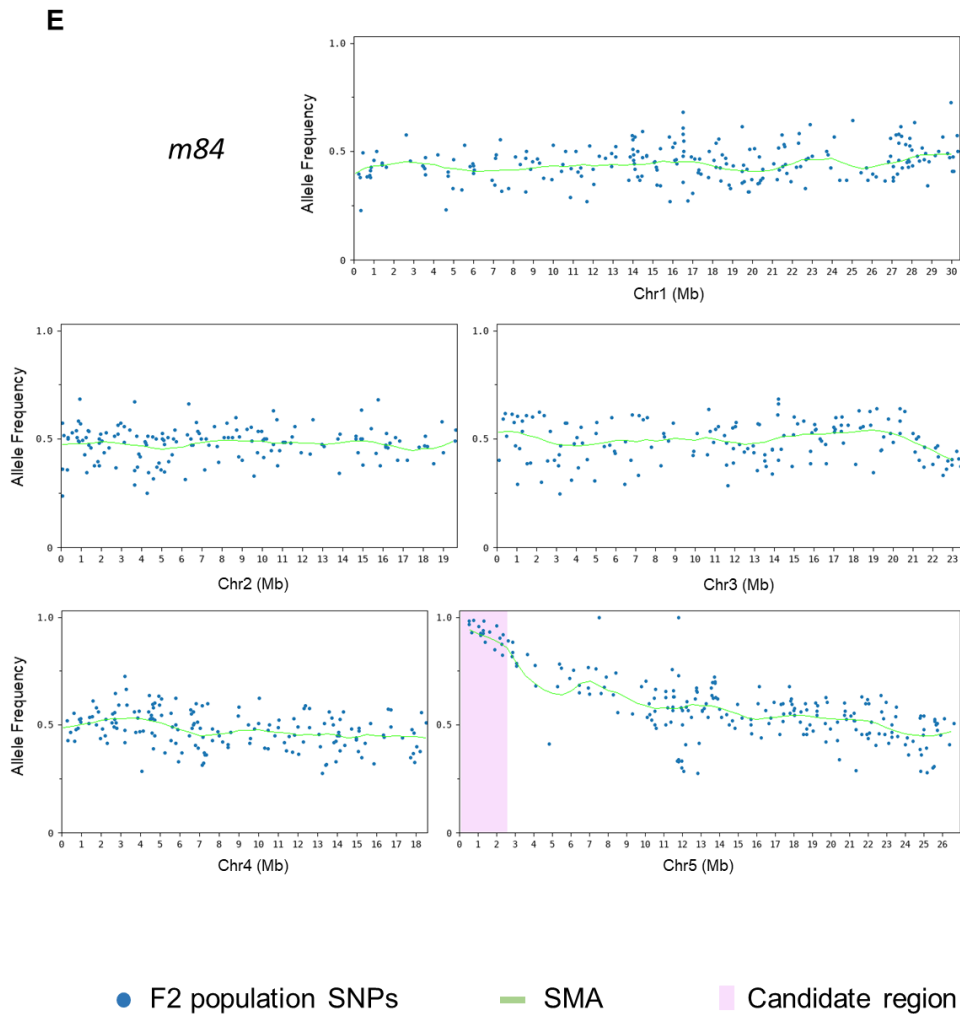


Figure 10. The allele frequency (AF) versus position plots show the single nucleotide polymorphisms (SNP, blue dots) common to the mapping population in the mutant line **(A)** m121, **(B)** m119, **(C)** m146, **(D)** m254 and **(E)** m84. All input contigs are displayed with all the polymorphisms used for mapping the causal mutation and their linear description. Blue dots: F2 population SNPs. Green line: SMA, which are boost values or AF difference between mapping populations. The candidate region determined by the analysis is highlighted.

In addition to *GED1*, *AT5G02310* is also known as *PROTEOLYSIS 6 (PRT6)*. By checking the DNA sequence, three of the mutants include an early stop codon that would affect the protein sequence (m84, m119 and m146) **(Fig 11A)**. In the m254 line, the mutation affects a splicing site during RNA processing and the

translation (**Table S2**) that potentially can alter the protein sequence. Interestingly, m254 and m84 are *adm* mutant, whereas m119 and m146 are *eva* mutants, whose hypocotyls elongated oppositely in the two shade conditions tested (**Fig 8**). These results suggested that (1) either this candidate gene is not the one responsible of the mutations or (2) the mutation location within the *PRT6* gene may have an influence on the phenotypes analyzed. Then, we obtained two mutant alleles of *prt6* (*prt6-1* and *prt6-5*) and compared their DIS phenotype in our screening condition (7W+10D). We observed that seedlings of both lines, as well as *pifq*, were greener than those of *At*^{WT} growing in the same conditions (**Fig 11B**): these results indicated that *PRT6* could be the one that regulates delayed DIS. We next also analyzed the hypocotyl elongation of *prt6-1* and *prt6-5* in response to simulated shade. As a result, seedlings of both mutant lines exhibited enhanced hypocotyl elongation in response to low R:FR compared to wild-type plants (**Fig. 11C**), which was consistent with the selected lines m254 and m84, whereas the other two lines m119 and m146 were in contrast, suggesting that mutations in different locations of the *PRT6* gene may cause differential responses of hypocotyls to shade.

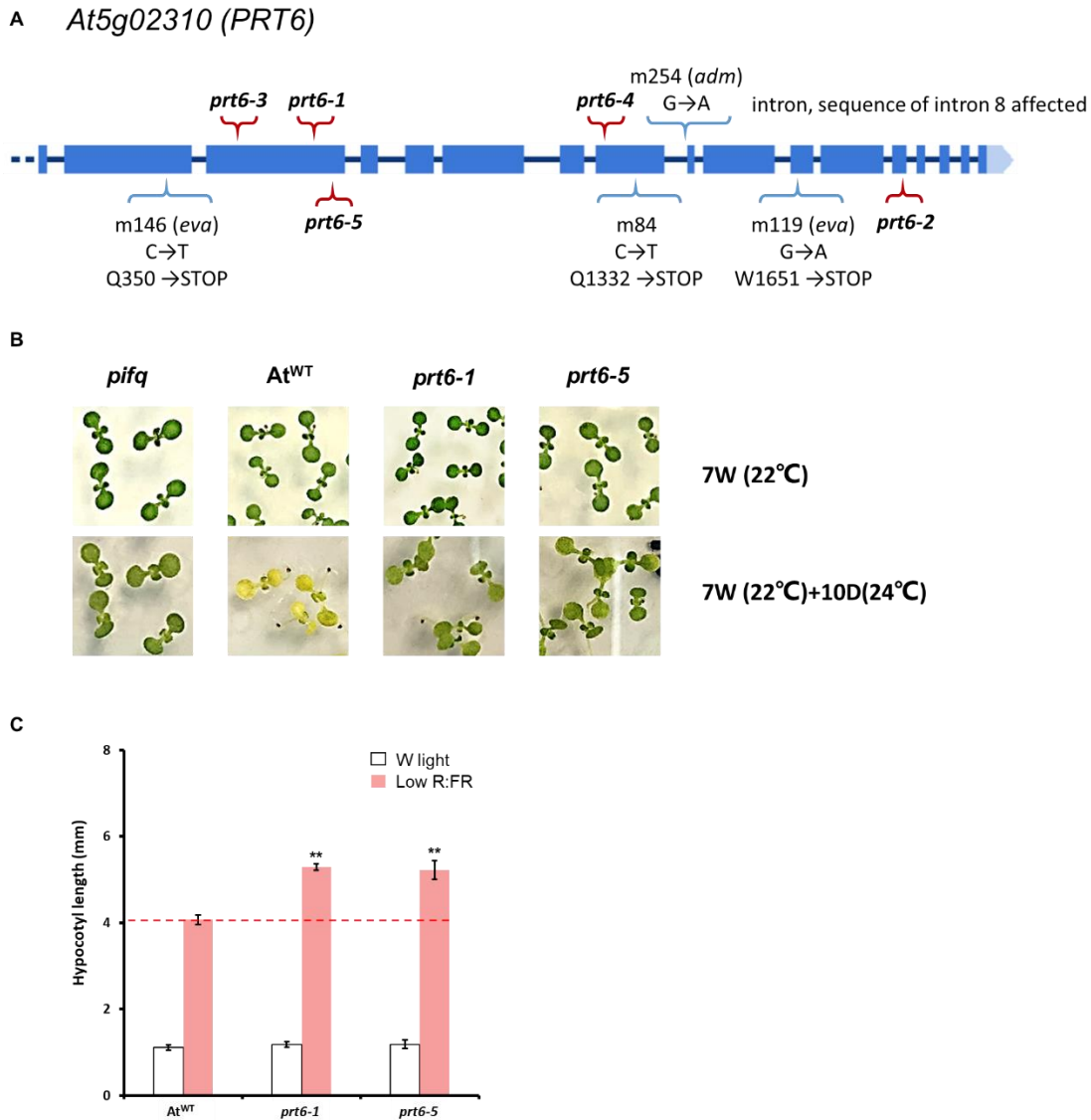


Figure 11. Annotation of putative causal mutations in the gene *AT5G02310* and the DIS phenotypes of related known mutants. **(A)** The genomic regions of EMS mutations in the gene *AT5G02310* in different mutant lines. Blue boxes indicate exons, blue lines indicate introns. Locations of EMS mutations that have putative effects on amino acid sequences are shown. **(B)** Aspect of *At^{WT}*, *pifq*, *prt6-1* and *prt6-5* seedlings grown for 7 days in W and 10 days in dark. **(C)** Hypocotyl length of *At^{WT}*, *prt6-1* and *prt6-5* seedlings in response to shade conditions. The values are the means \pm SE of at least 10 seedlings. Asterisks mark significant differences (student's t-test: *P-value < 0.05, **P-value < 0.01) between mutants and *At^{WT}*.

Table 3. Candidate genes selecting and the information of the genes or protein products related to shade, light, hormones and dark

Gene	Name & description	Amino acid		Paper or GO - related	Corresponding protein accumulation & interaction				
		Ref.	Alt.		degradation	interaction proteins			degradation
						heat	dark	light	
m119 (eva)									
AT5G02310	PROTEOLYSIS 6 (PRT6), GREENING AFTER EXTENDED DARKNESS 1 (GED1)	W	STOP		Yes	KAK			UPL4, ATE2
AT5G02400	PLL2, POL-LIKE 2	G	D		No			ARF10	
AT5G02600	HEAVY METAL ASSOCIATED PROTEIN 42 (HMP42)	R	C		No			LHT1	
AT5G03495	RNA-binding (RRM/RBD/RNP motifs) family protein			promoter	No				
AT5G03795	Exostosin family protein	P	L		No				
AT5G04070	NAD(P)-binding Rossmann-fold superfamily protein	G	R		No				
AT5G04770	CATIONIC AMINO ACID TRANSPORTER 6 (CAT6)			3'UTR	No				
AT5G06280	hypothetical protein	P	L		No			CAB3	
m121 (eva)									
AT2G15110	hypothetical protein	P	S		No				
AT2G15530	CTL03, MED25 BINDING RING-H2 PROTEIN 1 (MBR1)	A	T		Yes				
AT2G16950	IMB2, TRANSPORTIN 1 (TRN1)	A	T		No				

AT2G17700	SERINE/THREONINE/TYROSINE KINASE 8 (STY8)			5'UTR		No		
AT2G19430	HYPERSENSITIVE TO ABA 1 (DWA1)	G	D		ABA-hypersensitive	No	DDB1A	DWA2, CUL4
AT2G19930	RNA-dependent RNA polymerase family protein	A	V			No		
AT2G20990	ARABIDOPSIS THALIANA SYNAPTOTAGMIN A (ATSYT1),			5'UTR		No		
AT2G21230	BASIC LEUCINE-ZIPPER 30 (BZIP30), DRINK ME (DKM)	A	V			No		
AT2G21660	CIRCADIAN RHYTHM AND RNA BINDING 2 (CCR2)			5'UTR	GA biosynthetic pathway	No		
AT2G21730	CINNAMYL ALCOHOL DEHYDROGENASE HOMOLOG 2 (CAD2)	A	T			No		
AT2G22050	Galactose oxidase/kelch repeat superfamily protein	G	E			No		
AT2G22530	Alkaline-phosphatase-like family protein	P	S			No		
AT2G22530	Alkaline-phosphatase-like family protein			intron, putative splicing acceptor of intron 6		No		
AT2G23400	CIS-PRENYLTRANSFERASE 2 (CPT2)	T	M			Yes	LEW	
m146 (eva)								
AT5G01980	BCA2 ZINC FINGER ATL 16, BTL16	S	F			No		
AT5G02310	PROTEOLYSIS 6 (PRT6), GREENING AFTER EXTENDED DARKNESS 1 (GED1)	Q	STOP			Yes	KAK	UPL4, ATE2
AT5G02760	SENESCENCE-SUPPRESSED 51 PROTEIN PHOSPHATASE (SSPP)	S	F		Negative regulation of leaf senescence; promote hypocotyl elongation in TIM	No	SAUR22	

AT5G03070	IMPORTIN ALPHA ISOFORM 9 (IMPA-9)	G	E		No		
AT5G04920	protein_coding	D	N		No		
AT5G05030	protein_coding			promoter	No		
AT5G05365	ATHMP44, HEAVY METAL ASSOCIATED PROTEIN 44	Q	STOP		No		
AT5G06265	protein_coding			5'UTR	No		
AT5G07800	protein_coding	E	K		No		
AT5G07970	protein_coding	R	Q		No		
AT5G08490	SLG1, SLOW GROWTH 1	V	I	Response to abscisic acid	No		nMAT1
AT5G08670	protein_coding	G	D		No		
AT5G09280	protein_coding	D	N		No		
<hr/>							
m254 (adm)							
AT5G01970	protein_coding	P	L		No		
AT5G02310	PROTEOLYSIS 6 (PRT6), GREENING AFTER EXTENDED DARKNESS 1 (GED1)			intron, putative splicing acceptor of intron 8	Yes	KAK	UPL4, ATE2
AT5G02640	hypothetical protein			5' UTR	No		
AT5G03040	IQ-DOMAIN 2; Member of IQ67 (CaM binding) domain containing family.	P	S	Regulator of ABA signaling pathway	No	CESA1	CINV1, CPK4
AT5G03360	protein_coding	D	N		No		

AT5G03630	protein_coding			intron, putative splicing acceptor of intron 8	No		
AT5G03670	TON1 RECRUITING MOTIF 28 (TRM28)	E	K		No		
AT5G04590	SULFITE REDUCTASE (SIR)	V	I		No		
AT5G05430	RNA-binding protein	L	F		No		
AT5G05480	protein_coding	P	S		No		
AT5G05780	ASYMMETRIC LEAVES ENHANCER 3 (AE3)	3' UTR		Light & COP1-related	Yes		ATS9, RPT1A
m84 (adm)							
AT5G02250	ARABIDOPSIS THALIANA MITOCHONDRIAL RNASE II (MTRNASEII)	A	V		No		RRP4, RRP41
AT5G02310	PROTEOLYSIS 6 (PRT6), GREENING AFTER EXTENDED DARKNESS 1 (GED1)	Q	STOP		Yes	KAK	UPL4, ATE2
AT5G03730	CONSTITUTIVE TRIPLE RESPONSE 1 (CTR1), SUGAR-INSENSITIVE 1 (SIS1)	G	D	Negative regulator in the ethylene signal	No		
AT5G04040	SUGAR-DEPENDENT1 (SDP1)	L	F	Jasmonic acid biosynthesis	No		
AT5G04460	SUMO-TARGETED UBIQUITIN E3 LIGASE 5 (STUBL5)	P	S		No		PRT1
AT5G05350	protein_coding	5'UTR			No		
AT5G06140	SORTING NEXIN 1 (SNX1)	G	E	Auxin homeostasis	No		CAND1
AT5G06850	FT-INTERACTING PROTEIN 1 (FTIP1)	A	T		No		
AT5G07180	ERECTA-LIKE 2 (ERL2)	R	Q	Promote plant development	No		

3. Discussion

Plants have evolved to either tolerate or avoid being shaded by surrounding competitors in low-light conditions. Light quantity seems to be a key indicator of shade tolerance. In shade avoidance, by contrast, both light quantity and quality are important, however, changing only one of these two factors in a light environment can induce responses to avoid shade (Smith and Whitelam 1997, Franklin 2008). In our laboratory and therefore in this work, we are focused on light quality changes, particularly the R:FR ratio reduction that induces seedling responses. The shade-avoider, like *A. thaliana*, provided the foundation for our knowledge of the genetic components and regulatory systems involved in the control of the SAS, such as phytochromes and members of bHLH family (Martinez-Garcia, Galstyan et al. 2010, Casal 2012, Roig-Villanova and Martínez-García 2016), but there are still some other unknown components also related to regulate SAS. In order to identify molecular components involved in controlling the shade avoidance or shade tolerance habit, I have started a genetic screening looking for *A. thaliana* mutant plants with a shade tolerant phenotype, which is a strategy to select shade tolerant seedlings in the model system *A. thaliana*.

3.1 PIF-mediated processes of shade, DIS and TIM are related

The proximity of vegetation has a significant impact on plant development, particularly in its early stages (seedlings). Hypocotyl elongation is the first and most dramatic response to simulated shade (Martinez-Garcia, Galstyan et al. 2010). The elongation response after exposure to low R:FR was observed to be associated with the habit response to shade: the shade-avoiders showed elongation whereas the shade-tolerant showed a weak or no elongation response (Morelli, Paulišić et al. 2021). In addition, the attenuation of the warm temperature-induced hypocotyl elongation and DIS were also shown in a shade-tolerant plant *C. hirsuta*, which processes known to be PIF-regulated in *A. thaliana* (Quint, Delker et al. 2016, Paulišić, Qin et al. 2021). Therefore, we did the analysis on several *Brassicaceae* species with different shade habits. Among all shade-avoider species we found that they have a common behavior

in hypocotyl elongation in response to shade (SAS), warm temperature (TIM) and senescence in dark. In particular, we observed that in shade-tolerant species *C. hirsuta* and *S. irio*, the delay DIS and attenuated hypocotyl response in TIM overall associated with the shade tolerant habit, which were similar to those in *pifq* mutant. Whereas an exception to this observation is *A. alpina* (**Fig 2 and 3**). Genetic analyses indicate that these changes are mediated by PIFs (Hornitschek, Lorrain et al. 2009, Sagar and Singh 2020, Paulišić, Qin et al. 2021). This suggested that PIF activity is attenuated in shade-tolerant species *C. hirsuta* and *S. irio*. According to some published knowledge, some negative regulators in this signaling network, such as HFR1, can reduce PIF activity by dimerizing with them and preventing PIF binding to target genes (Hornitschek, Lorrain et al. 2009). Similarly, HY5 might compete with PIFs for the same promoter binding sites (Toledo-Ortiz, Johansson et al. 2014) and also contribute to the formation of the shade-tolerant habit. Furthermore, plants response to shade, dark and warm temperature are regulated by the same PIFs, which are PIF4, PIF5 and PIF7 (PIF7 not in the case of DIS), it may also give explanations on the connection between these PIF-mediated processes (Liebsch and Keech 2016, Quint, Delker et al. 2016, Roig-Villanova and Martínez-García 2016). In our experiments, as a shade-tolerant species, *A. alpina* has to be treated independently from the rest of shade-tolerant species (**Fig 3**), these results make us wonder if *A. alpina* is an authentic shade-tolerant plant. To deepen into this possibility, we explored the habitat of *A. alpina* in nature. The plants usually grow in mountainous areas characterized by an alpine climate, which occurs at high elevation and above the tree line, which means they usually grow without nearby vegetation and is commonly found in rocky soils or fissures of rocks (Koch, Kiefer et al. 2006), therefore, it seems unlikely that *A. alpina* frequently are found in shaded environments. In contrast to that, *C. hirsuta* and *S. irio* are plants characteristic of Mediterranean climate that usually grow in forests with closed vegetation (Hay, Pieper et al. 2014). In addition, it has been reported that *A. alpina* is shown to be shade-tolerant based on their photosynthetic parameters (Morelli, Paulišić et al. 2021). By reason of

the foregoing, *A. alpina* probably is not a true shade-tolerant plant, but has lost specifically its ability to elongate in response to shade, this loss may not involve PIF activity, this could be a reason to explain why *A. alpina* doesn't behave like the other shade-tolerant plants in the PIF-mediated responses of DIS and TIM.

Up to now, 8 different PIFs have been described in *A. thaliana* (Choi, Cho et al. 2021), we have to consider that only a subset of PIFs (e.g. PIF4, PIF5 and PIF7) might play an important role in modulating plant responses to vegetation proximity. Certainly, like in *A. thaliana*, 8 kinds of PIFs have been identified in *C. hirsuta*, but we cannot assume they work the same way. It also applies for the rest of the *Brassicaceae* species studied, of which no specific information about PIFs has yet been described. Altogether the data suggests that PIF-mediated responses of the delay DIS and attenuated hypocotyl response in TIM overall associated with the shade tolerant habit. According to this information, a genetic screening was initiated in our laboratory to get the novel molecular components involved in the control of PIF-based shade avoidance or shade tolerance habit.

3.2 A delayed DIS in *C. hirsuta* is modulated by an attenuated PIF activity

In shade-avoider plants, light deprivation associated with the shade produced by the perception of the presence of nearby vegetation might quickly induce senescence. Accordingly, implementation of the SAS responses may force the plant to redirect resources towards sustaining elongation and modifying plant architecture (Wolters and Jürgens 2009). Thus, start of the senescing process might help to energetically sustain these changes. In shade-tolerance plants, that usually grow in shaded or semi-shaded environments caused by the presence of nearby vegetation, low light quantities are common. Therefore, plants might have adopted mechanisms to slower the senescing process and extend survival under low light conditions. As a consequence, when transferred to the dark, which are the extreme circumstances of light deprivation in which we subject the plants in a typical DIS experiment, the

induction of senescence mechanisms is also delayed. Consistently, shade-tolerant species have a more conservative growth strategy with significantly longer time available to fill the storage when confronting the light deprivation caused by the shade of neighboring plants, likely contributing to their resilience in this unfavorable condition (Valladares & Niinemets 2008).

The analyses of 2 highly informative parameters from the chlorophyll fluorescence (CF) helped to understand better this strategy. The maximum quantum yield of PSII (Fv/Fm) serves as a good indicator to detect plant-stress, as a wide range of stresses converge in multiple affectations of the photosynthetic apparatus (Maxwell and Johnson 2000). The effective quantum yield of PSII (ϕ PSII) is considered as a solid indicator of the photosynthetic efficiency, as it estimates the proportion of energy flowing to photochemistry at the PSII (Murchie and Lawson 2013). Our Fv/Fm measurements indicated that plants were un-stressed before darkness transference; although the values of Fv/Fm detected (0.70-0.75) (**Fig 5**) were a bit lower than it has been widely described in un-stressed leaves for most species (0.79-0.85), this difference could be caused by the different development plant stages (Tian, Ungerer et al. 2017). The rapid and drastically drop in these two parameters in *A. thaliana* wild-type plants from the 4DD (**Fig 5 and 6**) agrees with seedlings implementing the senescence program induced upon darkness, which reflects a dismantling of the photosynthetic apparatus. This does not occur in *C. hirsuta* wild type plants (**Fig 6**). The genetic analyses also reproduce the key role of PIFs in the DIS process (*pifq* and *pif45*) revealed by a decreasing pattern of both parameters which is less acute than that of *A. thaliana* wild-type plants. The similar delayed decline in Fv/Fm and ϕ PSII values observed in *C. hirsuta* wild type plants support that these species has an attenuated PIF activity, as suggested (Paulišić, Qin et al. 2021).

The stability and activity of HY5, a negative regulator of the SAS, has been reported to rely on its interaction with the COP1/SPA complex (CONSTITUTIVELY PHOTOMORPHOGENIC 1 / SUPPRESSOR OF PHYA-105) that negatively regulates its abundance. As a result, HY5 abundance is

very low in the dark and it rapidly increases in the light (Burko, Seluzicki et al. 2020). Accordingly, even in an *HY5* overexpressing line as *HY5ox*, *HY5* activity remains very low in the absence of light and its implications in plant development, de-etiolation, and photomorphogenesis remain attenuated in the dark. Thereby, we did not observe a decreasing pattern of the photosynthetic-related responses of *HY5ox* as drastic as the one from *At*^{WT} but also, not as gradual as *Ch*^{WT}, indicating that *HY5* may be playing a minor role in modulating the senescing response. Moreover, *aba2* plants have an impaired ABA biosynthesis and are unresponsive to glucose/sucrose absence and FR:R treatment, proving that stress signaling and signal transduction are affected. Indeed, in our CF analysis, *aba2* seedlings behave as *pifq* and *pif45*, presenting a progressive drop in the Fv/Fm due to defective dark-stress signaling. However, the photosynthetic efficiency is highly affected in *aba2* but not in *pifq* and *pif45*, indicating that *aba2* mutants are senescing as *At*^{WT} (**Fig 6**). Altogether, the presented results have supported that a delayed DIS phenotype translates in *pifq*, *pif45*, and *Ch*^{WT} delayed decrease of the main fluorescence parameters by an attenuated PIF activity.

3.3 Novel molecular components involved in SAS

A novel genetic screening was carried out in our laboratory utilizing an EMS-mutagenized population in order to identify new molecular components involved in regulating the shade avoidance or tolerance behavior. This screening was based on characterized mutant or transgenic lines that have delayed DIS and altered hypocotyl length in both shade and warm temperature conditions. From this genetic screen, 12 mutant lines (from a total of 31 mutants) were identified as showing a delayed DIS phenotype (greener seedlings) and an altered (attenuated or enhanced) elongation response to simulated shade and warm temperature compared to the wild-type line (**Fig 8**), finding a subgroup of 12 mutations with impaired SAS and TIM responses from a total of 31 mutants with a delayed DIS reinforces our hypothesis that these processes might share some regulators. We expect that the identification of

their molecular identity will provide information about the shared mechanisms between SAS, TIM and DIS.

For the case of m121 (an *eva* mutant), mapping by sequencing identified a region in the middle of chromosome 2. In there, it was found *AT2G15530* (*MBR1, MED25 BINDING RING-H2 PROTEIN 1*), whose gene product binds to PHYTOCHROME AND FLOWERING TIME 1 (PFT1) and promotes PFT1 degradation in vivo (Iñigo, Giraldez et al. 2012). PFT1 acts as a positive regulator of *HY5* gene expression (Klose, Büche et al. 2012). Based on this, *HY5* expression in *mbr1* mutant seedlings should be induced to repress the hypocotyls elongation in shade and delay senescence in darkness. Another candidate mutation is *AT2G19430* (*DWD, DDB1-BINDING WD40 PROTEIN*), whose mutation (*dwa1*) resulted in an ABA hypersensitivity (Lee, Yoon et al. 2010). This may work similarly to *prt6-1*, as previously discussed. Similarly, *AT2G21660* (*CCR2, CIRCADIAN RHYTHM AND RNA BINDING 2*) is related to the GA biosynthetic pathway and its expression is up-regulated by shade (Ranade and García-Gil 2021). We deduced that the *ccr2* seedlings might have lower GA levels, showing an attenuated hypocotyl in shade condition. The gene *AT2G23400* (*CPT2, CIS-PRENYLTRANSFERASE 2*) also in this region, its protein product interacts with LEW1 (LEAF WILTING 1), a protein that keeps the dark insensitivity and delays senescence phenotypes in plants by suppressing the dark-inducible genes *DIN2* and *DIN9* and the leaf senescence marker gene *YLS4* (Zhang, Ohyama et al. 2008). The detailed elucidation of the function of these genes using mutant lines will be required to establish the identity of molecular lesion in the m112 mutant line.

After mapping by sequencing, four different alleles of *PRT6* were identified, suggesting this gene could be an important candidate in co-regulating these three PIF-mediated processes. These 4 lines include 2 *eva* mutants and 2 *adm* mutants. The different mutation locations might explain the variety of observed phenotypes. In the specific case of *PRT6*, it has also been reported that *prt6-5* was less sensitive to high sucrose than *prt6-1* (Castillo, Costa-Broseta et al. 2021), suggesting that different mutations in the same gene could lead the

different phenotypes. The implication of *PRT6* in the control of DIS was expected because of its initial identification of its altered ability to green on illumination after extended periods of darkness in a screening, and we could confirm that both *prt6-1* and *prt6-5* seedlings have delayed DIS phenotypes (**Fig 11B**). In addition, *prt6* mutants showed delayed leaf senescence in darkness for 12 days (Riber, Müller et al. 2015), similar to the delayed DIS phenotype that we showed here (**Fig 11B**). More importantly, the *PRT6* gene is involved in regulating some aspect of photomorphogenesis of seedlings and senescence in plants, according to the results of a physiological and genetic study of loss of function alleles (Choy, Sullivan et al. 2008, Abbas, Berckhan et al. 2015). In addition, *prt6* seedlings are hypersensitive to ABA (Holman, Jones et al. 2009). Shade increases the endogenous ABA levels to inhibit shade-induced hypocotyl elongation (Yang and Li 2017), this would be consistent with *eva* mutant lines having attenuated hypocotyl elongation in response to shade. Moreover, ABA acts as a primary signal that links the functional chloroplast, that are necessary for W light and shade responses, to modulate hypocotyl development (Ortiz-Alcaide, Llamas et al. 2019). In *prt6-1* seedlings chlorophyll accumulates to lower levels, most chloroplasts have less thylakoid membranes and are nearly devoid of starch grains when compared to the wild-type (Choy, Sullivan et al. 2008). Those incomplete functional chloroplasts may result in attenuated elongated hypocotyls in *eva* seedlings under shade. On the other hand, it has been reported that both Salicylic Acid (SA) and Jasmonic Acid (JA) inhibit hypocotyl elongation (Fernández-Milmanda and Ballaré 2021), and in *prt6-5* seedlings the level of SA and JA are lower than wildtype plants (De Marchi, Sorel et al. 2016), which means that also reduce the inhibitory effect of hypocotyl elongation, that could be the reason why *prt6-1*, *prt6-5* and *adm* seedlings have enhanced hypocotyl elongation (**Fig 14C**). Altogether, the phenotypes in shade of *prt6* mutant lines may depend on sensitivity to growth-related hormones, which could be influenced by the locations of mutations, like *hyd1* and *hyd2* mutant (Wassilewskija background) produced variable levels of ethylene (Souter, Topping et al. 2002). We identified other mutant alleles which

may have similar effects of the genetic background on the response to dark and simulated shade by causing the delayed DIS phenotypes and elongated hypocotyls in shade condition (**Table 3**).

4. Materials and methods

4.1 Plant material and growth conditions

A. thaliana accession Columbia-0 (At^{WT}), *pifq*, *pif45* (*pif4*, *pif5*), *35S:GFP-ΔNHFR1* (*HFR1ox*), *aba2*, *acd1-20*, *pif7-2*, *35S:HY5-GFP* (*HY5ox*) mutants (in the Col-0 background), and *C. hirsute*, of the reference Oxford accession (Ch^{WT}), have been described before (Hay et al., 2014; Martínez-García et al., 2014; Reed et al., 1993), in addition, *Capsella bursa-pastoris PHA* (Cbu-P), *Capsella bursa-pastoris SCH* (Cbu-S), *Capsella rubella* (Cru), *Sisymbrium irio* (Sir) and *Arabis alpina* (Aal) were used (Morelli, Paulišić et al. 2021). Also, plant growth conditions have been described elsewhere (seeds were sowed in growth medium without sucrose, 0.5xMS-), as well as the seeds surface-sterilization and the further stratification (4 days in the dark at 4°C) (Martínez-García et al., 2014). Normal light conditions also referred to as continuous white light (W), consisted of light emitted by cool-white vertical fluorescence tubes (PAR 20-24 $\mu\text{mol m}^{-2} \text{s}^{-1}$) located in a growth chamber at constant temperature 22°C.

For gene expression analysis of the DIS treatment, seeds were sown on sterilized nylon membranes placed on top of solid 0.5xMS-. After stratification, seeds were incubated in growth chambers under W to break dormancy and synchronize germination. After 7 days in W, seedlings were transferred to darkness (D) for 2 and 4 days. The plant material was harvested on the day of transfer (0DD) and after 2 and 4 days in D (2DD, 4DD). Three biological replicates per time point and genotype were performed.

About pigment quantification, seeds were sown on a sterilized nylon membrane placed on top of the solid 0.5xMS– medium. After stratification (dark at 4°C) of 4 days, plates with seeds were incubated in plant chambers at 22°C under continuous white light (W) for at least 2 h to break dormancy and synchronize germination (Paulišić, Molina-Contreras et al. 2017, Roig-Villanova, Paulišić et al. 2019).

For the shade experiments, after 4 days of stratification at 4°C in the dark, plates were incubated in growth chambers at 22°C under continuous W provided by 4 cool-white vertical fluorescent tubes for 3 hours and then transferred to simulated shade which was generated by enriching W with supplementary FR provided by LED lamps (www.quantumdev.com or www.philips.com/horti).

To conduct temperature-induced hypocotyl elongation experiments, plates containing seeds were placed in growth chambers at 22°C for 7 days, at 28°C for 7 days, or at 22°C and then 5 days at 28°C for a total of 7 days.

For de-etiolation experiments, after 4-day stratification, plates were incubated in growth chambers at 22°C under continuous W for 3 hours (as described below) and then were transferred to darkness for 24h. Then, plates were transferred to chambers provided by LED tubes that delivered a fixed amount of FR of 2.5 $\mu\text{mol}/\text{m}^2\text{s}$. The different light intensities were obtained using neutral filters as previously described (Paulišić, Molina-Contreras et al. 2017).

4.2 Pigment Extraction and chlorophyll content quantification

Photosynthetic pigments from seedlings of the plants were extracted from 50 mg of fresh weight with 2 ml of methanol: Tris-HCl+NaCl:chlorophorm (2:1:1 v/v) as described (Bou-Torrent, Toledo-Ortiz et al. 2015). The extract was dried in speedvac at room temperature (about 25°C). To quantify the concentration of chlorophyll *a* and chlorophyll *b* present in the pigment extracts of plant seedlings, the extracts were resuspended in 1 mL of acetone

and, using a spectrophotometer, the absorbance was measured in quartz cuvettes. Absorbance at 662 and 645 nm was used to determine the concentration of chlorophyll *a* and chlorophyll *b*, respectively. Absorbance measurements were used to calculate the concentration of the pigments using the equations described (Straumite, Kruma et al. 2015).

4.3 Chlorophyll fluorescence measurements

In vivo fluorescence measurements were performed at room temperature using an IMAGING-PAM Chlorophyll Fluorometer (Schreiber and Klughammer 2008). Seedlings were grown for 7 days in W and then transferred to D for 2, 4, and 7 days. The maximal PSII quantum yield (F_v/F_m) was calculated according to the equation:

$$F_v/F_m = (F_m - F_o)/F_m$$

Being F_m the maximal possible value for fluorescence, obtained after applying a saturating pulse (SP) (800 ms, 2700 $\mu\text{mol m}^{-2} \text{s}^{-1}$, 450 nm) to a dark-adapted seedling exposed to blue light (450 nm, 0.5 $\mu\text{mol m}^{-2} \text{s}^{-1}$). In this initial state, we know that the seedling has all the reaction centres opened ($F=F_o$) and non-photochemical energy dissipation (NPQ) is minimal ($q_N=NPQ=0$). In turn, F_o is calculated immediately after turning on the blue low-intensity light, which is unable to induce electron transport through PSII, but which elicits the minimum value for chlorophyll fluorescence (F_o). Hence, we obtained the fluorescence signal before (F_o) and after (F_m) the SP. Next, rapid light curves were generated by actinic irradiance (800 $\mu\text{mol m}^{-2} \text{s}^{-1}$), that allowed to drive photosynthesis. As a result, the effective quantum yield of the photosystem II in the light, ϕ_{PSII} was calculated as:

$$\phi_{PSII} = (F_m' - F')/F_m'$$

Being F_m' the light-adapted equivalent of F_m and F' , the steady-state level of fluorescence in the light. Measurements were taken at the same time of the day (12:00 am) on 10 different seedlings of each genotype ($n=10$).

4.4 Genomic DNA extraction for massive sequencing

Genomic DNA was extracted using DNeasy Plant Maxi Kit (QIAGEN) from ~1 g of grinded tissue and each sample was eluted twice, the remainders of grinded tissue were stored at -80°C . The integrity of the DNA was checked by loading 70-80 ng into a 1% agarose gel, the electrophoresis run at 120 V during 30 min and the first elutions were sent for NGS to Novogene. Novogene returned high-quality short reads amounting to around an 85x coverage of the genome. The reads were analyzed using custom software developed in our laboratory for the Easymap program, a tool to ease mapping-by-sequencing data analysis. The current *At*^{WT} genome assembly (TAIR10.1) was used as reference for the read alignments, using Hisat2 followed by the variant calling pipeline Samtools mpileup – Bcftools call to go from read files to variants.

Supplement Information

Table S1. Chi-Square Probabilities

Degrees of freedom (n)	Probability Values (P)				Deviation significant	Deviation highly significant
	Deviation from hypothesis not significant					
	0.99	0.95	0.90	0.10	0.05	0.01
1	---	0.004	0.016	2.706	3.841	6.635
2	0.020	0.103	0.211	4.605	5.991	9.210
3	0.115	0.352	0.584	6.251	7.815	11.345
4	0.297	0.711	1.064	7.779	9.488	13.277
5	0.554	1.145	1.610	9.236	11.070	15.086
6	0.872	1.635	2.204	10.645	12.592	16.812
7	1.239	2.167	2.833	12.017	14.067	18.475
8	1.646	2.733	3.490	13.362	15.507	20.090
Chi square value consistent with hypothesis					Not consistent	

Table S2. Candidate region analysis

ID	Contig	Position	AF	Nucleotide (Ref/Alt)	Gene (gene element)	Amino acid (Ref/Alt)
m119						
1	chr5	28043	0.93	G → A	-	-
2	chr5	120786	0.85	G → A	AT5G01290.1 (intron)	-
3	chr5	174697	0.95	G → A	-	-
4	chr5	192088	0.92	G → A	AT5G01470.1 (intron)	-
7	chr5	232989	0.93	G → A	AT5G01620.1 (cds)	-
10	chr5	480875	0.98	G → A	AT5G02310.1 (cds)	W → STOP

11	chr5	514927	0.96	G → A	AT5G02400.1 (cds)	G → D
12	chr5	586741	0.97	G → A	AT5G02600.1 (cds)	R → C
14	chr5	875319	0.97	G → A	AT5G03495.1 (promoter)	-
15	chr5	983643	0.94	G → A	AT5G03740.1 (cds)	-
16	chr5	1007861	0.98	G → A	AT5G03795.1 (cds)	P → L
17	chr5	1104085	0.94	G → A	AT5G04070.1 (cds)	G → R
18	chr5	1382334	1.00	G → A	AT5G04770.1 (three_prime_utr)	-
19	chr5	1392364	0.94	G → A	AT5G04810.1 (cds)	-
20	chr5	1523319	0.95	G → A	-	-
21	chr5	1607461	0.89	G → A	-	-
22	chr5	1656927	0.85	G → A	AT5G05570.1 (intron)	-
24	chr5	1888871	0.82	G → A	AT5G06240.1 (intron)	-
25	chr5	1918602	0.91	G → A	AT5G06280.1 (cds)	P → L

m121

1	chr2	6151382	0.87	G → A	-	-
2	chr2	6229415	0.95	G → A	-	-
3	chr2	6407789	0.89	G → A	AT2G14910.1 (intron)	-
5	chr2	6492999	0.96	G → A	AT2G15020.1 (cds)	-
6	chr2	6498638	0.87	G → A	-	-
7	chr2	6555766	0.88	G → A	AT2G15110.1 (cds)	P → S
8	chr2	6585136	0.92	G → A	-	-
9	chr2	6608919	0.83	G → A	AT2G15220.1 (cds)	-
10	chr2	6660738	0.92	G → A	-	-
11	chr2	6768450	0.88	G → A	-	-

12	chr2	6775788	0.95	G → A	AT2G15530.1 (cds)	A → T
16	chr2	6876673	0.90	G → A	-	-
17	chr2	6911609	0.88	G → A	-	-
18	chr2	7357047	0.95	G → A	AT2G16950.1 (cds)	A → T
20	chr2	7429868	0.96	G → A	-	-
21	chr2	7454722	0.97	G → A	-	-
22	chr2	7689281	0.91	G → A	AT2G17700.1 (five_prime_utr)	-
23	chr2	7725343	0.92	G → A	AT2G17780.1 (cds)	-
26	chr2	7809148	0.96	G → A	AT2G17950.1 (cds)	-
27	chr2	7828998	0.98	G → A	AT2G18000.1 (promoter)	-
29	chr2	7915678	0.97	G → A	AT2G18190.1 (cds)	-
30	chr2	8329681	0.92	G → A	AT2G19190.1 (intron)	-
31	chr2	8345636	0.85	G → A	AT2G19230.1 (intron)	-
32	chr2	8345698	0.94	G → A	AT2G19230.1 (cds)	-
33	chr2	8382145	0.92	G → A	AT2G19360.1 (intron)	-
34	chr2	8412865	0.86	G → A	AT2G19420.1 (intron)	-
35	chr2	8416771	0.88	G → A	AT2G19430.1 (cds)	G → D
36	chr2	8447868	0.89	G → A	-	-
37	chr2	8609770	0.95	G → A	AT2G19930.1 (cds)	A → V
38	chr2	9012183	0.85	G → A	AT2G20980.1 (cds)	-
39	chr2	9014721	0.93	G → A	AT2G20990.1 (five_prime_utr)	-
42	chr2	9020586	0.85	G → A	-	-
43	chr2	9093942	0.92	G → A	AT2G21230.1 (cds)	A → V
45	chr2	9266330	0.93	G → A	AT2G21660.1 (five_prime_utr)	-

47	chr2	9281153	0.90	G → A	AT2G21730.1 (cds)	A → T
48	chr2	9286646	0.95	G → A	AT2G21770.1 (cds)	-
49	chr2	9291704	0.83	G → A	-	-
50	chr2	9377414	0.89	G → A	AT2G22050.1 (cds)	G → E
52	chr2	9379012	0.90	G → A	-	-
53	chr2	9383573	0.91	G → A	AT2G22070.1 (promoter)	-
54	chr2	9515966	0.92	G → A	-	-
55	chr2	9576317	0.90	G → A	AT2G22530.1 (intron, putative splicing acceptor sequence of intron 6 affected)	-
56	chr2	9577163	0.99	G → A	AT2G22530.1 (cds)	P → S
57	chr2	9641567	0.85	G → A	-	-
58	chr2	9775042	0.95	G → A	AT2G22970.1 (intron)	-
61	chr2	9855067	0.85	G → A	-	-
62	chr2	9964788	0.81	G → A	AT2G23400.1 (cds)	T → M
63	chr2	9985243	0.89	G → A	-	-

m146

1	chr5	353875	0.95	C → T	-	-
2	chr5	376794	0.89	C → T	AT5G01980.1 (cds)	S → F
3	chr5	394254	0.83	C → T	-	-
4	chr5	475479	0.91	C → T	AT5G02310.1 (cds)	Q → STOP
5	chr5	538221	0.82	C → T	-	-
6	chr5	625753	0.90	C → T	AT5G02760.1 (cds)	S → F
7	chr5	701677	0.94	C → T	AT5G02990.1 (intron)	-
8	chr5	720194	0.91	C → T	AT5G03070.1 (cds)	G → E

9	chr5	1062400	0.82	C → T	AT5G03940.1 (intron)	-
10	chr5	1255435	0.89	C → T	AT5G04440.1 (cds)	-
11	chr5	1441218	0.96	C → T	AT5G04920.1 (cds)	D → N
12	chr5	1486293	0.88	C → T	AT5G05030.1 (promoter)	-
13	chr5	1553163	0.87	C → T	AT5G05230.1 (intron)	-
14	chr5	1590652	0.83	C → T	AT5G05365.1 (cds)	Q → STOP
15	chr5	1905854	0.88	C → T	AT5G06265.1 (intron)	-
18	chr5	2050003	0.80	C → T	AT5G06670.1 (cds)	-
19	chr5	2338860	0.90	C → T	AT5G07390.1 (cds)	-
21	chr5	2427357	0.84	C → T	AT5G07660.1 (intron)	-
22	chr5	2488845	0.83	C → T	AT5G07800.1 (cds)	E → K
23	chr5	2545350	0.84	C → T	AT5G07970.1 (cds)	R → Q
24	chr5	2579451	0.86	C → T	AT5G08055.1 (cds)	-
25	chr5	2745927	0.83	C → T	AT5G08490.1 (cds)	V → I
26	chr5	2819970	0.88	C → T	AT5G08670.1 (cds)	G → D
27	chr5	2881552	0.85	C → T	AT5G09280.1 (cds)	D → N

m254

1	chr5	64843	0.88	G → A	-	-
2	chr5	80208	0.96	G → A	-	-
3	chr5	149555	1.00	G → A	AT5G01360.1 (promoter)	-
5	chr5	316612	0.96	G → A	-	-
6	chr5	373093	0.98	G → A	AT5G01970.1 (cds)	P → L
7	chr5	479937	1.00	G → A	AT5G02310.1 (intron, putative splicing acceptor sequence of intron 8 affected)	-

8	chr5	594832	1.00	G → A	AT5G02640.1 (five_prime_utr)	-
9	chr5	621894	1.00	G → A	-	-
10	chr5	710586	0.96	G → A	AT5G03040.1 (cds)	P → S
13	chr5	771030	0.97	G → A	-	-
14	chr5	818515	0.96	G → A	AT5G03360.1 (cds)	D → N
16	chr5	922935	0.97	G → A	AT5G03630.1 (intron, putative splicingacceptor sequence of intron 8 affected)	-
17	chr5	947347	0.89	G → A	AT5G03670.1 (cds)	E → K
18	chr5	1039751	0.99	G → A	AT5G03880.1 (intron)	-
19	chr5	1153074	0.85	G → A	-	-
20	chr5	1321287	0.90	G → A	AT5G04590.1 (cds)	V → I
21	chr5	1605852	0.85	G → A	AT5G05430.1 (cds)	L → F
22	chr5	1623762	0.86	G → A	AT5G05480.1 (cds)	P → S
23	chr5	1738504	0.94	C → T	AT5G05780.2 (three_prime_utr)	-

m84

1	chr5	456526	0.97	C → T	AT5G02250.1 (cds)	A → V
2	chr5	479473	0.98	C → T	AT5G02310.1 (cds)	Q → STOP
3	chr5	608268	0.93	C → T	-	-
4	chr5	706819	0.99	C → T	-	-
5	chr5	979458	0.96	C → T	AT5G03730.1 (cds)	G → D
7	chr5	1091651	0.92	C → T	AT5G04040.1 (cds)	L → F
8	chr5	1101267	0.93	C → T	AT5G04060.1 (cds)	-
9	chr5	1230170	0.94	C → T	-	-

10	chr5	1230446	0.93	C → T	-	-
11	chr5	1262946	0.98	C → T	AT5G04460.1 (cds)	P → S
14	chr5	1321238	0.89	C → T	AT5G04590.1 (intron)	-
15	chr5	1585574	0.93	C → T	AT5G05350.1 (five_prime_utr)	-
16	chr5	1856291	0.85	C → T	AT5G06140.1 (cds)	G → E
17	chr5	1949826	0.96	C → T	AT5G06380.1 (cds)	-
18	chr5	2129581	0.91	C → T	AT5G06850.1 (cds)	A → T
19	chr5	2229924	0.88	C → T	AT5G07180.1 (cds)	R → Q
20	chr5	2260290	0.82	C → T	-	-
21	chr5	2285648	0.92	C → T	AT5G07280.1 (cds)	-

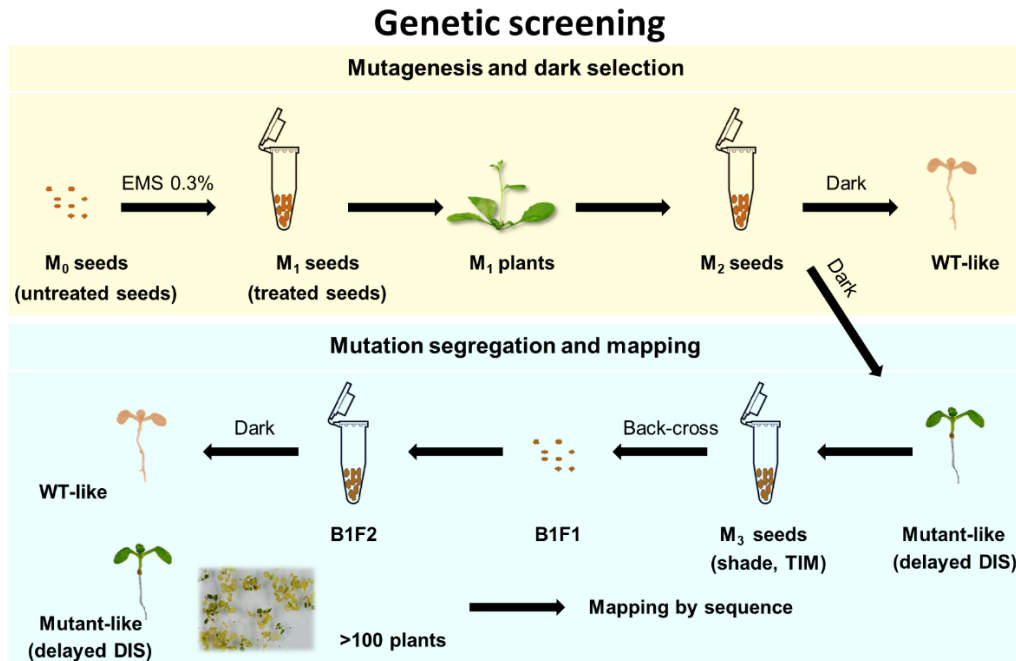


Figure S1. Overview of the experimental design of screening and detection of causal mutation by mapping-by-sequencing. The experiments start with the generation of a mutagenized EMS mutant collection. Alternatively, about EMS mutagenesis and phenotyping: Untreated seeds (M_0) are treated with 0.3% EMS to yield M_1 (EMS-treated) seeds. M_1 plants are grown, producing M_2 seeds, which are sown to give M_2 plants. M_2 plants are further screened using various phenotypic descriptors, the mutant collections can be screened for mutants displaying the delayed DIS. At each generation, seeds are collected and stored. Mutation segregation and detection of the causal mutation: The experimental design is shown for a recessive mutation that is the most commonly found mutation in EMS mutants. Once a homozygous mutant carrying a recessive mutation responsible for the phenotype of interest has been selected, the mutant is back-crossed with the wild type genotype used for generating the EMS mutant collection to get seeds (B1F1) and producing next generation (B1F2). B1F2 plants are further screened, mapping-by-sequence

was done with the mutant collections can be screened for mutants displaying the delayed DIS.

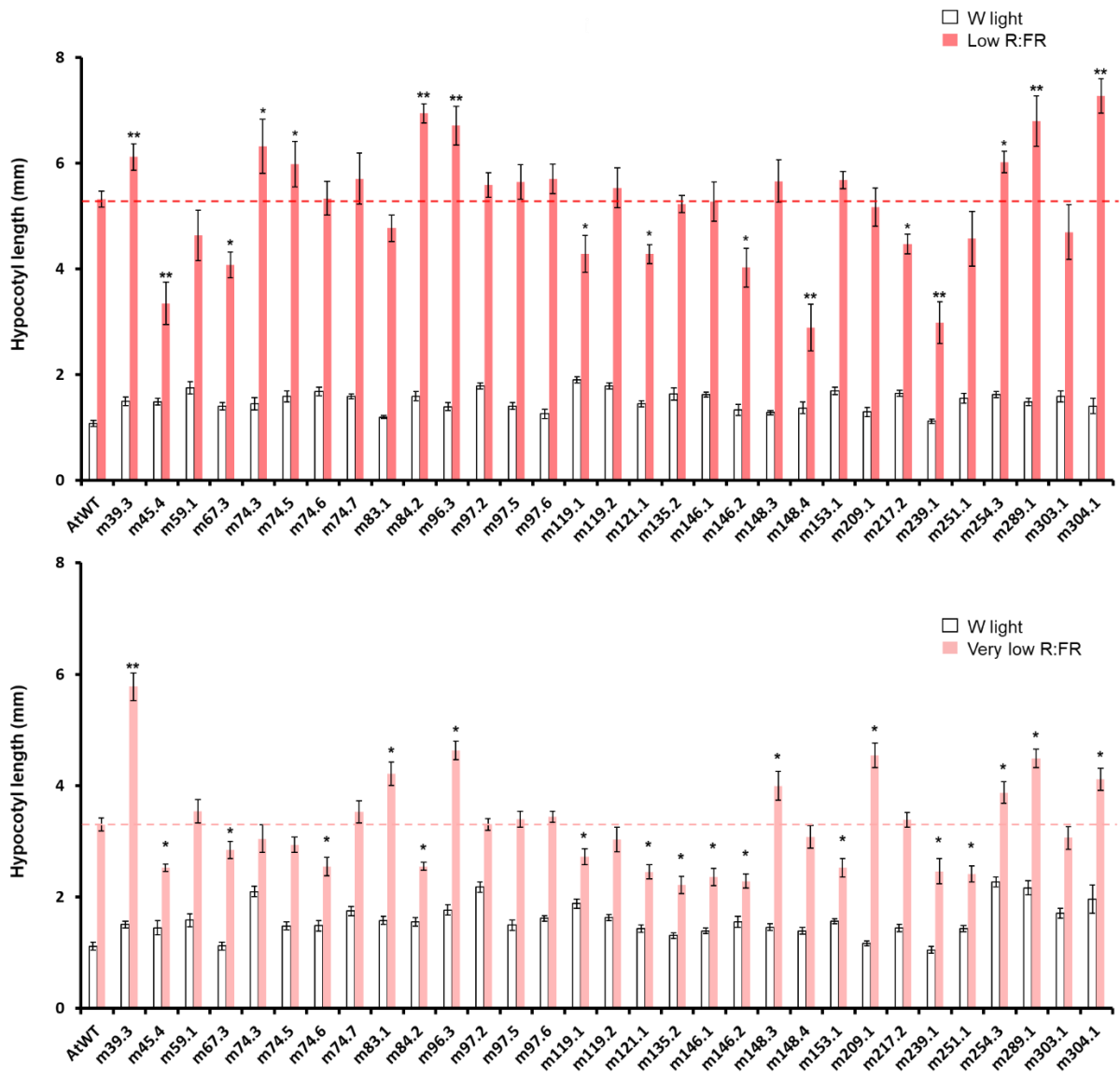
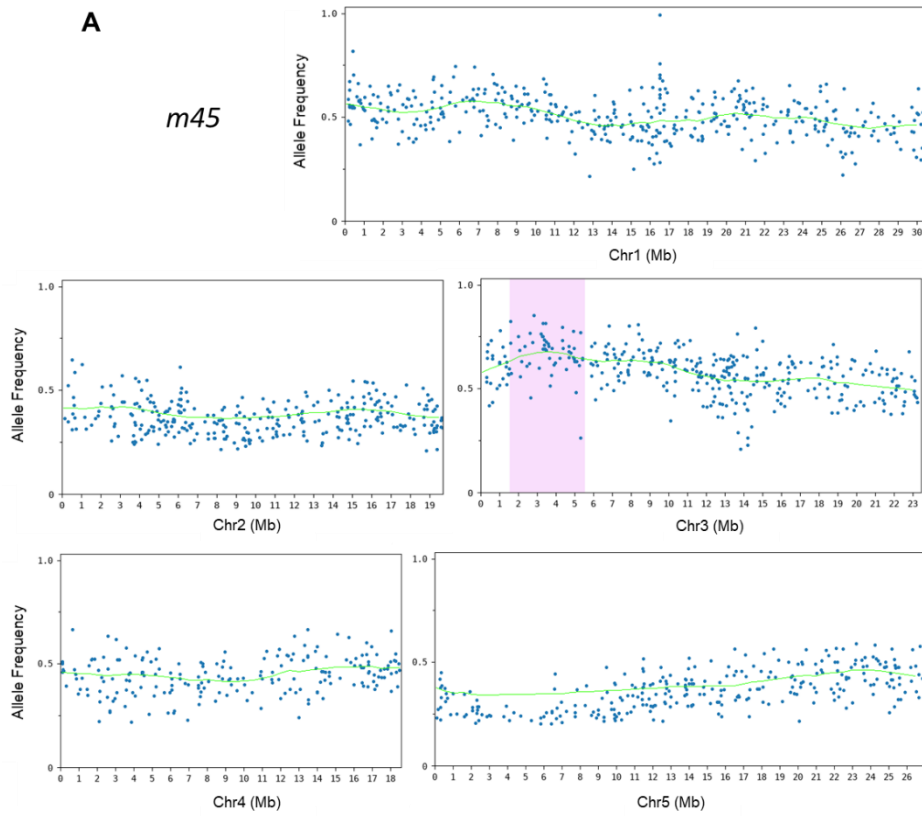
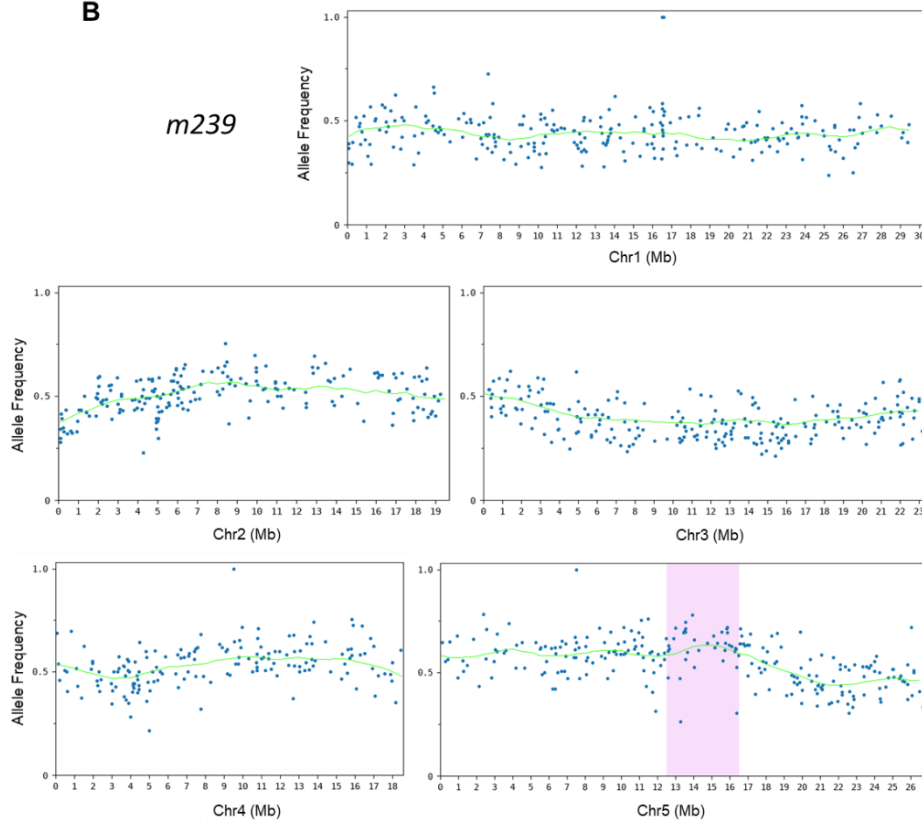


Figure S2. Hypocotyl length of *A. thaliana* seedlings in response to different shade condition. The values are the means \pm SE of at least 15 seedlings. Asterisks mark significant differences (student's t-test: *P-value < 0.05, **P-value < 0.01) between mutants and *At*^{WT} in the same light conditions.

A*m45***B***m239*

● F2 population SNPs

— SMA

■ Candidate region

Figure S3. The allele frequency (AF) versus position plots show the single nucleotide polymorphisms (SNP, blue dots) common to the mapping population in the mutant line **(A)** m45 and **(B)** m239. All input contigs are displayed with all the polymorphisms used for mapping the causal mutation and their linear description (SMA, boost values or AF difference between mapping populations). The candidate region determined by the analysis is highlighted.

Reference

Abbas, M., et al. (2015). "Oxygen sensing coordinates photomorphogenesis to facilitate seedling survival." Current Biology **25**(11): 1483-1488.

Adie, B. A., et al. (2007). "ABA is an essential signal for plant resistance to pathogens affecting JA biosynthesis and the activation of defenses in Arabidopsis." The Plant Cell **19**(5): 1665-1681.

Alonso, L., et al. (2017). "Diurnal cycle relationships between passive fluorescence, PRI and NPQ of vegetation in a controlled stress experiment." Remote Sensing **9**(8): 770.

Bai, S.-N. (2017). "Reconsideration of plant morphological traits: from a structure-based perspective to a function-based evolutionary perspective." Frontiers in plant science **8**: 345.

Ballaré, C. L. and R. Pierik (2017). "The shade-avoidance syndrome: Multiple signals and ecological consequences." Plant Cell Environ **40**(11): 2530-2543.

Ballaré, C. L., et al. (2017). "The shade-avoidance syndrome: Multiple signals and ecological consequences." **40**(11): 2530-2543.

Botto, J. and H. Smith (2002). "Differential genetic variation in adaptive strategies to a common environmental signal in Arabidopsis accessions: phytochrome-mediated shade avoidance." Plant Cell Environ **25**(1): 53-63.

Bou-Torrent, J., et al. (2014). "Plant proximity perception dynamically modulates hormone levels and sensitivity in Arabidopsis." Journal of Experimental Botany **65**(11): 2937-2947.

Bou-Torrent, J., et al. (2015). "Regulation of carotenoid biosynthesis by shade relies on specific subsets of antagonistic transcription factors and cofactors." Plant physiology **169**(3): 1584-1594.

Brouwer, B., et al. (2012). "The impact of light intensity on shade-induced leaf senescence." **35**(6): 1084-1098.

Burko, Y., et al. (2020). "Chimeric activators and repressors define HY5 activity and reveal a light-regulated feedback mechanism." The Plant Cell **32**(4): 967-983.

Casal, J. J. (2012). "Shade avoidance." The Arabidopsis book/American Society of Plant Biologists **10**.

Casal, J. J. (2013). "Photoreceptor signaling networks in plant responses to shade." Annual review of plant biology **64**: 403-427.

Casal, J. J. J. A. r. o. p. b. (2013). "Photoreceptor signaling networks in plant responses to shade." Annual review of plant biology **64**: 403-427.

Castillo, M.-C., et al. (2021). "NIN-like protein7 and PROTEOLYSIS6 functional interaction enhances tolerance to sucrose, ABA, and submergence." **187**(4): 2731-2748.

Choi, D.-M., et al. (2021). "Generation and characterization of a specific polyclonal antibody against Arabidopsis thaliana phytochrome-interacting factor 3." Journal of Plant Biology **64**(2): 181-191.

CHONG, L. (2001). "Molecular cloning." Science **292**(5516): 446-446.

Choy, M.-K., et al. (2008). "An Arabidopsis mutant able to green after extended dark periods shows decreased transcripts of seed protein genes and altered sensitivity to abscisic acid." Journal of Experimental Botany **59**(14): 3869-3884.

Choy, M.-K., et al. (2008). "An Arabidopsis mutant able to green after extended dark periods shows decreased transcripts of seed protein genes and altered sensitivity to abscisic acid." Journal of experimental botany **59**(14): 3869-3884.

Cloix, C., et al. (2012). "C-terminal region of the UV-B photoreceptor UVR8 initiates signaling through interaction with the COP1 protein." **109**(40): 16366-16370.

Cochran, W. G. (1952). "The χ^2 test of goodness of fit." The Annals of mathematical statistics: 315-345.

Dannehl, D., et al. (2021). "Increase of yield, lycopene, and lutein content in tomatoes grown under continuous PAR spectrum LED lighting." Frontiers in plant science **12**: 299.

Das, D., et al. (2016). "Ethylene-and shade-induced hypocotyl elongation share transcriptome patterns and functional regulators." Plant physiology **172**(2): 718-733.

De Lucas, M., et al. (2008). "A molecular framework for light and gibberellin control of cell elongation." Nature **451**(7177): 480-484.

De Marchi, R., et al. (2016). "The N-end rule pathway regulates pathogen responses in plants." Scientific Reports **6**(1): 1-15.

de Wit, M., et al. (2016). "Integration of phytochrome and cryptochrome signals determines plant growth during competition for light." Current Biology **26**(24): 3320-3326.

Djakovic - Petrovic, T., et al. (2007). "DELLA protein function in growth responses to canopy signals." The Plant Journal **51**(1): 117-126.

Duek, P. D., et al. (2004). "The degradation of HFR1, a putative bHLH class transcription factor involved in light signaling, is regulated by phosphorylation and requires COP1." Current Biology **14**(24): 2296-2301.

Eble, J. A. (2018). "Titration ELISA as a method to determine the dissociation constant of receptor ligand interaction." Journal of Visualized Experiments(132): e57334.

Eichers, E., et al. (2004). "Triallelic inheritance: a bridge between Mendelian and multifactorial traits." Annals of medicine **36**(4): 262-272.

Favero, D. S. (2020). "Mechanisms regulating PIF transcription factor activity at the protein level." Physiologia plantarum **169**(3): 325-335.

Feng, S., et al. (2008). "Coordinated regulation of Arabidopsis thaliana development by light and gibberellins." Nature **451**(7177): 475-479.

Fernández-Milmanda, G. L. and C. L. Ballaré (2021). "Shade avoidance: Expanding the color and hormone palette." Trends in plant science **26**(5): 509-523.

Fiorucci, A.-S. and C. Fankhauser (2017). "Plant strategies for enhancing access to sunlight." Current Biology **27**(17): R931-R940.

Fiorucci, A.-S., et al. (2020). "PHYTOCHROME INTERACTING FACTOR 7 is important for early responses to elevated temperature in Arabidopsis seedlings." New Phytologist **226**(1): 50-58.

Franklin, K. A. (2008). "Shade avoidance." New Phytologist **179**(4): 930-944.

Franklin, K. A., et al. (2011). "Phytochrome-interacting factor 4 (PIF4) regulates auxin biosynthesis at high temperature." Proceedings of the National Academy of Sciences **108**(50): 20231-20235.

Fraser, D. P., et al. (2016). "Photoreceptor crosstalk in shade avoidance." Current opinion in plant biology **33**: 1-7.

Frigerio, M., et al. (2006). "Transcriptional regulation of gibberellin metabolism genes by auxin signaling in Arabidopsis." Plant physiology **142**(2): 553-563.

Gallemí, M., et al. (2016). "DRACULA2 is a dynamic nucleoporin with a role in regulating the shade avoidance syndrome in Arabidopsis." Development **143**(9): 1623.

Gallemí, M., et al. (2016). "DRACULA2 is a dynamic nucleoporin with a role in regulating the shade avoidance syndrome in Arabidopsis." Development **143**(9): 1623-1631.

Gallemí, M., et al. (2017). "A non-DNA-binding activity for the ATHB 4 transcription factor in the control of vegetation proximity." New Phytologist **216**(3): 798-813.

Gallemí, M., et al. (2017). "A non-DNA-binding activity for the ATHB 4 transcription factor in the control of vegetation proximity." **216**(3): 798-813.

Galstyan, A., et al. (2011). "The shade avoidance syndrome in Arabidopsis: a fundamental role for atypical basic helix-loop-helix proteins as transcriptional cofactors." The Plant Journal **66**(2): 258-267.

Galstyan, A., et al. (2011). "The shade avoidance syndrome in Arabidopsis: a fundamental role for atypical basic helix-loop-helix proteins as transcriptional cofactors." **66**(2): 258-267.

Galvão, V. C., et al. (2019). "PIF transcription factors link a neighbor threat cue to accelerated reproduction in Arabidopsis." Nature communications **10**(1): 1-10.

Gan, X., et al. (2016). "The Cardamine hirsuta genome offers insight into the evolution of morphological diversity." Nature Plants **2**(11): 1-7.

Gommers, C. M. (2016). When growing tall is not an option: contrasting shade avoidance responses in two wild Geranium species, Utrecht University.

Gommers, C. M., et al. (2013). "Shade tolerance: when growing tall is not an option." Trends in plant science **18**(2): 65-71.

Gray, W. M. (2004). "Hormonal regulation of plant growth and development." PLoS biology **2**(9): e311.

Gray, W. M., et al. (1998). "High temperature promotes auxin-mediated hypocotyl elongation in Arabidopsis." Proceedings of the National Academy of Sciences **95**(12): 7197-7202.

Hardtke, C. S., et al. (2000). "HY5 stability and activity in Arabidopsis is regulated by phosphorylation in its COP1 binding domain." The EMBO Journal **19**(18): 4997-5006.

Hauvermale, A. L., et al. (2012). "Gibberellin signaling: a theme and variations on DELLA repression." Plant physiology **160**(1): 83-92.

Hay, A. S., et al. (2014). "Cardamine hirsuta: a versatile genetic system for comparative studies." The Plant Journal **78**(1): 1-15.

Hay, A. S., et al. (2014). "Cardamine hirsuta: a versatile genetic system for comparative studies." **78**(1): 1-15.

Hayes, S., et al. (2017). "UV-B perceived by the UVR8 photoreceptor inhibits plant thermomorphogenesis." **27**(1): 120-127.

Hersch, M., et al. (2014). "Light intensity modulates the regulatory network of the shade avoidance response in Arabidopsis." Proceedings of the National Academy of Sciences **111**(17): 6515-6520.

Hersch, M., et al. (2014). "Light intensity modulates the regulatory network of the shade avoidance response in Arabidopsis." Proceedings of the National Academy of Sciences of the United States of America **111**(17): 6515.

Holman, T. J., et al. (2009). "The N-end rule pathway promotes seed germination and establishment through removal of ABA sensitivity in Arabidopsis." Proceedings of the National Academy of Sciences **106**(11): 4549-4554.

Holtkotte, X., et al. (2017). "The blue light-induced interaction of cryptochrome 1 with COP1 requires SPA proteins during Arabidopsis light signaling." PLoS Genetics **13**(10): e1007044.

Hornitschek, P., et al. (2012). "Phytochrome interacting factors 4 and 5 control seedling growth in changing light conditions by directly controlling auxin signaling." The Plant Journal **71**(5): 699-711.

Hornitschek, P., et al. (2012). "Phytochrome interacting factors 4 and 5 control seedling growth in changing light conditions by directly controlling auxin signaling." **71**(5): 699-711.

Hornitschek, P., et al. (2009). "Inhibition of the shade avoidance response by formation of non-DNA binding bHLH heterodimers." The EMBO Journal **28**(24): 3893-3902.

Huang, X., et al. (2014). "Beyond repression of photomorphogenesis: role switching of COP/DET/FUS in light signaling." Current opinion in plant biology **21**: 96-103.

Iñigo, S., et al. (2012). "Proteasome-mediated turnover of Arabidopsis MED25 is coupled to the activation of FLOWERING LOCUS T transcription." Plant physiology **160**(3): 1662-1673.

Iqbal, N., et al. (2017). "Ethylene role in plant growth, development and senescence: interaction with other phytohormones." Frontiers in plant science **8**: 475.

Jaillais, Y. and G. Vert (2012). "Brassinosteroids, gibberellins and light-mediated signalling are the three-way controls of plant sprouting." Nature cell biology **14**(8): 788-790.

James, G. V., et al. (2013). "User guide for mapping-by-sequencing in Arabidopsis." **14**(6): 1-13.

Jang, I.-C., et al. (2005). "HFR1 is targeted by COP1 E3 ligase for post-translational proteolysis during phytochrome A signaling." Genes & Development **19**(5): 593-602.

Jang, I.-C., et al. (2005). "HFR1 is targeted by COP1 E3 ligase for post-translational proteolysis during phytochrome A signaling." **19**(5): 593-602.

Jia, Y., et al. (2020). "PIFs coordinate shade avoidance by inhibiting auxin repressor ARF18 and metabolic regulator QQS." New Phytologist **228**(2): 609-621.

Kami, C., et al. (2010). "Light-regulated plant growth and development." Current topics in developmental biology **91**: 29-66.

Kamiya, Y. and J. L. García-Martínez (1999). "Regulation of gibberellin biosynthesis by light." Current opinion in plant biology **2**(5): 398-403.

Keuskamp, D. H. and R. Pierik (2010). Photosensory cues in plant–plant interactions: regulation and functional significance of shade avoidance responses. Plant Communication from an Ecological Perspective, Springer: 159-178.

Keuskamp, D. H., et al. (2010). "Auxin transport through PIN-FORMED 3 (PIN3) controls shade avoidance and fitness during competition." **107**(52): 22740-22744.

Khanna, R., et al. (2004). "A novel molecular recognition motif necessary for targeting photoactivated phytochrome signaling to specific basic helix-loop-helix transcription factors." The Plant Cell **16**(11): 3033-3044.

Klose, C., et al. (2012). "The mediator complex subunit PFT1 interferes with COP1 and HY5 in the regulation of Arabidopsis light signaling." Plant physiology **160**(1): 289-307.

Koch, M. A., et al. (2006). "Three times out of Asia Minor: the phylogeography of *Arabis alpina* L.(Brassicaceae)." Molecular Ecology **15**(3): 825-839.

Koini, M. A., et al. (2009). "High temperature-mediated adaptations in plant architecture require the bHLH transcription factor PIF4." Current Biology **19**(5): 408-413.

Kurepin, L. V., et al. (2007). "Interaction of red to far red light ratio and ethylene in regulating stem elongation of *Helianthus annuus*." Plant Growth Regulation **51**(1): 53-61.

Lau, K., et al. (2019). "Plant photoreceptors and their signaling components compete for COP 1 binding via VP peptide motifs." The EMBO Journal **38**(18): e102140.

Lau, K., et al. (2019). "Plant photoreceptors and their signaling components compete for COP 1 binding via VP peptide motifs." **38**(18): e102140.

LeBlanc, C., et al. (2018). "Increased efficiency of targeted mutagenesis by CRISPR/Cas9 in plants using heat stress." The Plant Journal **93**(2): 377-386.

Lee, J.-H., et al. (2010). "DWA1 and DWA2, two Arabidopsis DWD protein components of CUL4-based E3 ligases, act together as negative regulators in ABA signal transduction." The Plant Cell **22**(6): 1716-1732.

Leivar, P., et al. (2008). "The Arabidopsis phytochrome-interacting factor PIF7, together with PIF3 and PIF4, regulates responses to prolonged red light by modulating phyB levels." The Plant Cell **20**(2): 337-352.

Leivar, P., et al. (2012). "Dynamic antagonism between phytochromes and PIF family basic helix-loop-helix factors induces selective reciprocal responses to light and shade in a rapidly responsive transcriptional network in Arabidopsis." **24**(4): 1398-1419.

Li, K., et al. (2016). "DELLA-mediated PIF degradation contributes to coordination of light and gibberellin signalling in Arabidopsis." Nature communications **7**(1): 1-11.

Li, L., et al. (2012). "Linking photoreceptor excitation to changes in plant architecture." Genes development **26**(8): 785-790.

Lichtenthaler, H., et al. (1982). "Adaptation of chloroplast-ultrastructure and of chlorophyll-protein levels to high-light and low-light growth conditions." **37**(5-6): 464-475.

Liebsch, D. and O. Keech (2016). "Dark-induced leaf senescence: new insights into a complex light-dependent regulatory pathway." New Phytologist **212**(3): 563-570.

Liebsch, D. and O. J. N. P. Keech (2016). "Dark-induced leaf senescence: new insights into a complex light-dependent regulatory pathway." **212**(3): 563-570.

Liu, B., et al. (2011). "Arabidopsis cryptochrome 1 interacts with SPA1 to suppress COP1 activity in response to blue light." Genes & Development **25**(10): 1029-1034.

Lorrain, S., et al. (2008). "Phytochrome-mediated inhibition of shade avoidance involves degradation of growth-promoting bHLH transcription factors." The Plant Journal **53**(2): 312-323.

Lorrain, S., et al. (2008). "Phytochrome-mediated inhibition of shade avoidance involves degradation of growth-promoting bHLH transcription factors." **53**(2): 312-323.

Lu, X.-D., et al. (2015). "Red-light-dependent interaction of phyB with SPA1 promotes COP1–SPA1 dissociation and photomorphogenic development in Arabidopsis." Molecular plant **8**(3): 467-478.

Lup, S. D., et al. (2021). "Easymap: a user-friendly software package for rapid mapping-by-sequencing of point mutations and large insertions." Frontiers in plant science **12**: 655286.

Martínez-García, J. F., et al. (2014). "The shade avoidance syndrome in Arabidopsis: the antagonistic role of phytochrome A and B differentiates vegetation proximity and canopy shade." PloS one **9**(10): e109275.

Martínez-García, J. F., et al. (2014). "The shade avoidance syndrome in Arabidopsis: the antagonistic role of phytochrome A and B differentiates vegetation proximity and canopy shade." **9**(10): e109275.

Martinez-Garcia, J. F., et al. (2010). Regulatory components of shade avoidance syndrome. Advances in botanical research, Elsevier. **53**: 65-116.

Martinez-Garcia, J. F., et al. (2010). "Regulatory components of shade avoidance syndrome." Advances in botanical research **53**: 65-116.

Maxwell, K. and G. N. Johnson (2000). "Chlorophyll fluorescence—a practical guide." Journal of Experimental Botany **51**(345): 659-668.

Molina-Contreras, M. J., et al. (2019). "Photoreceptor activity contributes to contrasting responses to shade in Cardamine and Arabidopsis seedlings." The Plant Cell **31**(11): 2649-2663.

Molina-Contreras, M. J., et al. (2019). "Photoreceptor activity contributes to contrasting responses to shade in Cardamine and Arabidopsis seedlings." **31**(11): 2649-2663.

Morelli, L., et al. (2021). "Light signals generated by vegetation shade facilitate acclimation to low light in shade-avoider plants." Plant physiology **186**(4): 2137-2151.

Morelli, L., et al. (2021). "Light signals generated by vegetation shade facilitate acclimation to low light in shade-avoider plants." Plant physiology **186**(4): 2137-2151.

Morelli, L., et al. (2020). "Light quality signals generated by vegetation shade facilitate acclimation to reduced light quantity in shade-avoider plants." bioRxiv.

Morgan, P. W., et al. (2002). "Opportunities to improve adaptability and yield in grasses: lessons from sorghum." Crop Science **42**(6): 1791-1799.

Müller-Moulé, P., et al. (2016). "YUCCA auxin biosynthetic genes are required for Arabidopsis shade avoidance." **4**: e2574.

Murchie, E., et al. (2009). "Agriculture and the new challenges for photosynthesis research." New Phytologist **181**(3): 532-552.

Murchie, E. H. and T. Lawson (2013). "Chlorophyll fluorescence analysis: a guide to good practice and understanding some new applications." Journal of Experimental Botany **64**(13): 3983-3998.

Murchie, E. H. and T. J. J. o. e. b. Lawson (2013). "Chlorophyll fluorescence analysis: a guide to good practice and understanding some new applications." **64**(13): 3983-3998.

Ortiz-Alcaide, M., et al. (2019). "Chloroplasts modulate elongation responses to canopy shade by retrograde pathways involving HY5 and abscisic acid." The Plant Cell **31**(2): 384-398.

Pacín, M., et al. (2013). "COP 1 re-accumulates in the nucleus under shade." The Plant Journal **75**(4): 631-641.

Pacín, M., et al. (2016). "Convergence of CONSTITUTIVE PHOTOMORPHOGENESIS 1 and PHYTOCHROME INTERACTING FACTOR signalling during shade avoidance." New Phytologist **211**(3): 967-979.

Pacín, M., et al. (2016). "Convergence of CONSTITUTIVE PHOTOMORPHOGENESIS 1 and PHYTOCHROME INTERACTING FACTOR signalling during shade avoidance." **211**(3): 967-979.

Paik, I., et al. (2017). "Expanding roles of PIFs in signal integration from multiple processes." Molecular plant **10**(8): 1035-1046.

Park, H.-J., et al. (2008). "Multisite phosphorylation of Arabidopsis HFR1 by casein kinase II and a plausible role in regulating its degradation rate." Journal of Biological Chemistry **283**(34): 23264-23273.

Paulišić, S., et al. (2017). Approaches to study light effects on brassinosteroid sensitivity. Brassinosteroids, Springer: 39-47.

Paulišić, S., et al. (2021). "Adjustment of the PIF7-HFR1 transcriptional module activity controls plant shade adaptation." The EMBO Journal **40**(1): e104273.

Pedmale, U. V., et al. (2016). "Cryptochromes interact directly with PIFs to control plant growth in limiting blue light." Cell **164**(1-2): 233-245.

Pierik, R. and M. de Wit (2014). "Shade avoidance: phytochrome signalling and other aboveground neighbour detection cues." Journal of Experimental Botany **65**(11): 2815-2824.

Pierik, R. and C. Testerink (2014). "The art of being flexible: how to escape from shade, salt, and drought." Plant physiology **166**(1): 5-22.

Pinstrup-Andersen, P. J. C. J. o. P. P. (2000). "The future world food situation and the role of plant diseases." **22**(4): 321-331.

Qi, L., et al. (2020). "PHYTOCHROME-INTERACTING FACTORS interact with the ABA receptors PYL8 and PYL9 to orchestrate ABA signaling in darkness." **13**(3): 414-430.

Quint, M., et al. (2016). "Molecular and genetic control of plant thermomorphogenesis." Nature Plants **2**(1): 1-9.

Quirino, B. F., et al. (2000). "Molecular aspects of leaf senescence." **5**(7): 278-282.

Ranade, S. S. and M. R. García-Gil (2021). "Molecular signatures of local adaptation to light in Norway spruce." Planta **253**(2): 1-18.

Rascher, U., et al. (2000). "Evaluation of instant light-response curves of chlorophyll fluorescence parameters obtained with a portable chlorophyll fluorometer on site in the field." Plant Cell Environ **23**(12): 1397-1405.

Riber, W., et al. (2015). "The greening after extended darkness¹ is an N-end rule pathway mutant with high tolerance to submergence and starvation." Plant physiology **167**(4): 1616-1629.

Roig-Villanova, I., et al. (2006). "Identification of primary target genes of phytochrome signaling. Early transcriptional control during shade avoidance responses in Arabidopsis." Plant physiology **141**(1): 85-96.

Roig-Villanova, I. and J. F. Martínez-García (2016). "Plant responses to vegetation proximity: a whole life avoiding shade." Frontiers in plant science **7**: 236.

Roig-villanova, I. and J. F. Martínez-García (2016). "Plant Responses to Vegetation Proximity: A Whole Life Avoiding Shade." Front. Plant Sci. **7**(February): 1-10.

Roig-Villanova, I. and J. F. J. F. i. P. S. Martínez-García (2016). "Plant responses to vegetation proximity: a whole life avoiding shade." **7**: 236.

Roig-Villanova, I., et al. (2019). Shade avoidance and neighbor detection. Phytochromes, Springer: 157-168.

Roig-Villanova, I., et al. (2007). "Interaction of shade avoidance and auxin responses: a role for two novel atypical bHLH proteins." The EMBO Journal **26**(22): 4756-4767.

Roig-Villanova, I., et al. (2007). "Interaction of shade avoidance and auxin responses: a role for two novel atypical bHLH proteins." Embo Journal **26**(22): 4756-4767.

Ruberti, I., et al. (2012). "Plant adaptation to dynamically changing environment: the shade avoidance response." **30**(5): 1047-1058.

Sagar, S. and A. Singh (2020). "Dark-induced hormonal regulation of plant growth and development." Frontiers in plant science **11**: 1527.

Sairanen, I., et al. (2012). "Soluble carbohydrates regulate auxin biosynthesis via PIF proteins in Arabidopsis." **24**(12): 4907-4916.

Sakuraba, Y., et al. (2014). "Phytochrome-interacting transcription factors PIF4 and PIF5 induce leaf senescence in Arabidopsis." Nature communications **5**(1): 1-13.

Sakuraba, Y., et al. (2014). "Phytochrome-interacting transcription factors PIF4 and PIF5 induce leaf senescence in Arabidopsis." **5**(1): 1-13.

Sasidharan, R., et al. (2008). "The regulation of cell wall extensibility during shade avoidance: a study using two contrasting ecotypes of *Stellaria longipes*." Plant physiology **148**(3): 1557-1569.

Schreiber, U. (2004). "Pulse-amplitude-modulation (PAM) fluorometry and saturation pulse method: an overview." Chlorophyll a fluorescence: 279-319.

Schreiber, U. and C. Klughammer (2008). "Non-photochemical fluorescence quenching and quantum yields in PS I and PS II: analysis of heat-induced limitations using Maxi-Imaging-PAM and Dual-PAM-100." PAM Application Notes **1**: 15-18.

Sessa, G., et al. (2005). "A dynamic balance between gene activation and repression regulates the shade avoidance response in Arabidopsis." **19**(23): 2811-2815.

Sheerin, D. J. and A. Hiltbrunner (2017). "Molecular mechanisms and ecological function of far-red light signalling." Plant Cell Environ **40**(11): 2509-2529.

Sibénil, Y., et al. (2001). "Plant bZIP G-box binding factors. Modular structure and activation mechanisms." European Journal of Biochemistry **268**(22): 5655-5666.

Smith, H. (1982). "Light quality, photoperception, and plant strategy." Annual review of plant physiology **33**(1): 481-518.

Smith, H. (2000). "Phytochromes and light signal perception by plants—an emerging synthesis." Nature **407**(6804): 585-591.

Smith, H. and G. Whitelam (1997). "The shade avoidance syndrome: multiple responses mediated by multiple phytochromes." Plant Cell Environ **20**(6): 840-844.

Solovchenko, A., et al. (2013). "Probing the effects of high-light stress on pigment and lipid metabolism in nitrogen-starving microalgae by measuring chlorophyll fluorescence transients: studies with a $\Delta 5$ desaturase mutant of *Parietochloris incisa* (Chlorophyta, Trebouxiophyceae)." Algal Research **2**(3): 175-182.

Sorin, C., et al. (2009). "ATHB4, a regulator of shade avoidance, modulates hormone response in *Arabidopsis* seedlings." Plant Journal **59**(2): 266-277.

Souter, M., et al. (2002). "hydra mutants of *Arabidopsis* are defective in sterol profiles and auxin and ethylene signaling." **14**(5): 1017-1031.

Stavang, J. A., et al. (2009). "Hormonal regulation of temperature-induced growth in *Arabidopsis*." The Plant Journal **60**(4): 589-601.

Straumite, E., et al. (2015). "Pigments in mint leaves and stems." *Agronomy research* **13**(4): 1104-1111.

Tian, Y., et al. (2017). "Direct impact of the sustained decline in the photosystem II efficiency upon plant productivity at different developmental stages." *Journal of plant physiology* **212**: 45-53.

Tissot, N. and R. Ulm (2020). "Cryptochrome-mediated blue-light signalling modulates UVR8 photoreceptor activity and contributes to UV-B tolerance in Arabidopsis." *Nature communications* **11**(1): 1-10.

Toledo-Ortiz, G., et al. (2014). "The HY5-PIF regulatory module coordinates light and temperature control of photosynthetic gene transcription." *PLoS Genetics* **10**(6): e1004416.

Ueda, H. and M. Kusaba (2015). "Strigolactone regulates leaf senescence in concert with ethylene in Arabidopsis." *Plant physiology* **169**(1): 138-147.

Valladares, F. and Ü. Niinemets (2008). "Shade tolerance, a key plant feature of complex nature and consequences." *Annual Review of Ecology, Evolution, Systematics* **39**: 237-257.

Wang, X., et al. (2022). "Label-Free Quantitative Proteomics Reveal the Involvement of PRT6 in Arabidopsis thaliana Seed Responsiveness to Ethylene." *International journal of molecular sciences* **23**(16): 9352.

Wolters, H. and G. J. N. R. G. Jürgens (2009). "Survival of the flexible: hormonal growth control and adaptation in plant development." *Nature Reviews Genetics* **10**(5): 305-317.

Xie, Y., et al. (2017). "Phytochrome-interacting factors directly suppress MIR156 expression to enhance shade-avoidance syndrome in Arabidopsis." **8**(1): 1-11.

Xu, X., et al. (2014). "PHYTOCHROME INTERACTING FACTOR1 enhances the E3 ligase activity of CONSTITUTIVE PHOTOMORPHOGENIC1 to

synergistically repress photomorphogenesis in Arabidopsis." The Plant Cell **26**(5): 1992-2006.

Yang, C. and L. Li (2017). "Hormonal regulation in shade avoidance." Frontiers in plant science **8**: 1527.

Yang, C., et al. (2018). "Phytochrome A negatively regulates the shade avoidance response by increasing auxin/indole acetic acid protein stability." Developmental Cell **44**(1): 29-41. e24.

Yang, J., et al. (2005). "Light regulates COP1-mediated degradation of HFR1, a transcription factor essential for light signaling in Arabidopsis." **17**(3): 804-821.

Yu, Y. and R. Huang (2017). "Integration of ethylene and light signaling affects hypocotyl growth in Arabidopsis." Frontiers in plant science **8**: 57.

Yu, Y., et al. (2013). "Ethylene promotes hypocotyl growth and HY5 degradation by enhancing the movement of COP1 to the nucleus in the light." PLoS Genetics **9**(12): e1004025.

Zhang, H., et al. (2008). "Dolichol biosynthesis and its effects on the unfolded protein response and abiotic stress resistance in Arabidopsis." The Plant Cell **20**(7): 1879-1898.

Zhang, Y., et al. (2013). "A quartet of PIF bHLH factors provides a transcriptionally centered signaling hub that regulates seedling morphogenesis through differential expression-patterning of shared target genes in Arabidopsis." **9**(1): e1003244.

Zhou, Y., et al. (2018). "TCP transcription factors regulate shade avoidance via directly mediating the expression of both PHYTOCHROME INTERACTING FACTORs and auxin biosynthetic genes." Plant physiology **176**(2): 1850-1861.

GENERAL DISCUSSION

GENERAL DISCUSSION

With limited arable land, growing more plants per unit area to increase the yield of plant supplies is one of the solutions to ensuring adequate resources and food for the increasing human world population (Pinstrup-Andersen 2000). However, since many crops are shade-avoiding or sun-loving, growing under high plant densities conditions triggers a SAS response, which in adult plants results in a reduction in the number of seeds, leaves, and fruits, which in turn reduces plant yield and productivity (Roig-Villanova and Martínez-García 2016). Moreover, some SAS responses occur even when the amount of sunlight that the plant receives is sufficient to promote photosynthesis, that is, when the plant is close to neighboring vegetation but not under its canopy (Ballaré, Pierik et al. 2017). Therefore, it is critical to understand the molecular mechanisms of SAS in detail to target these mechanisms in plant breeding and to produce crops that can grow at high plant densities without activating SAS and reducing its productivity.

Comparative genetic analysis between *C. hirsuta* and *A. thaliana* suggests that orthologous shade signaling components from these two related species may function differently in their native environment to modulate distinct responses (Molina-Contreras, Paulišić et al. 2019). Differential regulation and functional modification of genetically related components as mechanisms to achieve different responses to shade demonstrate the extent of plant evolutionary plasticity. In *A. thaliana*, HY5 and PIF7 are two functionally opposite components known to date, with HY5 helping to suppress the shade-induced hypocotyl elongation response, whereas PIF7 promoting this response. However, according to our experimental results that the negative regulation of HY5 is strengthened in *C. hirsuta*, but the positive regulation of PIF7 is weakened. It seems reasonable to assume that this is because of higher

biological activity of negative regulators and lower activity of positive regulators in *C. hirsuta* when compared with *A. thaliana*. A full understanding of the basis for the differential activity of orthologous components, and a better understanding of the regulators involved, will be key to translating this knowledge into crops.

On the other hand, although SAS regulation has been thoroughly analyzed and described in *A. thaliana* (Roig-villanova and Martínez-García 2016), new components implicated in this process are still being discovered. One of them might be PRT6, which we investigated. PRT6 seems to play an important role in several cellular processes, including DIS, TIM and SAS by regulating growth-related hormones, such as Abscisic acid (ABA) (Ortiz-Alcaide, Llamas et al. 2019), salicylic acid (SA) and jasmonic acid (JA) (Adie, Pérez-Pérez et al. 2007), as we talked before. In addition, it also has been reported that PRT6 is essential in *A. thaliana* seed response to ethylene (Wang, Davanture et al. 2022). In shade condition, the endogenous ABA levels were increased to inhibit shade-induced hypocotyl elongation (Yang and Li 2017), partly through limiting ethylene biosynthesis and partly by another mechanism (Iqbal, Khan et al. 2017), suggesting that biosynthesis of ethylene is restrained in *prt6* seedlings, this also would be consistent with *eva* mutant lines having delayed DIS and attenuated hypocotyl elongation in response to shade and warm temperature, because ethylene promotes DIS (Ueda and Kusaba 2015) and hypocotyl elongation (Das, St. Onge et al. 2016). However, the lower level of SA and JA were found in *prt6-5* seedlings than wildtype plants (De Marchi, Sorel et al. 2016), these two phytohormones inhibit hypocotyl elongation (Fernández-Milmanda and Ballaré 2021), suggesting the inhibitory effect of hypocotyl elongation was reduced, this would be consistent with *adm* mutant lines having delayed DIS and enhanced hypocotyl elongation in response to shade and

warm temperature. Altogether, the different sensitivities to growth-related hormones may lead to differences in plant phenotypes (Souter, Topping et al. 2002). In our cases, four different alleles of *PRT6* were identified, including 2 *eva* mutants and 2 *adm* mutants, 2 *eva* mutants may be hypersensitive to ABA than SA and JA; whereas 2 *adm* mutants are opposite, the similar situation happened in *prt6-1* and *prt6-5* mutant seedlings, which got different sensitivities to high sucrose (Castillo, Costa-Broseta et al. 2021).

In conclusion, HY5, PIF7 and PRT6 all affect plant growth under shade condition, as PHYA and HFR1 (Molina-Contreras, Paulišić et al. 2019, Paulišić, Qin et al. 2021), but the specific regulatory mechanism in shade tolerant plants remains to be answered. Furthermore, it will be interesting to explore the interconnections of these regulators in both *A. thaliana* and *C. hirsuta*, broadening the understanding of shade tolerance mechanisms in this species, including whether shade tolerance traits are maintained at all developmental stages.

CONCLUSIONS

CONCLUSIONS

1. AtHFR1 interacted more strongly with COP1 than ChHFR1, the stronger binding to COP1 results in lower HFR1 abundance.
2. The hypocotyl phenotype of *chy5* mutant indicate that HY5 in *C. hirsuta* (ChHY5) has a role in maintaining hypocotyls unresponsive to shade. (link) ChHY5 has higher stability than AtHY5 in shade.
3. The hypocotyl phenotype of *chpif7* mutant indicate that PIF7 promotes hypocotyl elongation in *C. hirsuta* (ChPIF7) only detected it in the background that absence of *phyA*.
4. Comparative genetic analyses of *A. thaliana* and *C. hirsuta* suggest that SAS regulators also have a role in implementing shade tolerant habit in shade tolerant species. But differential activity of related orthologous components can result in divergent shade responses. Moreover, negative SAS regulators have higher activity or stability in shade-tolerant species which helps to suppress the shade induced hypocotyl elongation.
5. Shade-tolerant species likely have weaker activities of PIFs compared to the shade-avoider ones based on their abolished or attenuated PIF-mediated responses of Thermal-Induced Morphogenesis (TIM), shade and delayed Dark-Induced Senescence (DIS). This suggested that TIM and DIS might be associated to the shade habit.
6. Based on the above conclusion, we established a genetic screening system to identify mutants in *A. thaliana* which have shade tolerant phenotype. As a result, we isolated mutants that confirmed the suggested association of TIM, DIS and shade traits.

7. Mapping by sequencing approach identified PRT6 in 4 different cases. Mutations in different locations of the PRT6 gene may cause differential responses of hypocotyls to shade.

GENERAL REFERENCE

Adie, B. A., et al. (2007). "ABA is an essential signal for plant resistance to pathogens affecting JA biosynthesis and the activation of defenses in Arabidopsis." The Plant Cell **19**(5): 1665-1681.

Bai, S.-N. (2017). "Reconsideration of plant morphological traits: from a structure-based perspective to a function-based evolutionary perspective." Frontiers in plant science **8**: 345.

Ballaré, C. L., et al. (2017). "The shade-avoidance syndrome: Multiple signals and ecological consequences." Plant, cell & environment **40**(11): 2530-2543.

Botto, J. and H. Smith (2002). "Differential genetic variation in adaptive strategies to a common environmental signal in Arabidopsis accessions: phytochrome-mediated shade avoidance." Plant Cell Environ **25**(1): 53-63.

Brouwer, B., et al. (2012). "The impact of light intensity on shade-induced leaf senescence." Plant, cell & environment **35**(6): 1084-1098.

Casal, J. J. (2013). "Photoreceptor signaling networks in plant responses to shade." Annual review of plant biology **64**: 403-427.

Castillo, M.-C., et al. (2021). "NIN-like protein7 and PROTEOLYSIS6 functional interaction enhances tolerance to sucrose, ABA, and submergence." Plant physiology **187**(4): 2731-2748.

Cloix, C., et al. (2012). "C-terminal region of the UV-B photoreceptor UVR8 initiates signaling through interaction with the COP1 protein." Proceedings of the National Academy of Sciences **109**(40): 16366-16370.

Dannehl, D., et al. (2021). "Increase of yield, lycopene, and lutein content in tomatoes grown under continuous PAR spectrum LED lighting." Frontiers in plant science **12**: 299.

Das, D., et al. (2016). "Ethylene-and shade-induced hypocotyl elongation share transcriptome patterns and functional regulators." Plant physiology **172**(2): 718-733.

De Lucas, M., et al. (2008). "A molecular framework for light and gibberellin control of cell elongation." Nature **451**(7177): 480-484.

De Marchi, R., et al. (2016). "The N-end rule pathway regulates pathogen responses in plants." Scientific Reports **6**(1): 1-15.

de Wit, M., et al. (2016). "Integration of phytochrome and cryptochrome signals determines plant growth during competition for light." Current Biology **26**(24): 3320-3326.

Djakovic - Petrovic, T., et al. (2007). "DELLA protein function in growth responses to canopy signals." The Plant Journal **51**(1): 117-126.

Favero, D. S. (2020). "Mechanisms regulating PIF transcription factor activity at the protein level." Physiologia plantarum **169**(3): 325-335.

Fernández-Milmanda, G. L. and C. L. Ballaré (2021). "Shade avoidance: Expanding the color and hormone palette." Trends in plant science **26**(5): 509-523.

Fiorucci, A.-S. and C. Fankhauser (2017). "Plant strategies for enhancing access to sunlight." Current Biology **27**(17): R931-R940.

Franklin, K. A. (2008). "Shade avoidance." New Phytologist **179**(4): 930-944.

Fraser, D. P., et al. (2016). "Photoreceptor crosstalk in shade avoidance." Current opinion in plant biology **33**: 1-7.

Gommers, C. M. (2016). When growing tall is not an option: contrasting shade avoidance responses in two wild *Geranium* species, Utrecht University.

Gommers, C. M., et al. (2013). "Shade tolerance: when growing tall is not an option." Trends in plant science **18**(2): 65-71.

Hauvermale, A. L., et al. (2012). "Gibberellin signaling: a theme and variations on DELLA repression." Plant physiology **160**(1): 83-92.

Hayes, S., et al. (2017). "UV-B perceived by the UVR8 photoreceptor inhibits plant thermomorphogenesis." Current Biology **27**(1): 120-127.

Hersch, M., et al. (2014). "Light intensity modulates the regulatory network of the shade avoidance response in Arabidopsis." Proceedings of the National Academy of Sciences **111**(17): 6515.

Holtkotte, X., et al. (2017). "The blue light-induced interaction of cryptochrome 1 with COP1 requires SPA proteins during Arabidopsis light signaling." PLoS Genetics **13**(10): e1007044.

Hornitschek, P., et al. (2012). "Phytochrome interacting factors 4 and 5 control seedling growth in changing light conditions by directly controlling auxin signaling." The Plant Journal **71**(5): 699-711.

Iqbal, N., et al. (2017). "Ethylene role in plant growth, development and senescence: interaction with other phytohormones." Frontiers in plant science **8**: 475.

Jaillais, Y. and G. Vert (2012). "Brassinosteroids, gibberellins and light-mediated signalling are the three-way controls of plant sprouting." Nature cell biology **14**(8): 788-790.

Jia, Y., et al. (2020). "PIFs coordinate shade avoidance by inhibiting auxin repressor ARF18 and metabolic regulator QQS." New Phytologist **228**(2): 609-621.

Kami, C., et al. (2010). "Light-regulated plant growth and development." Current topics in developmental biology **91**: 29-66.

Kamiya, Y. and J. L. García-Martínez (1999). "Regulation of gibberellin biosynthesis by light." Current opinion in plant biology **2**(5): 398-403.

Keuskamp, D. H. and R. Pierik (2010). Photosensory cues in plant–plant interactions: regulation and functional significance of shade avoidance responses. Plant Communication from an Ecological Perspective, Springer: 159-178.

Keuskamp, D. H., et al. (2010). "Auxin transport through PIN-FORMED 3 (PIN3) controls shade avoidance and fitness during competition." Proceedings of the National Academy of Sciences **107**(52): 22740-22744.

Koini, M. A., et al. (2009). "High temperature-mediated adaptations in plant architecture require the bHLH transcription factor PIF4." Current Biology **19**(5): 408-413.

Kurepin, L. V., et al. (2007). "Interaction of red to far red light ratio and ethylene in regulating stem elongation of *Helianthus annuus*." Plant Growth Regulation **51**(1): 53-61.

Leivar, P., et al. (2012). "Dynamic antagonism between phytochromes and PIF family basic helix-loop-helix factors induces selective reciprocal responses to light and shade in a rapidly responsive transcriptional network in *Arabidopsis*." **24**(4): 1398-1419.

Lichtenthaler, H., et al. (1982). "Adaptation of chloroplast-ultrastructure and of chlorophyll-protein levels to high-light and low-light growth conditions." **37**(5-6): 464-475.

Liu, B., et al. (2011). "Arabidopsis cryptochrome 1 interacts with SPA1 to suppress COP1 activity in response to blue light." Genes & Development **25**(10): 1029-1034.

Lorrain, S., et al. (2008). "Phytochrome-mediated inhibition of shade avoidance involves degradation of growth-promoting bHLH transcription factors." The Plant Journal **53**(2): 312-323.

Lu, X.-D., et al. (2015). "Red-light-dependent interaction of phyB with SPA1 promotes COP1–SPA1 dissociation and photomorphogenic development in Arabidopsis." Molecular plant **8**(3): 467-478.

Martínez-García, J. F., et al. (2014). "The shade avoidance syndrome in Arabidopsis: the antagonistic role of phytochrome A and B differentiates vegetation proximity and canopy shade." PloS one **9**(10): e109275.

Martínez-García, J. F., et al. (2014). "The shade avoidance syndrome in Arabidopsis: the antagonistic role of phytochrome A and B differentiates vegetation proximity and canopy shade." **9**(10): e109275.

Martinez-Garcia, J. F., et al. (2010). "Regulatory components of shade avoidance syndrome." Advances in botanical research **53**: 65-116.

Molina-Contreras, M. J., et al. (2019). "Photoreceptor activity contributes to contrasting responses to shade in Cardamine and Arabidopsis seedlings." The Plant Cell **31**(11): 2649-2663.

Morelli, L., et al. (2020). "Light quality signals generated by vegetation shade facilitate acclimation to reduced light quantity in shade-avoider plants." bioRxiv.

Morgan, P. W., et al. (2002). "Opportunities to improve adaptability and yield in grasses: lessons from sorghum." Crop Science **42**(6): 1791-1799.

Müller-Moulé, P., et al. (2016). "YUCCA auxin biosynthetic genes are required for Arabidopsis shade avoidance." **4**: e2574.

Ortiz-Alcaide, M., et al. (2019). "Chloroplasts modulate elongation responses to canopy shade by retrograde pathways involving HY5 and abscisic acid." The Plant Cell **31**(2): 384-398.

Paik, I., et al. (2017). "Expanding roles of PIFs in signal integration from multiple processes." Molecular plant **10**(8): 1035-1046.

Paulišić, S., et al. (2021). "Adjustment of the PIF7-HFR1 transcriptional module activity controls plant shade adaptation." The EMBO Journal **40**(1): e104273.

Pedmale, U. V., et al. (2016). "Cryptochromes interact directly with PIFs to control plant growth in limiting blue light." Cell **164**(1-2): 233-245.

Pierik, R. and M. de Wit (2014). "Shade avoidance: phytochrome signalling and other aboveground neighbour detection cues." Journal of Experimental Botany **65**(11): 2815-2824.

Pierik, R. and C. Testerink (2014). "The art of being flexible: how to escape from shade, salt, and drought." Plant physiology **166**(1): 5-22.

Pinstrup-Andersen, P. J. C. J. o. P. P. (2000). "The future world food situation and the role of plant diseases." **22**(4): 321-331.

Qi, L., et al. (2020). "PHYTOCHROME-INTERACTING FACTORS interact with the ABA receptors PYL8 and PYL9 to orchestrate ABA signaling in darkness." **13**(3): 414-430.

Quint, M., et al. (2016). "Molecular and genetic control of plant thermomorphogenesis." Nature Plants **2**(1): 1-9.

Quirino, B. F., et al. (2000). "Molecular aspects of leaf senescence." **5**(7): 278-282.

Rascher, U., et al. (2000). "Evaluation of instant light-response curves of chlorophyll fluorescence parameters obtained with a portable chlorophyll fluorometer on site in the field." Plant Cell Environ **23**(12): 1397-1405.

Roig-villanova, I. and J. F. Martínez-García (2016). "Plant Responses to Vegetation Proximity: A Whole Life Avoiding Shade." Front. Plant Sci. **7**(February): 1-10.

Roig-Villanova, I. and J. F. Martínez-García (2016). "Plant responses to vegetation proximity: a whole life avoiding shade." Frontiers in plant science **7**: 236.

Roig-Villanova, I. and J. F. J. F. i. P. S. Martínez-García (2016). "Plant responses to vegetation proximity: a whole life avoiding shade." **7**: 236.

Roig-Villanova, I., et al. (2007). "Interaction of shade avoidance and auxin responses: a role for two novel atypical bHLH proteins." The EMBO Journal **26**(22): 4756-4767.

Ruberti, I., et al. (2012). "Plant adaptation to dynamically changing environment: the shade avoidance response." **30**(5): 1047-1058.

Sairanen, I., et al. (2012). "Soluble carbohydrates regulate auxin biosynthesis via PIF proteins in Arabidopsis." **24**(12): 4907-4916.

Sasidharan, R., et al. (2008). "The regulation of cell wall extensibility during shade avoidance: a study using two contrasting ecotypes of *Stellaria longipes*." Plant physiology **148**(3): 1557-1569.

Sessa, G., et al. (2005). "A dynamic balance between gene activation and repression regulates the shade avoidance response in Arabidopsis." **19**(23): 2811-2815.

Sheerin, D. J. and A. Hiltbrunner (2017). "Molecular mechanisms and ecological function of far-red light signalling." Plant Cell Environ **40**(11): 2509-2529.

Smith, H. (1982). "Light quality, photoperception, and plant strategy." Annual review of plant physiology **33**(1): 481-518.

Smith, H. (2000). "Phytochromes and light signal perception by plants—an emerging synthesis." Nature **407**(6804): 585-591.

Souter, M., et al. (2002). "hydra mutants of Arabidopsis are defective in sterol profiles and auxin and ethylene signaling." **14**(5): 1017-1031.

Stavang, J. A., et al. (2009). "Hormonal regulation of temperature-induced growth in Arabidopsis." The Plant Journal **60**(4): 589-601.

Tissot, N. and R. Ulm (2020). "Cryptochrome-mediated blue-light signalling modulates UVR8 photoreceptor activity and contributes to UV-B tolerance in Arabidopsis." Nature communications **11**(1): 1-10.

Ueda, H. and M. Kusaba (2015). "Strigolactone regulates leaf senescence in concert with ethylene in Arabidopsis." Plant physiology **169**(1): 138-147.

Wang, X., et al. (2022). "Label-Free Quantitative Proteomics Reveal the Involvement of PRT6 in Arabidopsis thaliana Seed Responsiveness to Ethylene." International journal of molecular sciences **23**(16): 9352.

Xie, Y., et al. (2017). "Phytochrome-interacting factors directly suppress MIR156 expression to enhance shade-avoidance syndrome in Arabidopsis." **8**(1): 1-11.

Yang, C. and L. Li (2017). "Hormonal regulation in shade avoidance." Frontiers in plant science **8**: 1527.

Zhang, Y., et al. (2013). "A quartet of PIF bHLH factors provides a transcriptionally centered signaling hub that regulates seedling morphogenesis through differential expression-patterning of shared target genes in Arabidopsis." **9**(1): e1003244.

Zhou, Y., et al. (2018). "TCP transcription factors regulate shade avoidance via directly mediating the expression of both PHYTOCHROME INTERACTING FACTOR s and auxin biosynthetic genes." Plant physiology **176**(2): 1850-1861.

